

ACCEPTED MANUSCRIPT • OPEN ACCESS

A review of carbon monitoring in wet carbon systems using remote sensing

To cite this article before publication: Anthony Daniel Campbell *et al* 2022 *Environ. Res. Lett.* in press <https://doi.org/10.1088/1748-9326/ac4d4d>

Manuscript version: Accepted Manuscript

Accepted Manuscript is “the version of the article accepted for publication including all changes made as a result of the peer review process, and which may also include the addition to the article by IOP Publishing of a header, an article ID, a cover sheet and/or an ‘Accepted Manuscript’ watermark, but excluding any other editing, typesetting or other changes made by IOP Publishing and/or its licensors”

This Accepted Manuscript is © 2022 The Author(s). Published by IOP Publishing Ltd.

As the Version of Record of this article is going to be / has been published on a gold open access basis under a CC BY 3.0 licence, this Accepted Manuscript is available for reuse under a CC BY 3.0 licence immediately.

Everyone is permitted to use all or part of the original content in this article, provided that they adhere to all the terms of the licence <https://creativecommons.org/licenses/by/3.0>

Although reasonable endeavours have been taken to obtain all necessary permissions from third parties to include their copyrighted content within this article, their full citation and copyright line may not be present in this Accepted Manuscript version. Before using any content from this article, please refer to the Version of Record on IOPscience once published for full citation and copyright details, as permissions may be required. All third party content is fully copyright protected and is not published on a gold open access basis under a CC BY licence, unless that is specifically stated in the figure caption in the Version of Record.

View the [article online](#) for updates and enhancements.

A review of Carbon Monitoring in Wet Carbon Systems using Remote Sensing

Anthony D. Campbell^{1,2}, Temilola Fatoyinbo¹, Sean P. Charles³, Laura L. Bourgeau-Chavez⁴, Joaquim Goes⁵, Helga Gomes⁵, Meghan Halabisky⁶, James Holmquist⁷, Steven Lohrenz⁸, Catherine Mitchell⁹, L. Monika Moskal⁶, Benjamin Poulter¹, Han Qiu¹⁰, Celio H. Resende De Sousa¹, Michael Sayers⁴, Marc Simard¹¹, Anthony J. Stewart⁶, Debjani Singh¹², Carl Trettin¹³, Jinghui Wu⁵, Xuesong Zhang¹⁴, and David Lagomasino³

¹Biospheric Sciences Laboratory, NASA Goddard Space Flight Center, Greenbelt, MD, USA

²NASA Postdoctoral Program, Universities Space Research Association, Columbia, MD, USA

³Department of Coastal Studies, East Carolina University, Wanchese, NC 27981, USA

⁴Michigan Tech Research Institute, Michigan Technological University, Ann Arbor, MI, USA

⁵Marine Biology, Department of Marine Biology and Paleoenvironment, Lamont–Doherty Earth Observatory, Columbia University, 61 Route 9W, Palisades, New York 10964, USA

⁶School of Environment and Forest Sciences, University of Washington, Seattle, WA 98195, USA

⁷Smithsonian Environmental Research Center, Edgewater, MD 21037-0028, USA

⁸School for Marine Science and Technology, University of Massachusetts Dartmouth, New Bedford, MA 02744, USA

⁹Bigelow Laboratory for Ocean Sciences, East Boothbay, ME 04543, USA

¹⁰Department of Forest and Wildlife Ecology, University of Wisconsin-Madison, 1630 Linden Drive, Madison, WI, USA

¹¹Jet Propulsion Laboratory, California Institute of Technology, Pasadena, CA 91109, USA

¹²Environmental Sciences Division, Oak Ridge National Laboratory, Oak Ridge, TN 37830

¹³USDA-Forest Service, Southern Research Station, Cordesville, SC 29434, USA

¹⁴USDA-ARS Hydrology and Remote Sensing Laboratory, Beltsville, MD 20705-2350 USA

Abstract:

Carbon monitoring is critical for the reporting and verification of carbon stocks and change. Remote sensing is a tool increasingly used to estimate the spatial heterogeneity, extent and change of carbon stocks within and across various systems. We designate the use of the term wet carbon system to the interconnected wetlands, ocean, river and streams, lakes and ponds, and permafrost, which are carbon-dense and vital conduits for carbon throughout the terrestrial and aquatic sections of the carbon cycle. We reviewed wet carbon monitoring studies that utilize earth observation to improve our knowledge of data gaps, methods, and future research recommendations. To achieve this, we conducted a systematic review collecting 1,622 references and screening them with a combination of text matching and a panel of three experts. The search found 496 references, with an additional 78 references added by experts. Our study found considerable variability of the utilization of remote sensing and global wet carbon monitoring progress across the nine systems analyzed. The review highlighted that remote sensing is routinely used to globally map carbon in mangroves and oceans, whereas seagrass, terrestrial wetlands, tidal marshes, rivers, and permafrost would benefit from more accurate and comprehensive global maps of extent. We identified three critical gaps and twelve recommendations to continue progressing wet carbon systems and increase cross system scientific inquiry.

1 Introduction

The Paris Climate Agreement requires net neutral carbon emissions by reducing fossil fuel emissions and balancing sources and sinks by 2100 [1]. Monitoring, reporting, and verification (MRV) are foundational for tracking emission reductions from land-use change and carbon removal attributed to reforestation and afforestation [2,3]. Oceans, coasts, and wetlands are essential components of the global carbon cycle and are considered critical to achieving emission reductions necessary for fulfilling a variety of Sustainable Development Goals (Figure 1)[4-6]. Carbon monitoring of wetlands, water bodies, and oceans pose unique challenges because of their complex ecosystem structure, seasonality, and susceptibility to climate impacts such as sea-level rise, drought, and increased storms [7,8].

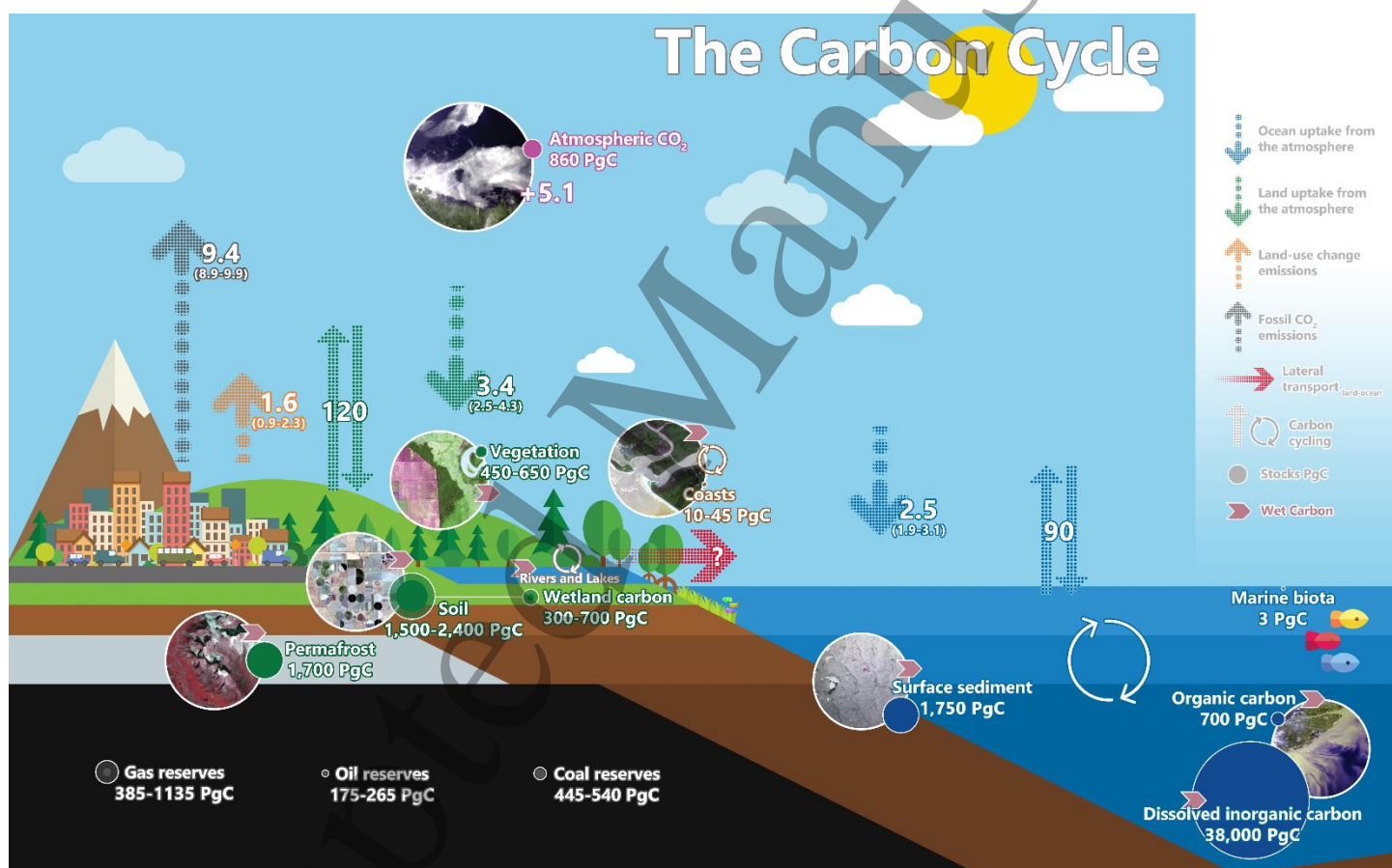


Figure 1. The global carbon cycle adapted from [9]. Wet carbon systems are highlighted with the interaction symbol from Systems Ecology [10]. Vegetation and soil are both denoted as wet carbon systems, but only a portion of these carbon stores are wet carbon. Images are Planetscope (permafrost, soil, vegetation, coasts), Sentinel-3 (atmospheric and organic carbon), and surface sediment camera system (photo credit Kevin Stokesbury). Wetland soil carbon value from Bridgham et al. [11]

This review focuses on the fluxes and stocks of carbon in wet carbon (WC) systems, a term used hereinafter to include all freshwater, saline, and brackish aquatic and wetland ecosystems, e.g., peatlands,

1 mangroves, and oceans. This term is not a paradigm shift away from 'blue carbon' but a broader grouping of
2 carbon cycle systems with shared data needs, restoration and preservation priority, and research direction. 'Blue
3 carbon' is a term used to describe carbon-dense coastal wetland ecosystems and has aided significant research
4 progress, with an expansive agenda for monitoring and applications [12]. However, focusing exclusively on
5 'blue carbon' ecosystems emphasizes ~20% of global wetlands (1,520-1,620 Mha) and excludes terrestrial
6 wetlands, permafrost, lakes, riverine, and marine systems [13,14]. We primarily consider the oceans a WC
7 system due to the interconnectedness between the oceans and other WC systems, i.e., the land–ocean aquatic
8 continuum (Figure 1)[15]. Here, we conducted a synthesis review of these interconnected systems to identify
9 shared data needs, convergent research directions, and carbon monitoring goals.
10
11
12
13
14
15
16

17 Carbon monitoring research has rapidly expanded over the last 10-20 years due to international
18 agreements targeted at reducing carbon emissions and establishing the need for accurate MRV of carbon. In
19 1997, the Kyoto Protocol prioritized the need for agricultural soils and forests to be managed as natural carbon
20 sinks [16], followed by the development of Reduce Emissions from Deforestation and Forest Degradation
21 (REDD) and REDD+ in 2009. The Paris Climate Agreement promotes wetland and coastal ecosystem
22 management and provides a mechanism for developing and implementing their Nationally Determined
23 Contributions (NDC) [16,17]. The goal of carbon-neutral land-use change set forth as part of the Paris Climate
24 Agreement has added additional exigency for developing MRV methods to inform carbon offsets and facilitate
25 the inclusion of WC ecosystems within NDCs. To continue the further expansion of carbon offsets to WC
26 systems requires high-quality remote sensing enabled MRV, a core goal of the NASA Carbon Monitoring
27 System (CMS) Program [18].
28
29
30
31
32
33
34
35
36

37 Remote sensing data provide spatial and temporal observations that can support carbon monitoring at
38 local, regional, and global scales. WC monitoring of terrestrial and coastal wetlands are concerned with both
39 aboveground and subsurface carbon as most most of these systems' carbon stock is below the surface [19]. Tier
40 3 Intergovernmental Panel on Climate Change (IPCC) estimates require the inclusion of modeled, local
41 processes that impact emissions and reduce uncertainty [20]. Therefore, spatially resolving subsurface carbon
42 requires modeling of hydrological, biophysical, and topographic indicators [21]. At local scales, carbon MRV
43 can be conducted exclusively with *in situ* data. However, WC monitoring at regional and global scales requires
44 combinations of *in situ* measurements and remote sensing observables. Remote sensing introduces uncertainty
45 but helps resolve spatial variability that *in situ* estimates cannot (Figure 2). Enabling our end goal of global
46 continuous monitoring of all WC systems and their interactions.
47
48
49
50
51
52
53
54
55
56
57
58
59
60

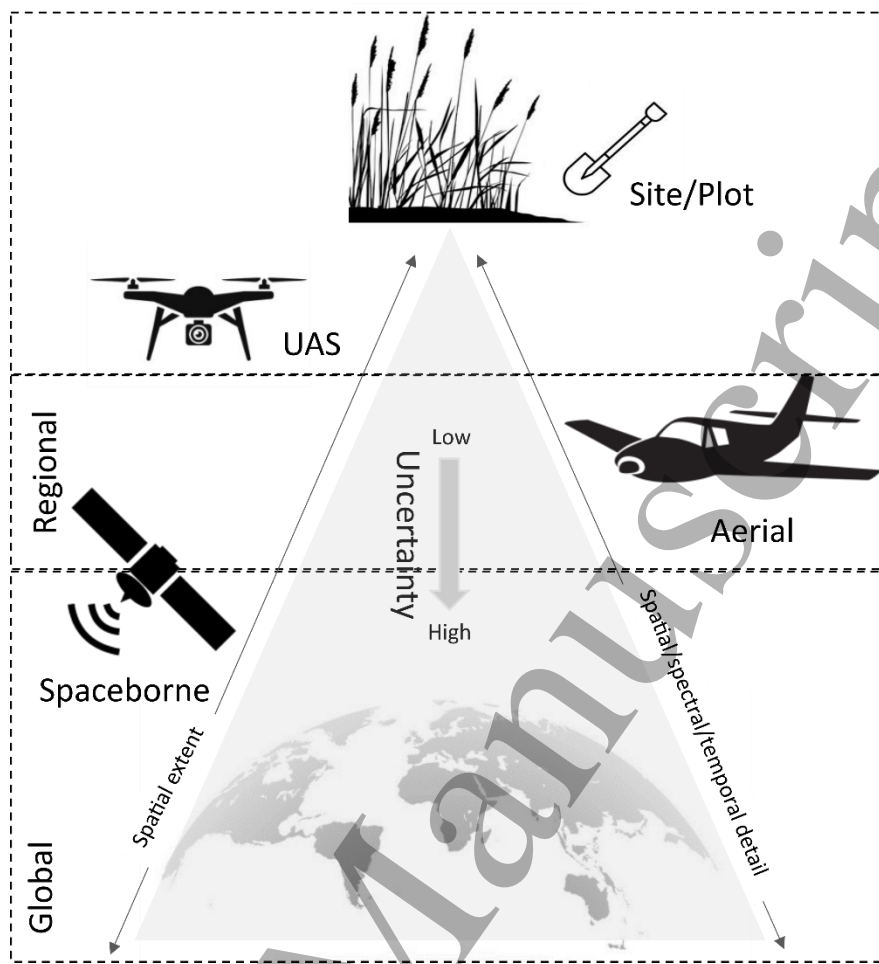


Figure 2. Terrestrial carbon monitoring extents, platforms in relation to uncertainty and remote sensing spatial, temporal, and spectral resolution domains.

The NASA CMS program seeks to prototype methods for MRV of the entire carbon cycle, and these WC systems represent an essential component with unique data needs and methodologies. As part of this review, we surveyed nine WC systems to determine earth observation-based WC monitoring status within each. The inclusion of more systems into global carbon budgets can reduce uncertainty, improve modeling outputs, and diversify climate mitigation solutions. WC monitoring is a relatively new field that we explore through a systematic review of the literature identifying gaps in our understanding, including location, ecosystem function, and methodological. We set forth the current state of carbon monitoring science within a subset of WC systems, including mangroves, peatlands and permafrost, tidal marsh and flats, terrestrial wetlands, oceans, coastal and continental shelf seas, lakes and ponds, rivers and streams, and submerged aquatic vegetation (including seagrasses, kelp). We focus on natural WC systems due to their connections and shared data needs; it should be noted that anthropogenic WC systems, such as, rice paddies, are also important, but beyond the scope of our review. We discuss the current state of carbon monitoring data, stakeholder engagement, and provide recommendations to inform the future of WC monitoring, the NASA CMS program, and carbon accounting.

2 Systematic Review

2.1 Methodology:

The Web of Science was used to conduct this review with the inclusion of the CMS literature archive, and Google Scholar searches. Our search descriptions and strings can be found in Supplemental Table 1. This example search string resulted in 466 references within the Web of Science and cumulatively all searches amounted to 1,622 records. The system terms used included salt marsh, tidal marsh, mangroves, wetland, coral, seagrass, forested wetland, riparian, bog, peat, benthic, ocean, tidal flat, mudflat, marsh, bog, vernal pool, salt flat, submerged aquatic vegetation, beach, kelp, and playa. The Google Scholar results, and CMS program outputs were screened with an automated text selection algorithm, ensuring that all abstracts had a remote sensing and WC system term. The resulting studies were input into Cadima, a webtool for facilitating systematic reviews. All abstracts were screened by at least two reviewers to identify if they fulfilled three requirements.

- 1) The study used remote sensing data
- 2) The study reports carbon monitoring findings (land cover mapping or solely *in situ* finding were excluded)
- 3) The study at least partially focuses on a WC system

If all these questions were answered in the affirmative, we included that paper in the data extraction step of the literature review. If reviewers disagreed on an abstract's relevancy, a three-reviewer panel adjudicated its inclusion with most references being passed to the next step i.e., full review by an expert on that system. This process found 496 relevant references. Additional references were added based on expert knowledge resulting in a total of 574 (Supplemental Data 1). The references were divided into WC systems including mangroves (n = 79), tidal marsh and flats (n = 47), submerged aquatic vegetation (SAV; n = 45), mineral wetlands (n = 55), peatlands (n = 129), permafrost (n=80), lakes (n = 64), rivers (n = 33), oceans (n = 102), and ocean shelf (n = 30). References were allowed to have multiple system designations.

3 Results

Since 2010, studies of WC monitoring with remote sensing have increased substantially (Figure 3). The research growth tracks with major literature milestones, e.g., Nellemann et al. [22], which first coined the term 'blue carbon,' and Page et al. [23], which demonstrated the importance of tropical peatland carbon. Interest further developed with a call for the use of remote sensing to identify land-use change, priority areas for

protection, and methods for measuring C stocks within sediments [24]. However, growth was not consistent between WC systems, with some having more research interest, including oceans, peatlands, and mangroves.

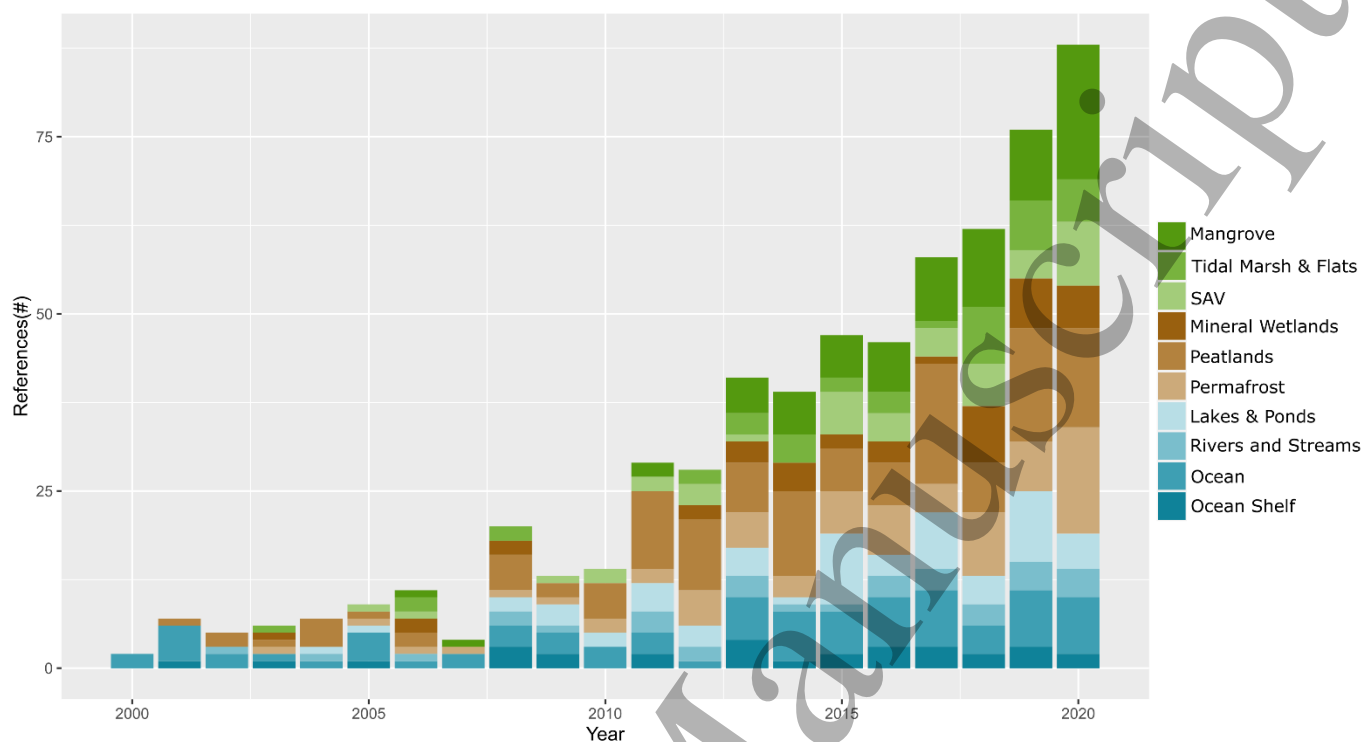


Figure 3: The results of the systematic review. References separated by year and WC system. We have separated peatlands and permafrost from terrestrial wetlands to demonstrate the disparity in research interest.

Disparate levels of research interest across remote sensing monitoring of WC systems are evident in this result. In the past, “blue carbon” research and media coverage were highly skewed towards coral [25]. Realignment of research interest, media attention, and funding is critical for understanding understudied WC systems and providing scientific justification and public support for WC mitigation. However, total yearly citations demonstrate that WC research utilization has remained relatively consistent since 2010 (Figure 4) despite more studies. Many systems are still developing remote sensing methodologies to enable carbon monitoring (see sections 3.1.2 Tidal marsh and flats; 3.1.3 Submerged Aquatic Vegetation; 3.2.1 Mineral wetlands; 3.3.2 Rivers). A shared language of carbon monitoring was evident across our WC systems. The use of earth observation to capture spatial heterogeneity is apparent in the two most common keywords, i.e., dynamics and variability. These keywords were identified in clusters across the literature and were areas of shared interest (Figure 5). Thematic mapping of the literature revealed that climate change, dynamics, and carbon were the most fundamental research themes and that forested WC systems were prominent in multiple clusters. These two forest-related clusters correspond with peatlands and mangroves, two systems with considerable growth in research interest from 2000-2019 (Figure 3). An emerging cluster associated with coastal remote sensing was evident, likely due to a recent focus on the data requirements for monitoring coastal

systems. These keywords were apparent within our detailed reviews of WC systems and framed our discussion of the status of carbon monitoring.

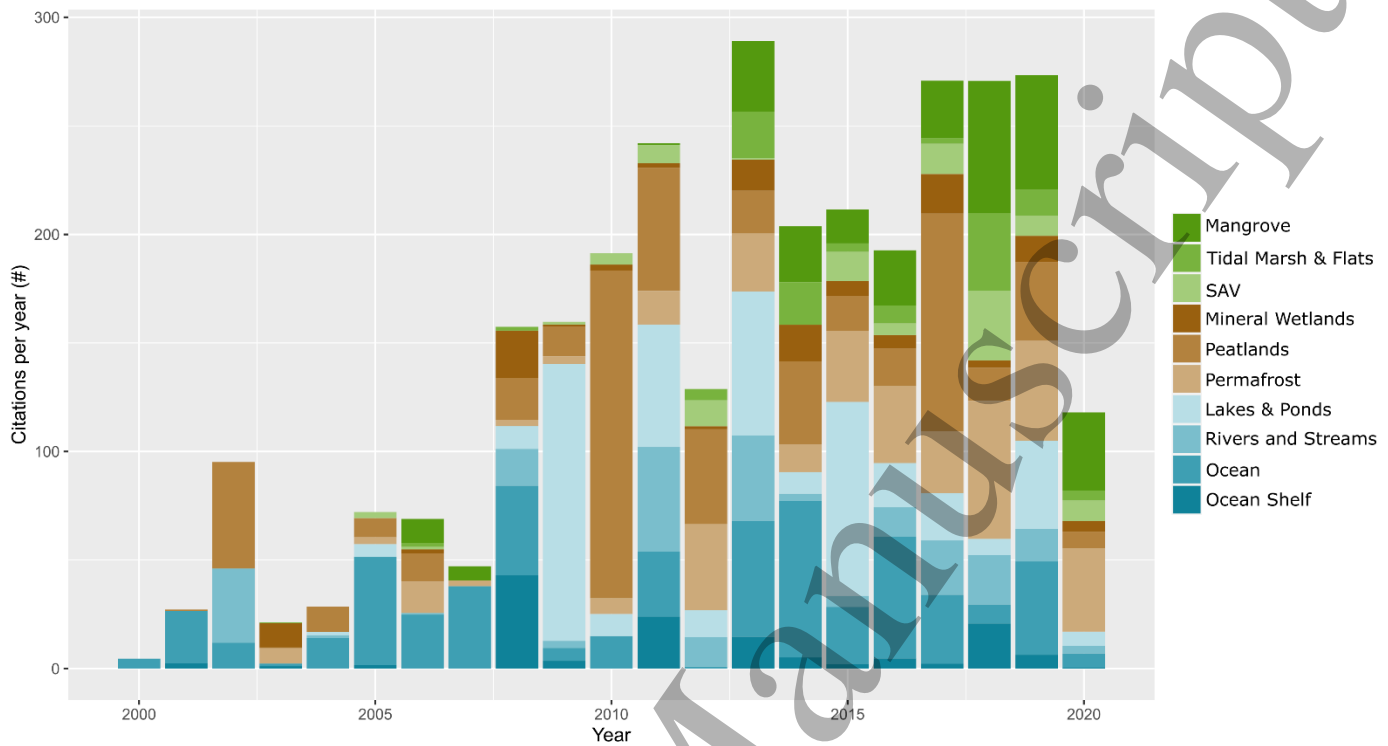
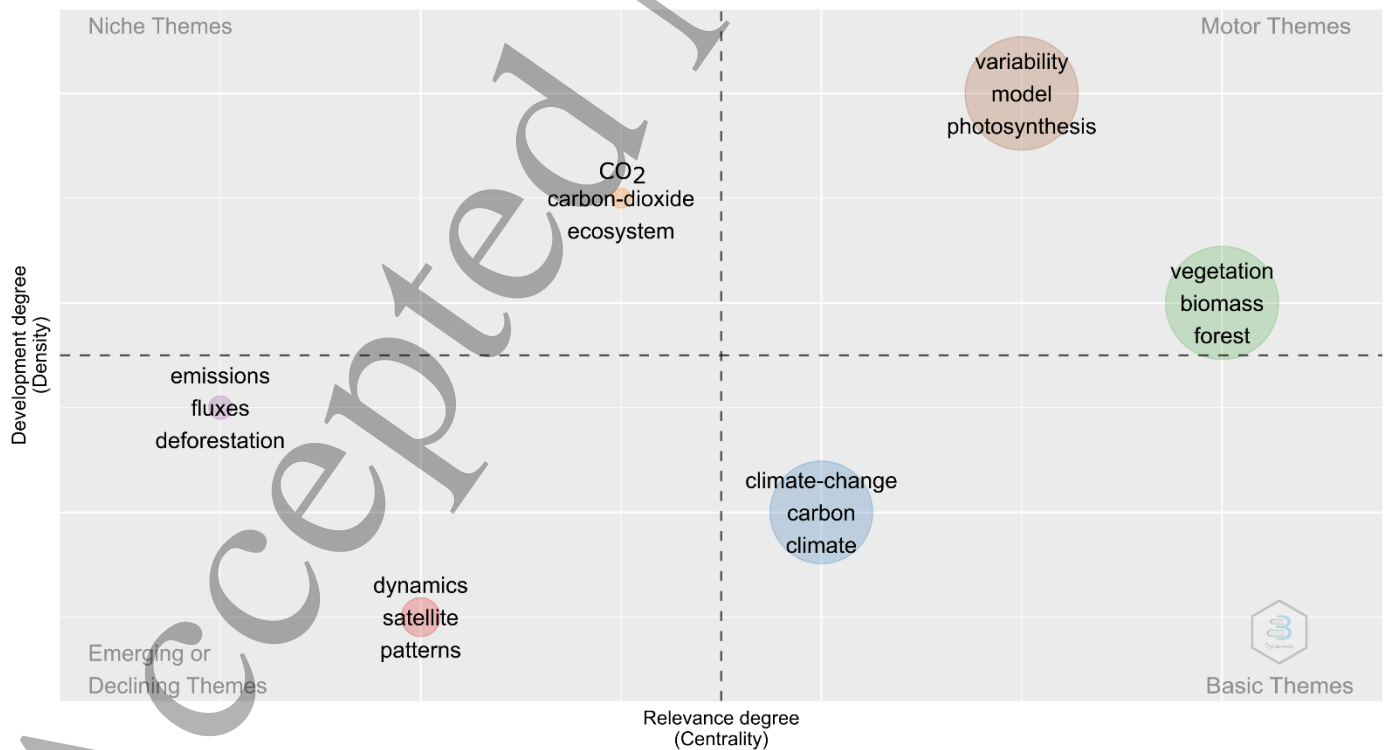


Figure 4: Total average citations per year by publication year and WC system category.



Accepted Manuscript

Figure 5: Thematic map created using keywords of WC research. We plotted relevance i.e., connection to the body of research on the x axis and development i.e., connections within a cluster on the y axis—each cluster's three most common keywords represent it. The Bibliometrix package in R 4.1.1 [26,27].

WC systems were separated into three categories for this review: coastal wetlands, inland wetlands, and ocean and shelves. Coastal wetlands included mangroves, submerged aquatic vegetation (SAV), and tidal marshes and flats. Inland wetlands comprised of mineral wetlands, peatlands and permafrost, whereas, inland waterbodies, lakes and ponds, and rivers and streams. Each of these system sections discusses the status of carbon monitoring within the system.

3.1 Coastal Wetlands:

Coastal wetlands are located along the terrestrial-aquatic interface and influenced by ocean and freshwater processes [28]. 'Blue carbon' ecosystems (seagrass, mangroves, tidal marshes and forests) comprise a portion of coastal wetlands. Coastal wetlands have consistently lost extent across the 19th and 20th century (-0.228% yr⁻¹), slightly less than inland wetland loss (-0.391% yr⁻¹) [29].

3.1.1 Mangroves:

In total, we found 79 papers relevant to carbon monitoring with remote sensing in mangrove ecosystems. Mangroves have some of the highest carbon (C) density (401 ± 48 Mg C ha⁻¹), with between 49-98% of carbon stored in the soils [30]. Mangroves are a small fraction of global forest area (0.3-0.5%) but a significant global C stock (5–10.4 PgC) [21,31-36]. Recently, Global Mangrove Watch identified 137,600 km² of mangrove extent in 2010 and has since measured change from 1996-2017 [35,37]. These forests are under significant threat from anthropogenic activity and sea-level rise [38-40]. In general, mangroves are difficult to survey, but remote sensing has increased our capacity to monitor their extent, C stocks, and change. We have grouped our synthesis of the status of carbon monitoring in mangroves into three sections: 1) carbon monitoring status, 2) data and applications.

Carbon Monitoring Status

Not long ago, mangrove biomass and carbon estimates relied upon the extrapolation of field data, environmental conditions, and partial extent maps [e.g., 31, 41-45]. Giri et al. [46] created the first global mangrove map using Landsat imagery. This map and other advances in remote sensing have enabled regional-to-global-scale analyses of mangrove carbon stocks and carbon stock change [21, 36, 38, 40, 47-49]. Mangrove carbon monitoring combining field-based surveys and remote sensing occurs across; local [e.g., 50-56], regional [e.g., 49,57-62], and global [21, 34, 36, 63-67] scales. Continued advancement, including machine learning,

1 have led to recent studies classifying species [68-71], quantifying height distributions and biomass [36, 72-74],
2 change in extent [40, 47, 49, 75] and stand age [60], and productivity [76, 77].
3
4

5 Passive sensors are used to map mangrove extent, change, and extrapolate C storage with field data [8,
6 59, 60, 78-81]. Active sensors (e.g., light detection and ranging (LiDAR) and radar) can measure mangrove
7 structural attributes, such as canopy height. Simard et al. [56] first derived accurate height estimates in the
8 Everglades with Shuttle Radar Topographic Mission (SRTM). Subsequently, canopy height was estimated using
9 satellite stereo images, Synthetic Aperture Radar (SAR) interferometry, and lidar [56, 60, 82-84]. Canopy
10 height enables estimates of aboveground biomass [e.g., 36, 85-88]. Additional active spaceborne sensors (e.g.,
11 SRTM, Sentinel-1, TanDEM-X, ICESat, and GEDI) have improved canopy height models [e.g., 82, 84, 89],
12 enabled the identification of change hotspots [40,49, 90], and the development of mangrove carbon monitoring
13 initiatives [37, 47, 60, 91]. The Japanese Aerospace Exploration Agency (JAXA) L-band SAR sensors (ALOS
14 and ALOS-2) are an important active sensor for mangrove mapping, including the identification of invasive
15 species [58], prediction of AGB [74, 92], and long-term monitoring [39, 93]. Medium resolution sensors have
16 enabled global-scale analysis but can miss small mangrove patches and edges or small-scale restoration efforts.
17
18
19
20
21
22
23
24
25

26 The recent increase in the resolution and accessibility of satellite imagery has provided fine-scale
27 mangrove data products suitable for MRV. The European Space Agency's (ESA) Sentinel-1 and Sentinel-2
28 launched in 2014 and 2015, respectively, increased the spatial resolution of new mangrove maps from 30 meters
29 (i.e., Landsat) to 10 and 20 meters [53, 95, 94]. Moreover, access to high-resolution satellite, aerial, and
30 unoccupied aerial systems (UAS) imagery has further increased the spatial resolution of mangrove maps (<5
31 meters) [51, 59, 60, 70, 71, 79, 95, 96]. Data fusion with combinations of multispectral, hyperspectral, lidar,
32 radar, and high-resolution data have been applied to increase the spatial and temporal resolution of mangrove
33 carbon storage and flux estimates [60, 88]. The increased temporal resolution also facilitates monitoring of
34 short-term disturbance and recovery [8,49].
35
36
37
38
39
40
41
42

43 Coarse spatial resolution sensors such as MODIS are also informative and often used with other satellite
44 imagery [97]. The high temporal resolution of MODIS is particularly beneficial when tracking net primary
45 productivity (NPP)[76] or gross primary productivity (GPP) change [55, 77], including due to disturbance
46 events like hurricanes [98] and insect outbreaks [77].
47
48
49
50

51 **Data and Applications**

52
53 Field and climate studies provided the first global mangrove carbon models [41, 63] and continue to be
54 essential for monitoring mangrove carbon [30, 66, 99, 100]. Mangrove height and biomass models have
55 increased in accuracy, providing improved estimates of aboveground C stocks and change through restoration
56 [101, 102], afforestation and encroachment [50, 51, 59, 103, 104], natural disturbances [40, 49, 57, 58] and
57
58
59
60

1 local anthropogenic impacts [40, 49, 57, 58]. Anne et al. [105] modeled mangrove soil carbon with
2 hyperspectral data, which improved on Landsat-based models. Global mangrove carbon density has been
3 extrapolated from 250 m to 30 m with a combination of machine learning, earth observation, and ancillary data
4 [e.g., 21,34].
5
6

7
8 Remote sensing further complicates the quantification of uncertainty in carbon monitoring (Figure 2).
9 Simard et al. [36,56] demonstrate that allometric equations can introduce considerable bias (>100%). However,
10 the remote sensing canopy height model error was low (RMSE of 2 m). *In situ* carbon monitoring samples are
11 limited globally. If these samples are not representative, uncertainty will be high and unquantified.
12 Extrapolating carbon stocks and fluxes from relatively few *in situ* measurements makes the accurate
13 quantification of spatial uncertainty extremely important. For example, Sanderman et al. [21] used the existing
14 250 m SoilGrid data, *in situ* training data, and Landsat imagery to create a 30 m organic carbon stock (OCS)
15 map. The study resulted in an average uncertainty of 40.4% of the mean OCS [21]. Remote sensing methods
16 can quantify the spatial uncertainty improving stakeholder understanding of regional carbon estimates and
17 accuracy.
18
19
20
21
22
23
24

25
26 Despite comprising only 0.3% of global coastal ocean area, mangroves contribute ~55% of air-sea CO₂
27 exchange from the world's wetlands and estuaries, 60% of dissolved inorganic carbon (DIC) and 27% of
28 dissolved organic carbon (DOC) from tropical rivers to the coastal ocean [106-108]. Over half of mangrove
29 carbon production was unaccounted for until recently [45, 109], when mangrove carbon export (particularly
30 DOC and DIC) were quantified [107,108]. Only 14 TgC yr⁻¹ of mangrove NPP is buried in soils, while export to
31 coastal oceans is approximately an order of magnitude higher (158 TgC yr⁻¹)[108]. Mangroves export an
32 estimated 15 Tg particulate organic carbon (POC) yr⁻¹, 51 Tg DOC yr⁻¹, and 124 Tg DIC yr⁻¹ to coastal oceans
33 [107,108]. Models of river and tidal flow through mangroves informed by remote sensing have improved
34 estimates of carbon export [276], identifying relationships between environmental conditions (tidal height,
35 river-flow, precipitation, biogeochemical constituents of water) and carbon export associated with tidal
36 pumping [45, 276], particularly of DIC [276]. Furthermore, ocean color techniques can identify the source of
37 organic matter through absorption coefficients [112, 113], allowing for detection of mangrove derived
38 chromophoric dissolved organic matter (CDOM) and DOC [114]. Carbon export from mangroves is spatially
39 and temporally heterogeneous, and remote sensing can help resolve this variability indirectly through
40 characterizing water flow and directly through the identification of CDOM.
41
42
43
44
45
46
47
48
49
50
51
52

53 Remote sensing has been essential for carbon monitoring of mangroves due to their unique landscape
54 position, structure, and spectral characteristics. These data have enabled relatively precise quantification of
55 mangrove extent, carbon stocks, and carbon fluxes from local-to-global scales (Table 1). Mangroves are among
56 the most carbon-dense ecosystems (Table 1)[108] and are likely to become increasingly impacted by
57
58
59
60

1 anthropogenic and natural disturbances [115]. Continued remote sensing carbon monitoring is necessary with a
2 particular focus on climate-related range-shifts associated with sea-level rise (coastal contraction and inland
3 expansion [116,117]) and poleward range expansion [118-121].
4
5
6
7
8
9
10
11
12
13
14
15
16
17
18
19
20
21
22
23
24
25
26
27
28
29
30
31
32
33
34
35
36
37
38
39
40
41
42
43
44
45
46
47
48
49
50
51
52
53
54
55
56
57
58
59
60

Accepted Manuscript

Table 1. Global carbon monitoring value for mangroves from the literature. Method refers to four categories, modeled, data synthesis, extrapolation (*in situ* combined with extent to upscale estimates), and remote sensing (mapping or predicting spatial heterogeneity for an indicator).

Carbon indicator	System	Value	Units	Method	Source
System Extent	Mangroves	0.137- 0.16	10 ⁶ km ²	Remote Sensing	[35,46,47]
System Extent Change	Mangroves	0.16% - 0.39% (2000- 2012), 2.1% (2000- 2016) * only losses, does not include gains, 0.214% (1995-2016)	percent loss yr ⁻¹	Remote Sensing	[35,40,47, 122]
Carbon stock	Mangrove (total)	7.29- 15.4	PgC	Remote Sensing, Extrapolation	[21, 67, 123]
	Mangrove (aboveground)	1.75- 2.83	PgC	Remote Sensing, Extrapolation	[63, 123]
	Mangrove (belowground)	2.6 - 6.4 (1 meter), 11.2- 12.6 (2 meters)	PgC	Remote Sensing, Extrapolation	[21, 34, 67]
Carbon burial	Mangroves	22.5 - 34.4	Tg OC yr ⁻¹	Extrapolation	[24, 109, 124]
Emissions	Mangrove (total emissions)	0.01-0.52	PgC yr ⁻¹	Extrapolation, Remote Sensing	[19,48, 125]
	Mangrove (belowground emissions)	2 - 8.1	TgC yr ⁻¹	Remote Sensing, Extrapolation	[21]
CH₄ Flux	Mangrove	0.191	Tg CH ₄ yr ⁻¹	Extrapolation	[124]
Net Primary Productivity	Mangrove	0.5 - 1.5	PgC yr ⁻¹	Extrapolation	[44, 126, 127, 128]

3.1.2 Tidal Marsh and Flats:

In total, we found 47 papers relevant to carbon monitoring with remote sensing in tidal marsh and flat ecosystems. Tidal marshes and flats share several characteristics, including tidal inundation and a relatively low energy environment; they may be salt, brackish, or fresh water. These ecosystems provide carbon storage and other valuable ecosystem services [129]. Tidal wetlands, like mangroves, are carbon-dense systems providing some of the highest carbon burial rates [24]. Global estimates of salt marsh and tidal flat extents are 54,950 km² and 127,921 km², respectively [130, 131]. Freshwater tidal wetlands also exist with ~ 2,000 km² around the great lakes [132]. Due to the results of our review, this section's primary focus was on salt marshes. However, carbon accounting of freshwater tidal and non-mangrove forested tidal wetlands would benefit from remote sensing integration. Tidal ecosystems are changing due to anthropogenic drivers, including sea-level rise [133], coastal development [134], and reduced sediment input [131, 135-137]. Coastal wetlands can also be a variable source of methane emissions [138]. These emissions can be classified as anthropogenic in cases where built impoundments block tidal flow, leading to artificial freshening and enhanced methane emissions [139]. We have grouped our synthesis of the status of carbon monitoring in tidal marsh and flats into three sections: 1) carbon monitoring status, and 2) data and uncertainty.

Carbon Monitoring Status

Tidal marsh studies utilized earth observation data to constrain and upscale *in situ* data, predict biomass and soil organic carbon (SOC) stocks, and model productivity. Land-use change was a primary theme, including migration, invasion, and long-term monitoring. The most common carbon indicators were GPP and biomass. Other indicators included sedimentation, leaf area index (LAI), vegetation fraction, nitrogen, and gas fluxes [105, 140-142]. Temporal dynamics of spectral indicators of biomass, i.e., normalized difference vegetation index (NDVI), were explored in tidal flats, too [143, 144]. Most tidal system studies (n = 33) pertained to marshes dictating this section's focus.

GPP is a common carbon indicator for tidal systems (n = 8). MODIS combined with eddy covariance towers was used to predict GPP in tidal environments [145-147]. Less common were gas flux chambers and incubation [140, 144]. Feagin et al. [148,149] improved on the MOD17 GPP product with an ecosystem-specific model. Tidal inundation is a source of uncertainty within GPP estimation, and studies addressed the tidal stage with spectral index filtering and tidal modeling [144, 146, 150]. These studies primarily rely on MODIS at a minimum spatial scale of 250 m, biomass, derived from Landsat or other high-medium resolution sensors is often used to track finer scale change.

In the 1980s, tidal marsh AGB was first predicted with *in situ* spectral measurement and expanded to Landsat imagery [151-153]. Since those foundational studies, researchers have assessed other sensors' capacity

to predict AGB, including Worldview-2, Hyperion, UAS, lidar, MODIS, AVIRIS-NG, Planetscope, and data fusion [142,154-161]. A major limitation of biomass prediction in tidal marshes is the site and species-specific limitations of the modeling results. Studies have sought to address this limitation with model transfer but resulted in inaccurate predictions [158], though regionally trained models have been successful [162-164]. AGB prediction scope and accuracy have increased since the first modeling approaches, but scale and uncertainty limit their applicability to global carbon monitoring.

Tidal marsh change was a frequent research topic, including tracking invasive species [165], determining marsh migration [166], time-series change analysis [167], and multitemporal regional change [168]. Studies frequently upscaled carbon measurements with land-use maps [168-171]. Braun et al. [172] determined that geomorphic change can dictate whether and how freshwater coastal wetlands serve as sources or sinks for terrestrial carbon and how carbon stocks can fluctuate on a geologically rapid timescale. A few studies used remote sensing data to constrain *in situ* sampling with land-use maps [166, 173]. The lack of baseline data availability and a focus on local methods limited regional monitoring applications.

Data and Uncertainty

CMS has supported the development of the US coastal wetland greenhouse gas inventory [174]. In the contiguous US between 2006-2011, coastal wetlands emitted 10.3 Tg CO_{2e} yr⁻¹ (1.6 to 21.3 Tg CO_{2e} yr⁻¹), and a robust sensitivity analysis demonstrates major sources of uncertainty where remote sensing could improve the model, including coastal salinity classifications -- and resulting CH₄ emission categories -- and the depth of soil deposits lost to erosion [175, 176]. Improved predictions on the fate of soil carbon following marsh loss events could combine earth observations and additional ocean physical modeling. Carbon stock values are well constrained compared to the uncertainty of methane emissions and loss events [175-176]. So far, strategies for mapping US coastal wetland soil carbon stocks using nationally available soil and wetland maps have not outperformed simpler strategies of applying a single average value for carbon stocks. Holmquist et al. [176, 177] utilized an extensive soil core database to predict tidal marsh soil carbon to 1 m depth (0.72 PgC) within the CONUS. The study also showed a way to improve future mapping would be to generate maps based on environmental drivers that differentiate between organic and inorganic soils, differentiated by a threshold of 13% organic matter by dry mass. Elevation relative to the tidal amplitude [178, 179], and long-term rates of relative sea-level rise [180] could be potential predictors of carbon stock. These CMS funded studies demonstrate the need for connecting earth observations and models between land, wetland, and open water; further *in situ* data collection of environmental driver data such as salinity and tidal elevation; and the development of tidal marsh class and change products that can be applied globally.

Table 2. Global carbon monitoring values for tidal marsh and tidal flat systems from the literature. Tidal marsh and salt marsh were considered interchangeably. Tidal flat and unvegetated sediments were also considered interchangeable. Method refers to 4 categories, modeled, data synthesis, extrapolation (*in situ* combined with extent to upscale estimates), and remote sensing (mapping or predicting spatial heterogeneity for an indicator). When available uncertainty is reported 95% confidence intervals in parenthesis and standard error after \pm .

Carbon indicator	System	Value	Units	Method	Source
System extent	Tidal marsh	0.055	10^6 km^2	Field and remote sensing	[130]
	Tidal flats	0.128 (0.124–0.132)	10^6 km^2	Remote sensing	[131]
System extent change	Tidal marsh	Not available			
	Tidal flats	0.5	$\% \text{ yr}^{-1}$	Remote sensing	[131]
Carbon burial	Tidal marsh	0.028–0.070	PgC yr^{-1}	Extrapolation	[181]
	Tidal flats	0.126	PgC y^{-1}	Extrapolation (total coastal burial in unvegetated sediments)	[182, 183]
Carbon stock	Tidal marsh	1.84	PgC	Extrapolation	[108]
	Tidal flats	Not available			
Carbon Loss	Tidal marsh	0.016 (0.005–0.065)	PgC yr^{-1}	Extrapolation	[19]

	Tidal flats	Not available			
CH₄ Flux	Tidal marsh	0.85±0.32	TgC yr ⁻¹	Extrapolation	[184]
	Tidal flats	Not available			
Net Primary Productivity	Tidal marsh	0.17–0.42	PgC yr ⁻¹	Extrapolation	[181]
	Tidal flats	0.01±0.013	PgC yr ⁻¹	Extrapolation (unvegetated sediments)	[185]

1 Additionally, global carbon export from tidal marshes to estuaries is uncertain. The connection between
2 tidal marshes and coastal waters is a long-standing consideration. Teal [186] identifies outwelling as an
3 important potential component of the system, and its magnitude and role have been debated since [187]. The
4 magnitude of C export is highly variable, with tidal marshes being both a sink and a carbon source to coastal
5 waters [188]. Salt marshes export an estimated 3.3 Tg POC yr⁻¹, 14 Tg DOC yr⁻¹, and 29 Tg DIC to coastal
6 oceans [108]. Remote sensing of ocean color to estimate DOC and CDOM can discern spatial and temporal
7 patterns of tidal marsh export [189]. Gao et al. [145] explored the connection between tidal marsh productivity
8 and detritus export using *in situ* sampling of detritus. Monitoring coastal waters is a difficult remote sensing
9 task (see sections 3.1.3 SAV and 3.3.1 Continental shelf). The use of ocean color methods and fine-scale
10 satellite imagery could enhance the capacity to monitor C export from tidal marshes.

19 **3.1.3 Submerged Aquatic Vegetation:**

21
22 In total, we found 45 papers relevant to carbon monitoring with remote sensing in SAV with a primary
23 focus on seagrass. Seagrass is found along all continents except Antarctica and refers to seventy-two species,
24 including *Zostera marina*, *Posidonia oceanica*, *Thalassia testudinum*, and *Zostera noltei* [190]. Seagrass is
25 estimated to store 10-20% of the ocean's carbon within 0.2% of the total ocean area [24, 128, 191]. However,
26 seagrass extent decreased ~30% in the last century [192]. During deterioration, seagrass beds can release their
27 carbon into the atmosphere [193]. Improvements in mapping seagrass extent, structure, and carbon storage will
28 enable management by valuing and including seagrass beds in REDD+ type programs. We have grouped our
29 synthesis of the status of carbon monitoring in SAV into two sections: 1) carbon monitoring status and 2) data
30 and limitations.

38 **Carbon Monitoring Status**

40
41 Seagrass biomass is below the water's surface; therefore, atmospheric and coastal water conditions
42 influence mapping [191]. Similarly, temporal and spatial variability in water quality and depth hinder seagrass
43 identification [e.g., 194-198]. These difficulties can result in misclassification between seagrass and algae [198-
44 202]. Due to the remote sensing challenges, seagrass mapped extent is an order of magnitude less than modeled
45 extents [203, 204]. Consequently, scientists lack a global map of seagrass extent, and recent estimates are
46 uncertain (160,387-266,562 km²) [205]. Seagrass aboveground carbon stocks are even more uncertain due to
47 mapping error and regional, intraspecies, and interspecies variability in biomass [200, 204, 206, 207]. Globally,
48 two-thirds of seagrass living carbon (2.52±0.48 Mg C ha⁻¹) is belowground, and seagrass SOC is ~65 times
49 greater (165.6 Mg C ha⁻¹)[191].

50
51 Novel methods for linking remote sensing and *in situ* data have improved our understanding of seagrass
52 cover and carbon storage. For example, seagrass cover estimates from UAS and *in situ* images can bridge the
53
54
55
56
57
58
59
60

1 scale differences of AGB samples and remote sensing imagery [195,197, 198]. Seagrass extent mapped with
2 UAS imagery has been used to scale *in situ* carbon samples to the landscape by percent cover [208]. Zoffoli et
3 al. [209] used a linear model to predict biomass with *in situ* radiance (RMSE = 5.31 g m⁻²) and applied that to
4 Sentinel-2 imagery, successfully capturing seasonality. Modeling optical properties of seagrass has led to the
5 development of a model to estimate leaf area index that does not require *in situ* data [210, 211]. In addition to
6 satellite and aerial platforms, ship-based acoustic sensors can identify species [212] and estimate biomass [206].
7 Data fusion between ship-based sensors, satellites, and UAS has improved seagrass extent maps [213] and
8 benefit biomass mapping.
9
10
11
12
13
14

15 **Data and Limitations**

16
17 Mapping was the primary seagrass research topic reviewed due to the challenges of modeling seagrass
18 carbon and the need to address data gaps in known seagrass extent. These challenges have resulted in high
19 uncertainty in seagrass extent estimates (Table 3). For example, high-resolution imagery, informed by a species
20 distribution model, was used to manually digitize seagrass beds within a single bay, resulting in a 44% increase
21 in mapped seagrass extent [214]. Poursanidis et al. [215] map change between submerged vegetation and other
22 benthic substrate following the cyclone season. Both Landsat and Sentinel-2 have the capacity for regional to
23 global mapping of seagrass.
24
25
26
27
28
29
30
31
32
33
34
35
36
37
38
39
40
41
42
43
44
45
46
47
48
49
50
51
52
53
54
55
56
57
58
59
60

Table 3. Global carbon monitoring value for seagrass from the literature. Method refers to the categories, modeled, data synthesis, extrapolation (*in situ* combined with extent to upscale estimates), and remote sensing (mapping or predicting spatial heterogeneity for an indicator).

Carbon indicator	System	Value	Units	Method	Source
System Extent	Seagrass	confirmed: 0.15- 0.35; potential: 1.6*	10 ⁶ km ²	Extrapolation	[191, 203*, 205, 216]
System Extent Change	Seagrass	0.9% (1879- 1940), 7% (1990- 2006)	percent loss yr ⁻¹	Extrapolation	[217]
Carbon stock	Seagrass	4.2 - 8.4	PgC	Extrapolation	[191]
Carbon burial	Seagrass	48-112	TgC yr ⁻¹	Extrapolation	[128]
Emissions	Seagrass	0.014- 0.09	PgC yr ⁻¹	Extrapolation	[19, 191]
CH₄ Flux	Seagrass	Not Available			
Net Primary Productivity	Seagrass	0.06-1.94	PgC yr ⁻¹	Extrapolation	[181]

1 Additionally, higher spatial resolution sensors, such as Planetscope, have improved classification
2 accuracy compared to Sentinel-2 [198]. UAS imagery (< 5 cm) has shown the capability to map local seagrass
3 extent and carbon [208, 218]. Object-based methods help separate areas of similar seagrass cover, water quality,
4 and depth [213] but do not necessarily improve accuracy [218]. Recent advancements in acoustic measurements
5 of photosynthesis-derived oxygen bubbles [219] and tracking seagrass grazing animals [220] have increased
6 seagrass mapped extent. Furthermore, machine learning has improved seagrass bed identification [196, 221,
7 222]. Remote sensing methods, including object-based image analysis, machine learning, physics-based
8 modeling, and integration of multiple scales of training data, have improved carbon monitoring of seagrass.
9

16 Estimating seagrass carbon fluxes with remote sensing is difficult due to varying light, tides, currents,
17 water quality, [e.g., 193, 198, 204], and biogeochemical process (i.e., carbon fixation and CaCO_3 [202, 223-
18 226]), even with *in situ* CO_2 flux measurements [227]. Furthermore, the major drivers of sediment carbon
19 changes within regions from autochthonous to allochthonous based on seagrass canopy complexity, turbidity,
20 and wave environment, further complicating carbon flux monitoring [228]. Water depth is an important factor
21 in estimating seagrass carbon storage [228-230]. Thomas et al. [231] demonstrate a data fusion approach using
22 ICESat-2 and Sentinel-2 to map bathymetry in shallow, optically clear coastal water addressing a key data gap
23 in most optical seagrass mapping approaches. Carbon fluxes are challenging to monitor, but modeling and
24 remote sensing have improved our understanding of the biogeochemical processes and site characteristics
25 contributing to flux variability.
26

34 The carbon impacts of seagrass loss are hard to quantify due to a lack of precise mapping and carbon
35 storage information. Local estimates of seagrass loss range from highs of $\sim 2.8\% \text{ yr}^{-1}$ [192, 232] to lows of $1.2\% \text{ yr}^{-1}$
36 [207], and globally, since 1990, seagrass loss rate is estimated to be $\sim 7\% \text{ yr}^{-1}$ [24]. The major drivers of
37 seagrass loss are direct anthropogenic impacts [233-235] from boats, development, dredging, and marine
38 pollution [192, 236], as well as overgrazing due to alterations to the food web [237]. Marine heat waves due to
39 climate change can exacerbate seagrass loss [193, 238], and temperature increases are likely to drive future
40 losses [207]. Seagrass beds experience multiple stressors associated with water quality, temperature increases,
41 and overgrazing which can shift seagrass beds from stable ecosystems to rapid deterioration [193, 207, 218].
42 However, both improvements in water quality [208, 232, 239] and planting have successfully restored seagrass
43 and increased carbon storage and ecosystem services [240, 241]. High but uncertain loss rates and the success
44 of restoration necessitate improved remotely sensed and *in situ* quantification of seagrass baseline and change in
45 extent to facilitate its inclusion into carbon monitoring and offset programs.
46

56 3.2 Inland Wetlands:

57
58
59
60

1 In total, we found 55 papers relevant to carbon monitoring with remote sensing in mineral wetlands. We
2 found an additional 129 papers relevant to carbon monitoring with remote sensing in peatlands and 80 in
3 permafrost due to the current status and prevalence of the research themes we have separated these into two
4 sections. Wetlands are defined by vegetation type, hydrology, and soil properties [242] and classified in the US
5 based on hydrogeomorphic position and vegetation [243]. These landscapes are dynamic with highly variable
6 carbon fluxes, changing hydrology, and impacted by anthropogenic disturbance such as draining for agricultural
7 development and deforestation [29, 244]. Palustrine wetlands span organic soil peatlands to mineral soil saline
8 wetlands in arid regions [243]. By this definition, inland wetlands disproportionately contribute to carbon
9 storage, storing 30% (202-754 PgC) of the global SOC stock (1500 PgC) while only occupying 8-11% of the
10 land surface [11, 245, 246]. Due to the magnitude of carbon storage in inland wetlands, Nahlik and Fennessy
11 [246] referred to this carbon as “teal carbon.” However, there is a distinction within inland wetlands between
12 peatlands and mineral soil wetlands. Peatland is a general term used to describe a wetland with an organic soil;
13 however, the definition of an organic soil varies by country and region. We have grouped our synthesis of the
14 status of carbon monitoring in inland wetlands into two sections: 1) mineral wetlands and 2) peatlands and
15 permafrost.

26 3.2.1 Mineral Wetlands

27 As previously mentioned, wetlands are defined by vegetation, soils, and hydrology but remotely
28 mapping wetland extent requires indirectly associating these attributes with remote sensing data and introduces
29 additional uncertainty. The extent of wetlands is a long, sought-after metric and has changed greatly over time
30 [247]. The United States National Wetland Inventory (NWI) demonstrated that baseline mapping followed by
31 subsequent updated digitization from aerial imagery can be utilized to create robust wetland change estimates
32 [248]. Mineral wetlands are difficult to map due to their high diversity, hydrologically dynamic, and variable
33 size. These factors impact carbon monitoring uncertainty and increase from local to global extent (Figure 2).
34 Mineral wetland carbon is challenging to measure, upscale, and monitor over both large spatial extents and at
35 fine scales. Recent research has utilized time-series analysis of satellite imagery to estimate inundation extents
36 and hydroperiods and, therefore, a variable approximation of wetland extent at the site level [249, 250].
37 Ignoring temporal variability, lidar has been used to map wetland extent via landform delineation. Lidar has
38 been especially effective for mapping wetlands under a forested canopy [251, 252]. SAR has also been
39 increasingly used in wetland extent mapping research, e.g., using the L-Band frequency to detect inundation at
40 various spatial scales [253]. We have grouped our synthesis of the status of carbon monitoring in mineral
41 wetlands into two sections: 1) carbon monitoring status and 2) data and uncertainty.

56 Carbon Monitoring Status

Wetland belowground carbon is primarily determined with field-intensive surveys to collect soil core samples, e.g., the National Wetland Condition Assessment in the United States [246]. Remote sensing has been increasingly deployed to upscale field observations from sample points to the plot or study area scale. For example, distribution maps of soil carbon stocks have been created from soil core measurements using satellite imagery [254, 255]. Satellite imagery has also aided measurements of carbon accumulation in sediments [256, 257]. Other fine-scale approaches have used UASs and Ground Penetrating Radar [277, 258, 259]. Despite these advances, high uncertainty in soil carbon estimates from remote sensing remain due to a lack of consistent depth measurements, including the depth of the upper horizons where most carbon is stored and can differentiate more mineral soil wetlands from peatlands [246].

The prediction of carbon storage in AGB with remote sensing is well studied, particularly in forested ecosystems. For mineral wetlands, studies have used remote sensing to upscale plot-level data of AGB to wider extents, such as the watershed-scale [260-262] including forested riparian wetlands [263]. Lidar has been used extensively in forest biomass research, and mineral wetland applications are increasing [264]. Studies scale site-level aboveground carbon metrics from estimates of AGB or carbon through land-use maps and spectral indices from Landsat [265], MODIS [266], Hyperion [267], and commercial satellites [268]. Budzynska et al. [269] predicted other carbon indicators, e.g., LAI and % soil moisture, with SAR and optical data. Riegel et al. [264] estimated aboveground carbon using aerial lidar and aerial imagery. Productivity rates, including both GPP [270, 278] and NPP [261], have been measured and upscaled to local, regional, and global scales.

Carbon gas fluxes, in particular methane (CH_4) emissions, have been of interest in recent research for mineral wetlands [271]. Most of this research has focused on peatlands in northern latitudes with fewer measurements and less a focus on mineral soil mineral wetlands [242]. In terms of scale, CH_4 has been evaluated with remote sensing at the regional or country level by combining satellite imagery with process models [272]. Inundation detection has been a key component to broad-scale CH_4 mapping with many models using the Global Inundation Extent from Multi-Satellites (GIEMS) dataset [273, 274]. However, more recent research has used fine-scale, 3 m resolution satellite imagery to map inundation detection at the watershed scale to evaluate CH_4 fluxes [275]. Lu et al. [276] used eddy covariance data from flux towers to demonstrate that mineral wetlands are net sinks and identify a need to incorporate remote sensing to predict CO_2 flux spatially.

Data and Uncertainty

Global assessment of mineral wetland carbon is limited by *in situ* carbon measurements and wetland map coverage. Recent assessments of global wetland coverage have utilized coarse-scale inundation mapping downscaled by topographic metrics [277, 279]. However, inundation approaches do not distinguish wetland types, e.g., these maps often include peatlands (Section 3.2.2) and mineral wetlands. Thus, the best-estimated extent comes from Lehner and Döll [280] and the Global Lakes and Wetlands Database (GLWD), which

1 estimated that non-peatland marshes, swamps, and forested wetlands cover 3.7×10^6 km² or ~2.5% of the
2 terrestrial land surface [13].
3
4

5 Global scale carbon measurements have yet to account for these changes in areal extent estimates. For
6 example, Bridgham et al. [11] used an average of two older sources [281, 282] for freshwater mineral soil
7 wetland area (2.315×10^6 km²) to upscale carbon burial, carbon soil stock, and CH₄ flux (Table 4). Similarly,
8 Roehm [283] utilized two older sources [284, 285] to combine areal extent estimates of northern and tropical
9 marshes and swamps (3.5×10^6 km²) to upscale NPP and CO₂ flux (Table 4). This latter estimate is closer to the
10 Lehner and Döll [280] estimate than the one used in Bridgham et al. [11]. Carbon monitoring research interest
11 in CH₄ is high due to its global warming potential. Thus, the global assessment of a CH₄ flux has been parsed by
12 wetland type and separated from peatlands [274].
13
14
15
16
17
18
19
20
21
22
23
24
25
26
27
28
29
30
31
32
33
34
35
36
37
38
39
40
41
42
43
44
45
46
47
48
49
50
51
52
53
54
55
56
57
58
59
60

Table 4. Global carbon monitoring values for inland wetlands from the literature. Method refers to categories: modeled, extrapolation (*in situ* combined with extent to upscale estimates), data synthesis, and remote sensing (mapping or predicting spatial heterogeneity for an indicator).

Carbon indicator	System	Value	Units	Method	Source
System extent	Global Inland Wetlands on Alluvial Soils	3.7	10 ⁶ km ²	Remote Sensing	[13, 280]
	North America Inland Mineral Soil Wetlands	0.93	10 ⁶ km ²	Mixed	[242]
System extent change	Global Long-term (Pre-1900s to 2000)	-0.39	% yr ⁻¹	Extrapolation	[29]
	Global Short-term (1990 to 2000s)	-0.48	% yr ⁻¹		
	Total loss of North America Inland Mineral Soil Wetlands	28.62	%	Extrapolation	[242]
Carbon burial (sediment accumulation)	Inland Freshwater Mineral Soil Wetlands	39±39	TgC yr ⁻¹	Extrapolation	[11]
Carbon stock (Soil)	Inland Freshwater Mineral Soil Wetlands	46±9	PgC	Extrapolation	[11]
	North America Inland Mineral Soil Wetlands	29.3	PgC	Mixed	[242]
Carbon emissions (CO₂ Flux)	Inland Freshwater Mineral Soil Wetlands	2.2	PgC yr ⁻¹	Extrapolation	[283]
Net Ecosystem CO₂ Exchange (Net CO₂ flux)	North America Inland Mineral Soil Wetlands	-64.3	TgC yr ⁻¹	Mixed	[242]
CH₄ Flux	Inland Freshwater Mineral Soil Wetlands	68±68	TgC yr ⁻¹	Remote Sensing and Modeling	[11]

1		North America Inland Mineral Soil Wetlands	25.2	TgC yr ⁻¹	Mixed	[242]
2						
3						
4	Net Primary Productivity	Inland Freshwater Mineral Soil Wetlands	3.2	PgC yr ⁻¹	Extrapolation	[283]
5						
6						
7						
8						
9						
10						
11						
12						
13						
14						
15						
16						
17						
18						
19						
20						
21						
22						
23						
24						
25						
26						
27						
28						
29						
30						
31						
32						
33						
34						
35						
36						
37						
38						
39						
40						
41						
42						
43						
44						
45						
46						
47						

3.2.1 Peatlands and Permafrost

Peatland extent comprises ~3% of the globe's terrestrial area [286], and their carbon stock is estimated to be between 528–600 Pg [287], representing 30% of the global belowground soil organic C stock [288-290]. Generally, peatland refers to a class of wetlands where the long-term rate of primary production is greater than the decomposition rate and losses from other sources such as wildfire and dissolved carbon export [291]. Thus, peatlands have soils with deep accumulations of organic matter, but the minimum thickness necessary to be considered peat varies significantly (~30-50 cm) [286, 291]. The accrual of peat over millennia leads to the formation of deep peat deposits, which may reach depths of 15–20 m [292-294]. We discuss peatlands by bioregion (tropical, temperate, and boreal). Considering peatlands by climatic region is necessary due to the latitudinal gradient in carbon accumulation, with colder regions having higher peat accumulation rates to a point [295, 296], also higher in tropical mountain peatlands [297]. We have grouped our synthesis of the status of carbon monitoring in peatlands into five sections: 1) tropical peatlands, 2) temperate peatlands, 3) boreal peatlands and permafrost, 4) peatland fires, and 5) data and uncertainty.

Tropical

Tropical peatland carbon indicators included AGB, degradation, subsidence, and canopy height. Southeast Asia ($n = 34$) was the primary focus of tropical peatland research, with additional studies focused on South America and Africa. South American studies mapped carbon stocks [298-301], extent and degradation [302], and mountain peatland stocks using SAR and multispectral imagery [303, 304]. In Africa, research focused on mapping the extent, depth [305] and estimating carbon stocks [306]. In Southeast Asia, degradation, loss, and recovery were major research topics enabled by lidar, SAR, and multispectral imagery. Studies have used lidar to detect illegal logging and carbon sequestration [307], map peat depth [308], and estimate AGB for tropical peatlands [309]. Minasny et al. detail an open data and mapping methodology with the ability to predict peat depth at a lower cost than lidar [310]. SAR particularly useful in tropical peatlands due to cloud and forest canopy penetration and its sensitivity to inundation and biomass [291, 298]. SAR applications included dinSAR to map subsidence across Southeast Asia [311] and predict AGB [312]. Studies have addressed remote sensing limitations by using multiple satellites to expand spatial and temporal coverage of fires [313] and the utilization of lidar to expand training data [312]. Despite the significant research interest, tropical peatlands lack regional and global scale monitoring due in part to data availability, extent uncertainty, and resources.

Temperate

Historically, temperate peatlands have frequently been managed for fuel, drained for agriculture, or other land-use [289, 314, 315]. Temperate peatland indicators included GPP [316], water table dynamics [317], erosion [318], disturbance [319], peat depth [320], and moisture [316]. Due to the prevalence of past

1 anthropogenic disturbance, restoration and recovery are common research topics [321-324]. High-resolution
2 imagery is common for site-scale studies, including satellite [318, 325, 326], UAS [327], aerial [328], and
3 handheld spectrometers [316]. Aitkenhead and Coull [320] conducted a regional carbon monitoring system
4 creating a national map of peat depth and Scotland's carbon content. The variety of temperate peatland
5 vegetation and the importance of subsurface carbon stocks are challenges for regional and global monitoring.
6
7
8
9

10 **Boreal and Permafrost Peatlands**

11
12 The boreal and tundra regions (n =35) are data-poor due to remoteness and the short field season
13 limiting *in situ* data collection. There are also significant human development pressures in parts of the boreal
14 zone for petroleum exploration, mining, forestry, agriculture, and infrastructure operations. Even low impact
15 disturbances such as seismic lines will increase the fragmentation of wetlands and have ecological impacts
16 [329]. Most degraded peatlands are tropical [289] but boreal peatlands and permafrost will change significantly
17 with warming and changes to precipitation [330].
18
19
20
21
22

23
24 Optical remote sensing data in boreal environments is limited due to sun angle, cloud cover, and the
25 short growing season [331]. The floristic similarity between peatlands and non-peatland ecotypes makes
26 identifying landform and hydrology with active sensors particularly important. The focus on topography and
27 landform included identifying permafrost peat mound degradation with aerial and high-resolution imagery
28 [332], classifying boreal bogs with microtopographic variation from lidar [333], mapping thermokarst lakes
29 with spectral imagery [334, 335], detecting freeze thaw dynamics with SAR [336], detecting permafrost extent
30 with electromagnetic imaging [337], and mapping lake extent with multispectral imagery [338]. An integration
31 of multi-season SAR and multispectral imagery was complementary in detecting vegetation and hydrologic
32 differences in bogs versus fens in the boreal zone [291, 339]. Carbon monitoring efforts included modeling gas
33 fluxes [271, 340, 341], upscaling *in situ* emission estimates with land cover maps [334, 342-344], and peat
34 extent [345]. Major change drivers within the system include increasing temperatures [335,346-348] and fire
35 [349, 350]. Boreal systems are critical for understanding the global carbon cycle, and unique challenges to *in*
36 *situ* and remote sensing data collection are being addressed by science programs such as the NASA Artic-
37 Boreal Vulnerability Experiment (ABoVE) [351].
38
39
40
41
42
43
44
45
46
47
48

49 **Fires**

50
51 The global importance of peatland fires in Southeast Asia has long been acknowledged, with peak yearly
52 emissions equaling 13-40% of the mean annual global carbon emissions from fossil fuels [23]. Earth
53 observation has enabled and verified peatland fires. Page et al. [23] primarily used fire extent mapped from
54 Landsat to understand peatland fires carbon emissions (2002). Lidar has been used to map fire scars and burn
55 depth improving emission estimates [352]. Emission estimates and burn area models have used satellite-derived
56
57
58
59
60

peatland fire data from the Global Fire Emissions Database for verification [353-355]. SMAP soil moisture data has been used to provide fire warnings, predict burn area [356], and as an input in emission models [357]. Drought can worsen emissions from forest fires within temperate/subtropical peatlands (0.32 PgC)[358]. Thus, earth observation is critical for modeling and verifying this important source of CO₂ emission. CMS has supported several fire mapping efforts of which peatlands are the focus [359] or included in more general fire data [360].

Fires in permafrost regions are also a major climate concern with remote sensing monitoring applications. Remote sensing has identified fires as the most prevalent disturbance in the permafrost region [361], leading to widespread permafrost thawing [362]. SAR has been used to track subsidence following vegetation loss in permafrost regions, including subsidence of 0.5-3 cm yr⁻¹ in deforested areas [363] and the rapidly developed thermokarst following fires with rates of subsidence up to 6.2 cm yr⁻¹ [364]. Studies have used SAR interferometry to model recovery and loss estimating that 4 m of permafrost is lost in a fire event and recovery takes up to 70 years [365]. For wildfire effects, algorithms were developed for assessing peat burn severity (depth) using Landsat-5 [294] and Landsat-8 [366]. Projections suggest rapid thawing will release 60-100 PgC, and gradual thaw regions will release another 200 PgC by 2030 [367].

Data and Uncertainty

Globally, peatlands represent a massive SOC stock (Table 5) and a remote sensing challenge due to their disparate data needs and global range. Peatland extent is ~4.0106 x 10⁶ km² and 4.5104 x 10⁴ km² in the northern and southern hemispheres, respectively [288, 291]. Boreal regions of the northern hemisphere are 25-30% peatland and comprise most of the global extent [291, 368]. Tropical peatland carbon (88.6 Pg) is estimated to be 15% of the global peatland carbon, with boreal and temperate peatland carbon estimated to be 521.4 Pg [369]. Temperate peatland carbon is understudied and as a result has high uncertainty in the carbon estimates [370]. The area of tropical peatlands is uncertain (387,201 to 657,430 km²), and the largest area (56%) and most of the carbon stock (77%) are in Southeast Asia [371], followed by the Amazon basin [372]. Africa's lowland peatland area is largely unknown except for the Congo Basin [306]. Tropical alpine peatlands are numerous in the Andes, many islands, and Africa [291, 373, 374]. Permafrost peatlands are estimated to contain 277 PgC and are changing rapidly due to global warming and fire [375-377]. The carbon store within the permafrost region is estimated to be ~1300 Pg (1100-1500 Pg) with 500 Pg within the active layer [378].

Table 5. Existing global carbon monitoring indicator values for peatlands and permafrost. Method refers to the categories, modeled, data synthesis, extrapolation (*in situ* combined with extent to upscale estimates), and remote sensing (mapping including remote sensing derived spatial heterogeneity). No isolated values for CH₄ flux or carbon export found.

Carbon indicator	System	Value	Units	Method	Source
System extent	Total Peatlands	4.2	10 ⁶ km ²	Various	[286]
	Tropical Peatlands	0.387-1.7	10 ⁶ km ²	Various	[371, 379]
	Temperate /Boreal Peatlands	4.06	10 ⁶ km ²	Various	[288]
	Permafrost	22.0	10 ⁶ km ²	Modeled	[380]
System Extent Change	Peatlands	0.5	% yr ⁻¹ (1990-2008)	Various methods	[13, 381]
Carbon burial	Peatlands	0.14±0.007	PgC yr ⁻¹	Extrapolation	[382]
	Tropical Peatlands	0.02	PgC yr ⁻¹	Extrapolation	[288]
	Temperate/Boreal Peatlands	0.09	PgC yr ⁻¹	Extrapolation	[288]
	Peatlands				

1		Permafrost	-0.55	PgC yr ⁻¹	Modeled	[383]
2						
3	Carbon stock	Tropical peatlands	81.7–91.9	PgC	Extrapolation	[369]
4		Temperate/Boreal	473–621	PgC	Various	[288]
5		Peatlands				
6		Permafrost	1700	PgC	Extrapolation	[9]
7	Carbon emissions	Tropical peatlands	1.26±0.77 (includes CH ₄)	Pg CO _{2e} yr ⁻¹ (2015)	Extrapolation	[384]
8		Temperate/Boreal	0.27±0.03	Pg CO _{2e} yr ⁻¹ (2015)	Extrapolation	[384]
9		peatlands	(includes CH ₄)			
10		Permafrost	Not available			
11						
12						
13						
14						
15						
16						
17						
18						
19						
20						
21						
22						
23						
24						
25						
26						
27						
28						
29						
30						
31						
32						
33						
34						
35						
36						
37						
38						
39						
40						
41						
42						
43						
44						
45						
46						
47						

3.3 Inland Waterbodies:

3.3.1 Lakes and Ponds

In total, we found 64 papers relevant to carbon monitoring with remote sensing in lakes and ponds. Freshwater lakes are an important component of the global carbon cycle, but this has not always been acknowledged [385-390]. This oversight is primarily due to the small fraction of the earth's surface area covered by lakes, the large number, the diversity of freshwater lake type, and the complex carbon cycle of individual lakes [385, 387, 388, 390]. Recent work suggests that the carbon cycle of individual lakes can vary significantly across time and space depending on thermal stratification, allochthonous loading, trophic state, and degree of anthropogenic influence [15, 389, 391, 392]. Large lakes are common in the boreal region and freshwater lakes play a crucial role in transforming and storing carbon [390]. We have grouped our synthesis of the status of carbon monitoring in lakes into two sections: 1) carbon monitoring status and 2) data and applications.

Carbon monitoring status

Phytoplankton photosynthesis is the primary process by which carbon dioxide is fixed from the water column and overlying atmosphere. Remote sensing applications to estimate phytoplankton photosynthesis or primary production in the marine environment are numerous (See Ocean and Shelves 3.4). However due to the spatial variability and optical complexity, applications to freshwater systems are scarce. Advances in remote sensing platforms and algorithm development have allowed for the characterization of phytoplankton abundance and productivity in various freshwater environments [e.g., 393-398]. Remote sensing approaches hold much promise for sampling many lakes on the planet [399] and understanding global trends in phytoplankton [400].

Globally, freshwater lakes exhibit a wide range in size and shape, creating a unique challenge for applying remote sensing methods. Accurate estimates of freshwater phytoplankton biomass require remote sensing data with specific wavelengths associated with spectrally narrow chlorophyll-*a* absorption features and high signal-to-noise ratios [401]. Satellite sensors with these spectral requirements often target oceans and typically have a coarser spatial resolution (300m-1000m), limiting their ability to observe smaller freshwater features. These requirements limit how carbon monitoring of freshwater lakes. The Plankton, Aerosol, Clouds, ocean Ecosystem (PACE) will address spectral needs of ocean color remote sensing but is still too coarse (<1 km²) to discern small-scale waterbodies [402]. Instead, data fusion using high-resolution imagery and ocean color remote sensing are likely necessary to improve mapping of phytoplankton biomass in lakes and ponds.

Carbon fixation

Several recent works have used a mechanistic carbon fixation model adapted for use in the Laurentian Great Lakes [397, 398] to estimate carbon fixation in the world's large lakes [403]. Additionally, a simple depth integrated model approach (DIM) was refined to estimate growing season carbon fixation of ~80,000 freshwater lakes [404]. The DIM approach relies on the light-utilization index, which relates to latitude providing a straightforward method to estimate carbon fixation rates when minimal limnological data is available. The marine standard Vertically Generalized Production Model has also been applied to estimate carbon fixation in large lakes [410]. Remote sensing approaches to estimate freshwater phytoplankton carbon fixation have been developed and applied for small lakes [411, 412].

Lake carbon budgets are highly dependent on carbon fixation rates, yet these rates are unknown for most lakes. McDonald et al. [413] estimated that there are over 60 million lakes. Estimating carbon fixation in all these lakes would be impossible with *in situ* methods. Therefore, the development of remote sensing methods to estimate carbon fixation rates is a current focus. Still, global-scale estimates remain elusive due to the lack of readily available remote sensing products appropriate for optically and spatially complex inland lakes. However, several recent works have estimated global scale freshwater carbon fixation for satellite observable lakes [403, 404]. These works also examined carbon fixation on multiple temporal scales ranging from a single year growing season snapshot for ~80,000 lakes [404] to a 15-year time-series for the world's eleven largest lakes [403]. The latter work revealed significant changes in carbon fixation for several lakes, likely in response to changes in climate. The use of remote sensing to understand spatial variability across lakes is lacking in many of the existing global carbon monitoring values (Table 6).

Table 6. Global carbon monitoring values for lakes. Method refers to the categories, modeled, extrapolation (*in situ* combined with extent to upscale estimates), data synthesis, and remote sensing (mapping including remote sensing derived spatial heterogeneity).

Carbon indicator	System	Value	Units	Method	Source
System extent	Lakes	5	10 ⁶ km ²	Remote sensing	[405]
Carbon burial (sediment accumulation)	Lakes and Reservoirs	0.15 (0.06-0.25)	Pg CO ₂ -C yr ⁻¹	Modeling	[406]
Carbon fixation	Lakes	0.376	PgC yr ⁻¹	Remote sensing	[404]
Carbon fixation	Lakes	1.3	PgC yr ⁻¹	Modeling	[407]
Carbon storage	Lakes	820	PgC	Extrapolation	[385, 408]
Carbon Flux	Lakes	0.75- 1.65	PgC yr ⁻¹	Extrapolation	[385]
CH ₄ Flux	Lakes	71.6	Tg CH ₄ yr ⁻¹	Extrapolation	[409]

1 Additionally, common carbon monitoring measurements in lakes include chlorophyll-*a*, DOC, CO₂ flux,
2 and GPP. Kuhn et al. [414] calculated boreal lake GPP with aerial and satellite imagery and verified the result
3 with *in situ* measurements. Remote sensing combined with *in situ* measurements clarified that boreal lakes may
4 have a limited role in carbon mineralization [415]. Lake color in the region has been tracked with the satellite
5 record identifying increased connection with the surrounding landscape [416]. The combination of
6 electromagnetic imaging and satellite imagery has mapped the temporal dynamics of hydrological connectivity
7 between boreal lakes and permafrost [417]. Remote sensing is critical for understanding the effect of climate
8 change on the carbon cycle in permafrost regions.

15 Methods to estimate chlorophyll-*a* concentrations range from empirical and semi-analytical approaches
16 and, more recently, machine learning and artificial intelligence-based techniques (Reviews in [418, 419]). Initial
17 work has been done to estimate global freshwater lake chlorophyll concentrations [399]. However, more robust
18 methods to account for the varying optical complexity of lakes should be developed. The GloboLakes initiative
19 has developed a freshwater chlorophyll retrieval algorithm, generated a global time-series of chlorophyll
20 concentrations for ~1000 lakes, and provided monitoring products for the ESA Climate Change Initiative [420].

26 DOC and CDOM are also frequently monitored in lake environments with remote sensing. CDOM
27 algorithm comparisons found that remote sensing algorithms did not predict the highs or lows well [421], but
28 continued algorithm refinements are promising [422]. Brezonik et al. [423] demonstrated a strong relationship
29 between CDOM and DOC but were cautious about assuming a consistent relationship. Geographically diverse
30 study sites suggest the possibility of applying these methods globally [424].

36 CO₂ flux has been estimated with partial pressure of CO₂ (*p*CO₂) in coastal oceans [425]. Simple
37 relationships have also been developed between bio-geochemical properties and freshwater carbon flux through
38 comparisons with Eddy-covariance flux tower measurements [426]. While these methods show promise,
39 applications in freshwater lakes are infrequent. Similarly, very few efforts have been made to fully characterize
40 carbon fractions in freshwater systems, although initial efforts seem promising [427] and are worthy of
41 continued research.

47 3.3.2 Rivers

50 In total, we found 33 papers relevant to carbon monitoring with remote sensing of rivers. Rivers and
51 streams receive a large amount of carbon from terrestrial ecosystems and actively cycle carbon through them by
52 outgassing CO₂ and CH₄ into the atmosphere, burying particulate carbon in the riverbed, and exporting organic
53 and inorganic carbon into estuaries and coasts [15, 385, 428-435]. Meanwhile, the flowing waters in river
54 networks link the carbon cycle in non-flowing (or slowly flowing) waterbodies and wetlands. Here we
55 summarize and discuss carbon monitoring of rivers and streams based on the literature. We do not include
56
57
58
59
60

1 terrestrial carbon inputs due to the lack of direct observations as that carbon flux is often inferred through mass
2 balance analysis by assuming no accumulation of carbon in inland waters [436]. We have grouped our synthesis
3 of the status of carbon monitoring in rivers into three sections: 1) carbon export, 2) outgassing of CO₂ and CH₄,
4 and 3) carbon burial.
5
6

8 **Carbon Export**

9
10 Riverine C export is well constrained using global streamflow discharge and measurements of aqueous
11 carbon concentrations [385, 434]. Stream gauge and water quality data can provide the necessary data for the
12 extrapolation of C export at continental scales [437] and global scales [438, 439]. Mass balance analysis and
13 data initiatives have refined global estimates [15, 440]. Many studies have established empirical relationships
14 between surface organic C concentrations (e.g., POC, DOC, and phytoplankton) and remote sensing data across
15 various aquatic systems, including river reaches [e.g., 441-448].
16
17
18
19
20

21 Remote sensing derived C concentrations have been used to estimate riverine export to estuaries and
22 coasts. For example, Chunhock et al. [449] calculated river-to-ocean fluxes with remote sensing derived DOC
23 concentrations near the river mouth in conjunction with discharge data. Liu et al. [450] used Landsat-derived
24 POC concentrations and monthly river discharges near the mouth of the Yangtze River to assess long-term
25 patterns of riverine POC fluxes from 2000-2017. Successful application of remote sensing methods requires
26 continual monitoring of constituent concentrations and a large enough water body (e.g., river with a width
27 larger than 90m) to be observed from satellite imagery [451], making it challenging to apply them in small
28 rivers and streams. High-resolution UAS imagery was applied to detect water quality parameters in small
29 rivers/streams, such as chlorophyll-*a*, Secchi disc depth, and turbidity, with limited success [452, 453].
30 Therefore, carbon monitoring of rivers and small streams with remote sensing requires further research and
31 technological advancement.
32
33
34
35
36
37
38
39
40

41 **Outgassing of CO₂ and CH₄**

42
43 In the past two decades, quantification of regional and global CO₂ outgassing from streams and rivers
44 has made great progress. Richey et al. [454] in a pioneering study of regional-scale CO₂ outgassing in the
45 Amazon River basin, used field observations to estimate CO₂ emissions per unit area in mainstem and
46 floodplains. They used JERS-1 L-band SAR to estimate areal coverage and inundation status of rivers and
47 floodplains (>100m in width) and developed empirical relationships for smaller streams. Since then, multiple
48 studies have continued to use remote sensing to refine estimates of CO₂ emissions from the running waters in
49 the Amazon. For example, Johnson et al. [455] constrained their analysis to seasonally inundated areas based on
50 SAR detected high and low water periods. De Fátima et al. [456, 457] used a 100 m DEM to improve the
51 surface area calculation. Recently, Sawakuchi et al. [432] used model estimates of surface area to estimate
52 outgassing in the lower Amazon River Basin. These advances have resulted in an estimate of ~0.96 PgC yr⁻¹
53
54
55
56
57
58
59
60

1 CO₂-C outgassing from the rivers and streams in the Amazon [434], nearly double the estimate by Richey et al.
2 [454], which included both rivers and floodplains. In another salient example of regional carbon accounting,
3 Butman and Raymond [458] used numerous USGS field observations and the National Hydrography Dataset
4 plus (NHDplus) [459] river networks to estimate surface water area. These studies demonstrate the need for
5 high-resolution river networks and water surface area data to monitor CO₂ outgassing from rivers reliably.
6
7

8
9
10 At the global scale, Richey et al. [454] upscaled their estimates of CO₂ outgassing in the Amazon River
11 Basin to calculate outgassing from rivers and floodplains in the global humid tropics. This was much higher
12 than contemporary estimates not informed by remote sensing [385, 460]. Battin et al. [461] analyzed the net
13 heterotrophy (respiration - GPP) of 130 rivers and streams and extrapolated the results to the global scale by
14 multiplying average emissions of streams and rivers by global surface area. Utilizing remote sensing data
15 including hydrological data derived from the SRTM, Raymond et al. [431] reported a 1.8 PgC yr⁻¹ of CO₂
16 outgassing from global streams and rivers. Recently, the global relevance of dry inland waters to the carbon
17 cycle has been identified [462-464], representing unreported CO₂ emissions [431].
18
19
20
21
22
23

24
25 Progress has also been made for accounting CH₄ emissions from global freshwaters. Bastviken et al.
26 [409] synthesized and calculated average areal field observations of CH₄ fluxes of various types of freshwaters
27 (including lakes, reservoirs, wetlands, and lakes) by different latitudes to estimate a total of 103.3 Tg CH₄ yr⁻¹,
28 of which rivers contributed ~1.5 Tg CH₄ yr⁻¹ (or ~10 Tg C (CO₂-e) yr⁻¹). The scarcity of observed data points
29 and the exclusion of small streams in the river surface area likely contributed to low river flux [465]. Overall,
30 CH₄ emissions from streams and rivers are less studied than CO₂ emissions.
31
32
33
34
35

36 In general, current riverine CO₂ and CH₄ outgassing estimates are subject to large uncertainties due to
37 difficulty in accurately measuring surface water area, partial pressure of CO₂, and gas exchange rates [428].
38 More field data and high spatial resolution remote sensing are needed to refine surface water area and gas
39 exchange rates. The global studies rely on river networks primarily based on NASA's global SRTM DEM at 90
40 m. In the US, 10 m DEM-derived high-resolution hydrological data is available [466]. Still, higher resolution
41 lidar derived DEM with (~2 m) can improve river network delineation [467]. Additionally, SAR, multispectral,
42 and hyperspectral data collected from aerial, satellite, and UAS, have been used to map surface water area and
43 characterize river channel morphology [468-471]. Although those applications achieved noticeable success,
44 upscaling them to continental or global scales face many challenges [472].
45
46
47
48
49
50
51

52 The Surface Water and Ocean Topography (SWOT) satellite mission [473], will measure terrestrial
53 water at a spatial resolution of 50 m and provide river vector products that represent reaches with a collection of
54 nodes spanning every 200 m [474, 475]. Researchers estimate gas exchange coefficient with remote sensing
55 derived width and water surface slope measurements, while surface water area can be multiplied with estimated
56
57
58
59
60

1 gas emissions per unit area to estimate total C degassing. Note that small streams are difficult to discern at
2 SWOT's spatial resolution; therefore, data fusion of SWOT river vectors with high-resolution DEMs holds
3 promise to provide more accurate data regarding rivers and streams.
4

6 **Carbon Burial**

8 Global estimates of aquatic organic C burial are between 0.15 and 1.6 Pg CO₂-C yr⁻¹ [406, 476]. These
9 studies focus on sedimentation in reservoirs, lakes, and wetlands, without explicit global-scale C burial in rivers
10 and streams. Watershed models that explicitly integrate terrestrial and aquatic carbon cycling processes are
11 being developed to quantify the burial of particulate OC in rivers. For example, Qi et al. [477, 478] incorporated
12 OC deposition, resuspension, and diagenesis processes in the Soil and Water Assessment Tool (SWAT) and
13 showed that a significant fraction of terrestrially originated POC is deposited on the bed of small streams and
14 further decomposes into CO₂ and CH₄. These results indicate that the inclusion of C burial in rivers and streams
15 would improve the accounting of global C burial in inland waters. High-resolution riverine networks will be
16 critical for updating and improving existing carbon monitoring (Table 7). Additionally, certain carbon pathways
17 are relatively unknown, e.g., how much carbon enters wetlands and subsequently enters rivers.
18
19
20
21
22
23
24
25
26
27
28
29
30
31
32
33
34
35
36
37
38
39
40
41
42
43
44
45
46
47
48
49
50
51
52
53
54
55
56
57
58
59
60

Table 7. Global carbon monitoring values for rivers. Method refers to three broad categories, modeled, extrapolation (*in situ* combined with extent to upscale estimates), data synthesis (combination of data sources and methods), and remote sensing (mapping including remote sensing derived spatial heterogeneity).

Carbon indicator	System	Value	Units	Method	Source
System extent	Rivers and streams	0.773±0.08	10 ⁶ km ²	Remote sensing/modeling for rivers less than 90 m in width	[479]
Carbon input	Inland waters	2.7–5.1	PgC yr ⁻¹	Data synthesis	[15, 386, 428, 434]
Carbon export to estuaries	Rivers and streams	1.06	PgC yr ⁻¹	Data synthesis	[440]
Carbon flux to atmosphere	Rivers and streams	1.8±0.25	PgCO ₂ yr ⁻¹	Extrapolation	[431]
CH₄ Flux	Rivers and streams	~1.5	Tg CH ₄ yr ⁻¹	Extrapolation	[409]

3.4 Ocean and Shelves:

In total, we found 102 papers relevant to carbon monitoring with remote sensing of oceans. Earth observation-derived oceanic carbon indicators have been used to characterize a variety of carbon-related properties and processes. The global oceans represent a substantial sink for anthropogenic CO₂, accounting for more than 40% of the global sink of anthropogenically produced CO₂ (Figure 1) [9]. Moreover, the magnitude of the ocean sink appears to be increasing with the buildup of CO₂ in our planet's atmosphere. Approaches to estimate the ocean sink have relied on a combination of global ocean biogeochemistry models (GOBMs) along with comparison to observation-based estimates, including *p*CO₂-based interpolations. These interpolations, in some cases, have relied on remote sensing products as described in Rödenbeck et al. [480], involving regression to remotely sensed external drivers such as sea surface temperature (SST), sea surface salinity (SSS), and chlorophyll-*a* concentration. Many of the GOBMs also use remote sensing for model implementation and model-data comparisons [e.g., 481-483].

Several studies have examined regional time-series changes in values averaged over the 17 biomes of Fay and McKinley [484], which were defined based on various environmental datasets including the SeaWiFS chlorophyll-*a* product. These times-series have revealed substantial interannual and decadal variability as well as regional patterns in atmosphere-ocean CO₂ fluxes [9, 485, 486]. Interannual and multi-year variability can be related to climate oscillations including El Niño as well as decadal scale oscillations in the North Pacific and Southern Ocean, as described by Liao et al. [487] in a NASA CMS-supported study. The Liao et al. [487] simulations expanded on prior observational studies that have identified negative anomalies in eastern Pacific surface *p*CO₂ during El Niño events as well as other seasonal and interannual variations and regional patterns [e.g., 480, 488-490]. More recently, Watson et al. [491] provided a revised estimate of observation-based CO₂ atmosphere-ocean fluxes, accounting for temperature gradients between the surface and sampling at a few meters' depth, or for the effect of the cool ocean surface skin. Their estimate resulted in an upward revision of the net flux into the oceans of 0.8-0.9 PgC yr⁻¹, with a best estimate for the period 1994-2007 of -2.5±0.4 PgC yr⁻¹ (where negative values denote net uptake into the ocean) that is consistent with ocean interior inventory increases [492]. This estimate is considerably less than that of Wang et al. [493], who applied an atmospheric inversion approach to GOSAT and *in situ* observations of atmospheric CO₂ and derived estimates for ocean fluxes of -3.1±0.5 PgC yr⁻¹. Considerable progress has been made in the assessment of oceanic CO₂ flux, with different approaches converging.

Sedimentation/Benthic-Pelagic Coupling

Satellite observations have also been used to observe coupling between surface and benthic biogeochemical processes with implications for carbon transport from the surface to the deep ocean. Waga et al.

[494] found evidence of linkages between surface phytoplankton size structure, derived with ocean color proxies, and deep ocean benthic macrofaunal distributions. Corliss et al. [495] reported lower benthic foraminiferal diversity in North Atlantic latitudes coinciding with high seasonality in primary production as inferred from SeaWiFS satellite imagery. Surface patterns of SeaWiFS-derived chlorophyll-*a* were also found to be related to regional differences in macrobenthic community structure in the deep Gulf of Mexico [496]. Satellite observations have also been used to assess transport to offshore waters of unattached benthic algae and found to be associated with a substantial carbon footprint [497]. These studies highlight the apparent coupling between surface ocean carbon dynamics, as observed by remote sensing, and deep ocean biogeochemistry.

Ocean Chlorophyll and Primary Production

Oceanic NPP, estimated as diurnal photosynthesis minus diel respiration, is responsible for almost half of global NPP ($\sim 50 \text{ Pg C yr}^{-1}$) and is the primary source of energy for marine food webs [498]. NPP draws down CO_2 levels in the surface ocean, thus shifting net fluxes from the atmosphere to the ocean and thereby exerting an important control on global climate [499]. The export of fixed carbon from the surface ocean by sinking particles to the deep through the 'biological pump' stores carbon on time scales ranging from seasons to centuries and is a critical estimate of how oceans regulate our planet's climate [500-502]. Thus, accurate and well-characterized regional, basin, and global scale NPP products are essential for understanding how ocean biology influences ocean carbon dynamics.

NPP estimates derived from satellite data, have the advantage of providing unprecedented spatial and temporal coverage. However, despite considerable progress over the past two decades, remotely sensed NPP estimates continue to suffer from large uncertainties [503-506]. At present, satellite-based global annual NPP estimates range from 32 to 79 PgC yr^{-1} [503], and annual carbon export fluxes range from 5 to $>12 \text{ PgC yr}^{-1}$ [507, 508]. The uncertainties associated with these measurements are clearly as large as the annual anthropogenic CO_2 emission rates of between ~ 7 and 11 PgC yr^{-1} [509]. Necessitating that we continue improving remote sensing methods to estimate NPP.

Satellite-based NPP models span a wide range of complexity from empirical [510] to semi-analytical models [511, 512], but can be generally categorized into one of three modeling strategies [513]. Two of these, are the biology-based models, of which one uses phytoplankton biomass (chlorophyll-*a*) derived from remote sensing reflectance (R_{rs}) [503, 514-520], while the other, the carbon based Productivity Model (CbPM), uses phytoplankton carbon stock (C_{phyto}) retrieved from backscattering coefficients at 443 nm ($b_{bp}(443)$). The latter is also derived from R_{rs} . The term ocean color is described with the spectrum of $R_{rs}(\lambda)$ and defined as the ratio of water-leaving radiance to downwelling irradiance just above the surface. A major problem in using chlorophyll-*a* as a critical input parameter is the disparate and often opposing responses of cellular chlorophyll-*a* content to nutrient availability, light limitations, and temperature conditions that can confound any simple relationship

1 between NPP and chlorophyll-*a*. To alleviate this, Behrenfeld et al. [521] used the “carbon-based approach” and
2 replaced chlorophyll-*a* with C_{phyto} . However, this method includes a new uncertainty due to scattering by non-
3 phytoplankton particles including bubbles [522-524].
4

5
6 The third category is the absorption-based models (AbPM), which rely on the absorption coefficient of
7 phytoplankton (a_{ph}) an inherent optical property, derived directly from R_{rs} . The recent model, Carbon
8 Absorption Fluorescence Euphotic resolving (CAFE) [506], belongs to this category. AbPM’s derive NPP as
9 the product of a_{ph} , photosynthetically active radiation (PAR) [525] and the efficiency (ϕ) with which absorbed
10 energy is converted into carbon biomass [526-534]. Currently, broad use of AbPM models has been hampered
11 by the lack of adequate *in situ* ϕ measurements, forcing reliance on estimates that ignore large, temporal
12 (diurnal, seasonal) and spatial (regional and vertical) variability [527, 530, 535-537]. One approach to
13 circumventing this problem is via modeling ϕ as a function of PAR and temperature [534, 538]. While this
14 approach will continue to be useful for application to ocean color from polar orbiting satellites, full realization
15 of AbPM for use with the new generation of geostationary ocean color satellites such as GOCI-1, GOC1-2 and
16 NASA GLIMR will rely on our ability to measure diurnal variability in ϕ . In conclusion, while it is clear AbPM
17 models will help reduce uncertainty in deriving NPP from satellite data, their usefulness for obtaining NPP will
18 require community efforts to accurately derive a_{ph} , diurnal PAR, and ϕ .
19
20
21
22
23
24
25
26
27
28
29

30 Satellite observations have improved global estimates of organic carbon export from the surface ocean.
31 DeVries and Weber [539] combined satellite and ship-based observations in an assimilative global carbon cycle
32 model to estimate a global POC flux out of the euphotic zone of $\sim 9 \text{ PgC yr}^{-1}$. Their study showed that carbon
33 export ratios (ratios of NPP to carbon export) were highest in higher latitudes, even though export from lower
34 latitudes was higher than previously estimated. Satellite-derived NPP and particle size as variables in a food
35 web model enabled estimation of a climatological mean global carbon export from the euphotic zone of $\sim 6 \text{ PgC}$
36 yr^{-1} [509]. Regional and basin-scale estimates of carbon export with satellite-derived NPP and empirical
37 relationships are prevalent [496, 540-542]. The NASA Exports program [543] focused on developing new
38 approaches to characterize global carbon export using satellite observations of ocean surface properties,
39 specifically considering different mechanisms. These include settling of particulate carbon in the form of intact
40 phytoplankton, aggregates, and zooplankton byproducts; net vertical transport of suspended particulate and
41 dissolved organic carbon by physical and microbial processes; and vertical transport of organic carbon
42 associated with migration of zooplankton and their predators.
43
44
45
46
47
48
49
50
51
52

53 **Satellite Assessments of Ocean Carbon Stocks**

54 Remotely sensed observations have also been used to derive stocks of different forms of carbon in ocean
55 waters (Table 8). Estimations of basin scale DOC have been explored on the basis of relationships to satellite-
56 observable optical properties, specifically CDOM absorption [e.g., 544]. The method requires a priori
57
58
59
60

1 knowledge of the relationship between DOC and CDOM, the latter comprising only a small portion of the total
2 DOC pool. Various approaches have also been developed to estimate global satellite-based estimates of total
3 surface POC [e.g., 523, 545], and PIC [547, 548]. Estimates of mixed-layer integrated global POC range
4 between 0.77 and 1.3 PgC of carbon [549]. A space-based lidar system (CALIOPS) was used to derive global
5 average mixed-layer standing stocks of phytoplankton carbon (C_{phyto}) and total POC, with estimated values of
6 0.44 PgC for C_{phyto} and 1.9 PgC for POC [550]. Balch et al. [551] extended the PIC surface algorithms by
7 developing approaches for estimation of PIC concentrations integrated over both the upper 100 m and the
8 euphotic zone depths, based on relationships between ship-based PIC concentrations.

9
10
11
12
13
14
15
16
17
18
19
20
21
22
23
24
25
26
27
28
29
30
31
32
33
34
35
36
37
38
39
40
41
42
43
44
45
46
47
48
49
50
51
52
53
54
55
56
57
58
59
60

Table 8. Existing carbon monitoring indicators for oceans and continental shelves. Method refers to broad categories, modeled, extrapolation (*in situ* combined with extent to upscale estimates), data synthesis, and remote sensing (mapping or predicting spatial heterogeneity for an indicator).

Carbon indicator	System	Value	Units	Method	Source
Carbon stocks	<u>Ocean</u>				
	POC (upper mixed layer)	0.77 – 1.9	PgC	Remote Sensing	[549, 550]
	Total Organic C	700	PgC	Extrapolation	[9]
	DIC	38,000	PgC	Extrapolation	[9]
	PIC (euphotic zone)	0.63-0.7	PgC	Remote Sensing	[547]
	Surface Sediments	1750	PgC	Extrapolation	[9]
	Carbonate Rock	60x10 ⁶	PgC	Extrapolation	[552]
	<u>Shelf</u>				
Surface Sediments	10-45	PgC	Extrapolation	[9]	
Carbon export from upper mixed layer	<u>Ocean</u>				
	Organic Carbon	5 - >12	PgC yr ⁻¹	Extrapolation and Remote Sensing	[507-509, 553, 554]
	PIC	0.59	PgC yr ⁻¹	Model	[555]

	<u>Shelf</u>				
	Organic Carbon	0.2-0.7	PgC yr ⁻¹	Extrapolation and Remote Sensing	[556, 557]
Carbon Burial	Ocean	0.012±0.02	PgC yr ⁻¹	Extrapolation	[553]
	Shelf	0.29±0.15	PgC yr ⁻¹	Extrapolation	[553]
CO₂ flux (negative values correspond to net ocean uptake)	Ocean	-2.5±0.4	PgC yr ⁻¹	Remote Sensing and Extrapolation	[491]
		-3.1±0.5	PgC yr ⁻¹	Remote Sensing (inversion)	[493]
		-1.6 – 2.8	PgC yr ⁻¹	Various	[9]
	Shelf	-0.1-0.2	PgC yr ⁻¹	Extrapolation and Model	[558, 559]
Primary Production	Ocean	32-79	PgC yr ⁻¹	Remote Sensing (<i>in situ</i> extrapolation)	[503]
	Shelf	9 – 11	PgC yr ⁻¹	Remote Sensing; Extrapolation	[556, 557, 560]
Calcification	Ocean	1.1-1.6	PgC yr ⁻¹	Remote Sensing; Model	[555, 547, 561]

3.4.1 Coastal and Continental Shelf Seas:

Coastal and continental shelf seas make up 7-11% of the total area of the ocean, yet have a significant impact on the global carbon cycle relative to their size [562]. Shelf seas are estimated to contribute almost a third of the total marine primary production, up to 50% of the inorganic carbon burial, and up to 80% of the organic carbon burial [552, 553, 556, 557, 560, 563], and therefore significantly contribute to oceanic-atmosphere carbon exchange [558, 564]. Each coastal region is different, and carbon monitoring tends to focus on each one individually, but there are a number of robust synthesis and review papers on coastal carbon cycling [e.g., 562, 563, 565], and we refer the reader to those for recent coastal carbon budgets. Here, we review the status of carbon monitoring in these regions (n = 30).

Carbon Monitoring Status

The carbon cycle in coastal shelf seas is very similar to that of the open oceans. Thus, carbon monitoring methods in shelf seas tend to overlap with oceanic approaches. However, the coastal shelf has unique data needs i.e., spatial resolution to discern coastal features, spectral influence of depth and terrestrial hydrology. Thus, oceanic remote sensing methods require alteration for use in coastal shelf regions. NPP monitoring has used methods derived for ocean systems both directly and with slight modifications [505, 556], but the performance of these methods is lowest in coastal shelf seas [505]. One region of particular focus is the Arctic Ocean and its surrounding shelf seas, where many regional algorithms exist [e.g., 515, 566, 567]. Lee et al. [513] provide an assessment of 32 Arctic NPP satellite models, finding the models performing relatively well in low-productivity seasons and deep-water regions. However, the algorithms tended to overestimate NPP, but yielded underestimates when a subsurface chlorophyll-*a* maximum was present.

Given that the shelf sea represents the continuum between terrestrial and ocean ecosystems, there are additional factors to be considered compared to carbon monitoring in ocean systems. NASA CMS studies have focused on improved observation and modeling of lateral transport of terrestrial carbon into the watershed and ultimately to the coasts [568-575]. Other studies have focused on the estimation of DOC and CDOM [189, 576-579]. As described in section 3.3.1, CDOM only makes up a fraction of the total DOC pool, but in coastal systems dominated by terrestrial discharge, CDOM and DOC co-vary. The exact form of the relationship between CDOM and DOC varies both temporally and spatially, driven by terrestrial source characteristics and biogeochemical processes, thus the need for regional approaches. However, Vantrepotte et al. [580] demonstrated the potential of a generalized approach in deriving DOC from CDOM in very contrasting coastal environments.

The CMS program has supported carbon monitoring in the northern Gulf of Mexico and the region influenced by the Mississippi River. This included efforts to map $p\text{CO}_2$ and estimate fluxes [581-585], model

1 simulations using a coupled physical-biogeochemical model [586] and satellite-derived estimation of $p\text{CO}_2$ and
2 air-sea flux of CO_2 [425]. Studies have also examined patterns in phytoplankton community composition and
3 potential relationships to carbon dynamics [587, 588]. Other CMS program efforts examined carbon properties
4 in both the Gulf of Mexico and the Atlantic coast [565, 589], and other studies have focused on sedimentation
5 and flux of various carbon forms to the seafloor [556, 590-593].
6
7
8
9

10 There remains considerable uncertainty in the estimate of global coastal ocean uptake of CO_2 . Some of
11 this is related to differences in the extent to which estuarine and inland waters are included in the inventory.
12 However, estimates based on *in situ* extrapolations as well as global models have generally converged around -
13 0.1 to -0.3 PgC yr^{-1} [558,559, 594].
14
15
16
17

18 **4 Stakeholders**

19
20 Although there are different approaches for monitoring WC systems, the full potential of satellite WC
21 products requires and thrives with stakeholder involvement to utilize and disseminate the resulting maps and
22 perpetuate monitoring. WC stakeholders are diverse across systems, scales, and studies. In general, stakeholders
23 for carbon monitoring and climate action are cities, international organizations, non-government organizations
24 (NGOs), and other governing bodies. Several international agreements include carbon monitoring such as The
25 UN Sustainable Development Goals, which encourages national monitoring. The IPCC outlines carbon
26 monitoring methods and the Paris Agreements NDCs, which outline carbon monitoring and mitigation
27 activities.
28
29
30
31
32
33
34

35 The inclusion of WC systems within these agreements varies. In 1997, the Kyoto protocol had no
36 mention of wetlands [595], in 2006, the first IPCC guidelines included only peatlands and flooded lands [20],
37 and in 2013, a supplement added recommendations for monitoring additional WC systems [596]. Oceans were
38 conspicuously absent [597] but have subsequently been addressed in a special report [598] due in part to their
39 importance for achieving climate goals [4]. The IPCC methods are focused on anthropogenic emissions and
40 recommend isolating these by identifying a change in managed lands [20]. Defining managed lands is
41 straightforward in forestry and agriculture; however, the term is ambiguous in WC systems. Therefore, national
42 monitoring programs have addressed this ambiguity by considering all wetlands managed [174]. Codifying this
43 approach within an update to the IPCC protocols would ensure a uniform application of WC monitoring. Many
44 countries cite the IPCC guidelines in their NDCs and seek to report and mitigate land-use, land-use change, and
45 forestry emissions; however, only a few directly stated their intention to track wetland restoration [599].
46 Enhanced stakeholder capacity will improve the MRV of carbon stocks and fluxes for NDCs, and carbon
47 markets [600]. The gaps in WC monitoring within international agreements and resulting national monitoring
48 leave a critical role for NGOs, universities, and subnational governing bodies to fill.
49
50
51
52
53
54
55
56
57
58
59
60

1 The transition from remote sensing methodology, often prototyped over a subnational region, to globally
2 consistent time-series is difficult and requires stakeholder involvement. For example, the Global Mangrove
3 Watch, a scientific data initiative has mapped mangrove change, provided carbon monitoring data, and
4 disseminated data [35]. Carbon monitoring can inform management of protected areas, as an example, with no
5 intervention, the Great Dismal Swamp would have emitted 6.5 million tons of CO₂ through 2062 (Net Present
6 Value (NPV): \$232 million) but due to informed management practices, it is expected to offset 9.9 million tons
7 of CO₂ emissions (NPV: \$326 million) [601]. Similarly, peatland restoration approaches, project size, and
8 stakeholder involvement have advanced over the last 25 years [602]. Local, regional, and international
9 stakeholders are critical for taking the science from space to policy.
10
11
12
13
14
15

16 **5 Recommendations**

17
18
19
20 Upon review of the status of WC monitoring, clear gaps exist. Several systems lack fundamental remote
21 sensing baselines, such as, location, extent, and change. Complete global extent maps are a priority for seagrass,
22 tidal marsh, and mineral wetlands. Similarly, peatlands could benefit from an improved extent map, e.g.,
23 peatlands in Africa [306]. There are additional systems that were not a focus of this review due to limited
24 remote sensing-based carbon monitoring research that would benefit from global mapping forested wetlands,
25 freshwater tidal marshes, and riparian wetlands. Also, thematic classifications that focus on differences in
26 carbon storage, e.g., separating mineral wetlands and peatlands or species of mangroves. Existing wetland
27 inventories can have high classification errors, and omission bias for wetlands that are difficult to detect, e.g.,
28 forested wetlands obscured by tree canopy. Another major challenge in understanding carbon stocks and fluxes
29 is the limited availability of data on the factors contributing to the variability of carbon stocks and fluxes, such
30 as the hydroperiod, hydrologic connectivity, plant and microbial communities, soil properties, chemical
31 characteristics, and disturbance. This data would improve the ability to quantify change uncertainty and
32 outcomes as they relate to carbon stocks and flows. Remote sensing research can fill these gaps by providing
33 improved up to date wetland inventories [603], reconstruction of both seasonal and long-term changes in
34 wetland hydroperiod [249, 554], monitoring disturbance [131, 604], and improving subsurface measurements
35 [231]. Terrestrial and coastal carbon budgets can be enhanced by determining the type of disturbance [40] and
36 quantifying the carbon impacts of varied change processes including degradation, loss, and restoration [605].
37 Poulter et al. [370] proposed reducing global-scale wetland carbon uncertainty with additional field collection,
38 continuous flux measurements, new satellite data sources, improved modeling of biogeochemical processes, and
39 harnessing high-performance computing. While initially proposed for wetlands, these methods for reducing
40 uncertainty are helpful for all wet carbon monitoring.
41
42
43
44
45
46
47
48
49
50
51
52
53
54
55
56

57 Carbon fluxes are an area of research across WC systems. The flows and interactions between systems
58 are still understudied, e.g., ocean carbon fluxes and linkages across the terrestrial-shelf-ocean continuum as a
59
60

constraint on terrestrial carbon fluxes. Remote sensing has the potential to reduce carbon stock and flux uncertainty by optimizing and fusing techniques that take advantage of the spatial, e.g., morphology, spectral, e.g., species, and temporal, e.g., phenology and change, remote sensing resolution domains, including the limitations and tradeoffs of applying these techniques. The next generation of carbon monitoring will capture the complex linkages between WC systems, e.g., the linked permafrost and boreal lake carbon cycle [415-417]. As we address these challenges and opportunities, our ability to understand WC storage and fluxes will improve, and in turn, our understanding of how these ecosystems function, allowing for sustainable management and conservation. Our suggestions and recommendations to accelerate the development of WC monitoring fall into four categories remote sensing, *in situ*, terrestrial and blue carbon and aquatic recommendations.

Table 10: Recommendations for future wet carbon monitoring with remote sensing.

Type	Recommendation	Potential outcome
Remote Sensing	Continued evaluation of new sensors and technology for WC monitoring.	Increased temporal, spatial, and thematic coverage. Reduced uncertainty.
Remote Sensing	The perpetuation of long running earth observation missions to ensure a continuous observation of global carbon processes.	Improved monitoring reporting and verification
Remote Sensing	Access to long-term archives to resolve trends, regional patterns, and their underlying mechanisms	Elucidate climate effects on carbon cycle
Remote Sensing	Data consistency to support development of remote sensing algorithms and model data assimilation.	Improved accuracy and applicability of methodologies
Remote Sensing	The use of spatial-temporal data to determine fine-phase temporal effects (e.g., extreme events, river plumes, drought) and how these affect WC systems.	Improved carbon budgets and understanding of carbon cycle interactions
Remote Sensing	Increased spatial and temporal coverage of lidar [550, 606].	Expanded understanding of vegetation and landscape structure and change
Remote Sensing	Coordination of carbon monitoring across boundaries including terrestrial-aquatic boundary, fresh-saline gradient, and peat-mineral wetlands.	Determination of WC linkages
<i>In situ</i>	Open access to <i>in situ</i> data.	Reducing barriers to carbon monitoring research and expanded impact of <i>in situ</i> data
<i>In situ</i>	Methods for scaling the limited <i>in situ</i> data for use in prediction and modeling of carbon products from satellite data.	Reduced uncertainty and spatial biases in carbon monitoring

<i>In situ</i>	Greater geographic distribution of <i>in situ</i> samples collection.	Global data products with reduced uncertainty and spatial biases in carbon monitoring e.g., $p\text{CO}_2$ across ocean basins [607]
Terrestrial and Blue carbon	Spatial variability of belowground carbon [34, 608]	Improved spatial estimates of carbon stock and change impacts
Terrestrial and Blue carbon	Impact of disturbance and recovery [8, 118, 608-610]	Determine carbon stock stability and major change drivers
Terrestrial and Blue carbon	Concurrent loss, gain [49], and restoration monitoring [611]	Improved change maps and extents
Aquatic	Development and refinement of ocean color remote sensing methods in optically complex coastal shelf sea and nearshore environments	Improved carbon budgets and understanding of carbon cycle interactions in coastal margins

As noted by Shutler et al. [612] satellite observations, international collaboration, and methodological advancement have resulted in accurate and robust oceanic carbon monitoring. Following a similar roadmap robust carbon monitoring can be achieved in all WC systems. The global-scale WC monitoring relies on remote sensing often as ancillary data. Our remote sensing WC agenda prioritizes the integration of remote sensing within WC monitoring at local to global scales identifying the importance of change locations and types. To summarize, major priorities are: 1) mapping or improving existing baselines will benefit all systems and the ability to understand their interconnections 2) determining linkages between systems and how climate change will alter these, 3) leveraging local remote sensing and *in situ* measurements to facilitate global analysis, and 4) continued and expanded global-scale remote sensing-based MRV to enable, subnational, national, and international carbon budgets.

6 Conclusions

Carbon monitoring depends heavily on *in situ* measurements (e.g., shipboard water and spectral sampling, soil cores, allometric equations, and biomass collection). These data are limited in WC systems due to inaccessibility and cost. Global carbon monitoring often uses mass balance equations and modeling with limited need for measurements of individual systems. Local estimates rely on *in situ* samples to estimate site-level carbon budgets. The gap between these scales will increasingly rely on earth observation. System-specific estimates are often extrapolated from limited *in situ* data, but remote sensing can capture spatial variability, quantify uncertainty, and improve carbon estimates. Remote sensing is critical for national carbon monitoring programs that fulfill IPCC level 3 data requirements. Therefore, NDCs supplement the existing need for remote sensing monitoring of WC systems. All these recommendations culminate in a primary goal for all WC systems, quantifying their contribution to global and national carbon budgets with associated uncertainties.

Acknowledgements

This research was in part supported by NASA Carbon Monitoring Systems Program (grant numbers: 18-CMS18-0052, 16-CMS16-0073, 80NSSC17K0712, 80NSSC20K0013, NNH18ZDA001-CMP, 80NSSC20K0084, 80NSSC20K0427, NNX14AO73G). This research was supported in part by the U.S. Department of Agriculture, Agricultural Research Service. This work was partly conducted by the Jet Propulsion Laboratory, California Institute of Technology, under contract with the National Aeronautics and Space Administration. Anthony Campbell was supported by the NASA Postdoctoral Program administered by the University Space Research Association.

Data Availability

Any data that support the findings of this study are included within the article or supplemental.

Accepted Manuscript

References

- 1 Walsh, B., Ciais, P., Janssens, I.A., Penuelas, J., Riahi, K., Rydzak, F., Van Vuuren, D.P. and Obersteiner, M. 2017, "Pathways for balancing CO₂ emissions and sinks", *Nature communications*, vol. 8, no. 1, pp. 1-12.
- 2 Herold, M. and Skutsch, M. 2011, "Monitoring, reporting and verification for national REDD programmes: two proposals", *Environmental Research Letters*, vol. 6, no. 1, pp. 014002.
- 3 Joseph, S., Herold, M., Sunderlin, W.D. and Verchot, L.V. 2013, "REDD readiness: early insights on monitoring, reporting and verification systems of project developers", *Environmental Research Letters*, vol. 8, no. 3, pp. 034038.
- 4 Hoegh-Guldberg, O., Northrop, E. and Lubchenco, J. 2019, "The ocean is key to achieving climate and societal goals", *Science*, vol. 365, no. 6460, pp. 1372-1374.
- 5 Seifollahi-Aghmiuni, S., Nockrach, M. and Kalantari, Z. 2019, "The potential of wetlands in achieving the sustainable development goals of the 2030 Agenda", *Water*, vol. 11, no. 3, pp. 609.
- 6 Moomaw, W.R., Chmura, G.L., Davies, G.T., Finlayson, C.M., Middleton, B.A., Natali, S.M., Perry, J.E., Roulet, N. and Sutton-Grier, A.E. 2018, "Wetlands in a changing climate: science, policy and management", *Wetlands*, vol. 38, no. 2, pp. 183-205.
- 7 Saintilan, N., Rogers, K., Kelleway, J.J., Ens, E. and Sloane, D.R. 2019, "Climate change impacts on the coastal wetlands of Australia", *Wetlands*, vol. 39, no. 6, pp. 1145-1154.
- 8 Taillie, P.J., Roman-Cuesta, R., Lagomasino, D., Cifuentes-Jara, M., Fatoyinbo, T., Ott, L.E. and Poulter, B. 2020, "Widespread mangrove damage resulting from the 2017 Atlantic mega hurricane season", *Environmental Research Letters*, vol. 15, no. 6, pp. 064010.
- 9 Friedlingstein, P., O'Sullivan, M., Jones, M.W., Andrew, R.M., Hauck, J., Olsen, A., Peters, G.P., Peters, W., Pongratz, J. and Sitch, S. 2020, "Global carbon budget 2020", *Earth System Science Data*, vol. 12, no. 4, pp. 3269-3340.
- 10 Odum, H.T., 1983. *Systems Ecology; an introduction*.
- 11 Bridgman, S.D., Megonigal, J.P., Keller, J.K., Bliss, N.B. and Trettin, C. 2006, "The carbon balance of North American wetlands", *Wetlands*, vol. 26, no. 4, pp. 889-916.
- 12 Macreadie, P.I., Anton, A., Raven, J.A., Beaumont, N., Connolly, R.M., Friess, D.A., Kelleway, J.J., Kennedy, H., Kuwae, T. and Lavery, P.S. 2019, "The future of Blue Carbon science", *Nature communications*, vol. 10, no. 1, pp. 1-13.
- 13 Davidson, N.C. & Finlayson, C.M. 2018, "Extent, regional distribution and changes in area of different classes of wetland", *Marine and Freshwater Research*, vol. 69, no. 10, pp. 1525-1533.
- 14 Tootchi, A., Jost, A. and Ducharme, A. 2019, "Multi-source global wetland maps combining surface water imagery and groundwater constraints", *Earth System Science Data*, vol. 11, no. 1, pp. 189-220.
- 15 Regnier, P., Friedlingstein, P., Ciais, P., Mackenzie, F.T., Gruber, N., Janssens, I.A., Laruelle, G.G., Lauerwald, R., Luysaert, S. and Andersson, A.J. 2013, "Anthropogenic perturbation of the carbon fluxes from land to ocean", *Nature geoscience*, vol. 6, no. 8, pp. 597-607.
- 16 Krug, J.H. 2018, "Accounting of GHG emissions and removals from forest management: a long road from Kyoto to Paris", *Carbon balance and management*, vol. 13, no. 1, pp. 1-11.
- 17 UNFCCC. 2016, "Canada intended nationally determined contributions (INDCs)", *United Nations Framework Convention on Climate Change 2015-05-15*.
- 18 Hurtt, G., Wickland, D., Jucks, K., Bowman, K., Brown, M.E., Duren, R.M., Hagen, S. and Verdy, A. 2014, "NASA carbon monitoring system: prototype monitoring, reporting, and verification".
- 19 Pendleton, L., Donato, D.C., Murray, B.C., Crooks, S., Jenkins, W.A., Sifleet, S., Craft, C., Fourqurean, J.W., Kauffman, J.B. & Marbà, N. 2012, "Estimating global "blue carbon" emissions from conversion and degradation of vegetated coastal ecosystems", *PloS one*, vol. 7, no. 9, pp. e43542.
- 20 Eggleston, H.S., Buendia, L., Miwa, K., Ngara, T. and Tanabe, K. 2006, "2006 IPCC guidelines for national greenhouse gas inventories".
- 21 Sanderman, J., Hengl, T., Fiske, G., Solvik, K., Adame, M.F., Benson, L., Bukoski, J.J., Carnell, P., Cifuentes-Jara, M. and Donato, D. 2018, "A global map of mangrove forest soil carbon at 30 m spatial resolution", *Environmental Research Letters*, vol. 13, no. 5, pp. 055002.
- 22 Nellemann, C., Corcoran, E., Duarte, C.M., Valdes, L., DeYoung, C., Fonseca, L. and Grimsditch, G. 2009, "Blue carbon: The role of healthy oceans in binding carbon. A rapid response assessment".
- 23 Page, S.E., Siegert, F., Rieley, J.O., Boehm, H., Jaya, A. and Limin, S. 2002, "The amount of carbon released from peat and forest fires in Indonesia during 1997", *NATURE*, vol. 420, no. 6911, pp. 61-65.
- 24 Mcleod, E., Chmura, G.L., Bouillon, S., Salm, R., Björk, M., Duarte, C.M., Lovelock, C.E., Schlesinger, W.H. and Silliman, B.R. 2011, "A blueprint for blue carbon: toward an improved understanding of the role of vegetated coastal habitats in sequestering CO₂", *Frontiers in Ecology and the Environment*, vol. 9, no. 10, pp. 552-560.
- 25 Duarte, C.M., Dennison, W.C., Orth, R.J. and Carruthers, T.J. 2008, "The charisma of coastal ecosystems: addressing the imbalance", *Estuaries and coasts*, vol. 31, no. 2, pp. 233-238.
- 26 Aria, M. and Cuccurullo, C. 2017, "Bibliometrix: An R-Tool for comprehensive science mapping analysis", *Journal of Informetrics*, vol. 11, no. 4, pp. 959-975.

- 1 27. Cobo, M.J., López-Herrera, A.G., Herrera-Viedma, E. and Herrera, F. 2011, "An approach for detecting, quantifying,
2 and visualizing the evolution of a research field: A practical application to the fuzzy sets theory field", *Journal of*
3 *informetrics*, vol. 5, no. 1, pp. 146-166.
- 4 28. Perillo, G., Wolanski, E., Cahoon, D.R. and Hopkinson, C.S. 2018, *Coastal wetlands: an integrated ecosystem*
5 *approach*, Elsevier.
- 6 29. Davidson, N.C. 2014, "How much wetland has the world lost? Long-term and recent trends in global wetland area",
7 *Marine and Freshwater Research*, vol. 65, no. 10, pp. 934-941.
- 8 30. Rovai, A.S., Coelho-Jr, C., de Almeida, R., Cunha-Lignon, M., Menghini, R.P., Twilley, R.R., Cintrón-Molero, G. &
9 Schaeffer-Novelli, Y. 2021, "Ecosystem-level carbon stocks and sequestration rates in mangroves in the Cananéia-
10 Iguape lagoon estuarine system, southeastern Brazil", *Forest Ecology and Management*, vol. 479, pp. 118553.
- 11 31. Donato, D.C., Kauffman, J.B., Murdiyarto, D., Kurnianto, S., Stidham, M. and Kanninen, M. 2011, "Mangroves among
12 the most carbon-rich forests in the tropics", *Nature geoscience*, vol. 4, no. 5, pp. 293-297.
- 13 32. Jardine, S.L. & Siikamäki, J.V. 2014, "A global predictive model of carbon in mangrove soils", *Environmental*
14 *Research Letters*, vol. 9, no. 10, pp. 104013.
- 15 33. Keenan, R.J., Reams, G.A., Achard, F., de Freitas, J.V., Grainger, A. & Lindquist, E. 2015, "Dynamics of global forest
16 area: Results from the FAO Global Forest Resources Assessment 2015", *Forest Ecology and Management*, vol. 352, pp.
17 9-20.
- 18 34. Atwood, T.B., Connolly, R.M., Almahsheer, H., Carnell, P.E., Duarte, C.M., Lewis, C.J.E., Irigoien, X., Kelleway,
19 J.J., Lavery, P.S., Macreadie, P.I. and Serrano, O., 2017. Global patterns in mangrove soil carbon stocks and losses.
20 *Nature Climate Change*, 7(7), pp.523-528.
- 21 35. Bunting, P., Rosenqvist, A., Lucas, R.M., Rebelo, L., Hilarides, L., Thomas, N., Hardy, A., Itoh, T., Shimada, M. and
22 Finlayson, C.M. 2018, "The global mangrove watch—a new 2010 global baseline of mangrove extent", *Remote*
23 *Sensing*, vol. 10, no. 10, pp. 1669.
- 24 36. Simard, M., Fatoyinbo, L., Smetanka, C., Rivera-Monroy, V.H., Castañeda-Moya, E., Thomas, N. & Van der Stocken,
25 T. 2019, "Mangrove canopy height globally related to precipitation, temperature and cyclone frequency", *Nature*
26 *Geoscience*, vol. 12, no. 1, pp. 40-45.
- 27 37. Worthington, T.A., Andradi-Brown, D.A., Bhargava, R., Buelow, C., Bunting, P., Duncan, C., Fatoyinbo, L., Friess,
28 D.A., Goldberg, L. & Hilarides, L. 2020, "Harnessing big data to support the conservation and rehabilitation of
29 mangrove forests globally", *One Earth*, vol. 2, no. 5, pp. 429-443.
- 30 38. Richards, D.R. & Friess, D.A. 2016, "Rates and drivers of mangrove deforestation in Southeast Asia, 2000–2012",
31 *Proceedings of the National Academy of Sciences*, vol. 113, no. 2, pp. 344-349.
- 32 39. Thomas, N., Lucas, R., Bunting, P., Hardy, A., Rosenqvist, A. & Simard, M. 2017a, "Distribution and drivers of global
33 mangrove forest change, 1996–2010", *PloS one*, vol. 12, no. 6, pp. e0179302.
- 34 40. Goldberg, L., Lagomasino, D., Thomas, N. and Fatoyinbo, T. 2020, "Global declines in human-driven mangrove
35 loss", *Global Change Biology*, vol. 26, no. 10, pp. 5844-5855.
- 36 41. Twilley, R.R., Chen, R.H. & Hargis, T. 1992, "Carbon sinks in mangroves and their implications to carbon budget of
37 tropical coastal ecosystems", *Water, air, and soil pollution*, vol. 64, no. 1, pp. 265-288.
- 38 42. Chmura, G.L., Anisfeld, S.C., Cahoon, D.R. & Lynch, J.C. 2003, "Global carbon sequestration in tidal, saline wetland
39 soils", *Global Biogeochemical Cycles*, vol. 17, no. 4.
- 40 43. Alongi, D.M. 2002, "Present state and future of the world's mangrove forests", *Environmental Conservation*, pp. 331-
41 349.
- 42 44. Alongi, D.M. 2014, "Carbon cycling and storage in mangrove forests", *Annual review of marine science*, vol. 6, pp.
43 195-219.
- 44 45. Bouillon, S., Borges, A.V., Castañeda-Moya, E., Diele, K., Dittmar, T., Duke, N.C., Kristensen, E., Lee, S.Y.,
45 Marchand, C. and Middelburg, J.J. 2008, "Mangrove production and carbon sinks: a revision of global budget
46 estimates", *Global Biogeochemical Cycles*, vol. 22, no. 2.
- 47 46. Giri, C., Ochieng, E., Tieszen, L.L., Zhu, Z., Singh, A., Loveland, T., Masek, J. & Duke, N. 2011, "Status and
48 distribution of mangrove forests of the world using earth observation satellite data", *Global Ecology and Biogeography*,
49 vol. 20, no. 1, pp. 154-159.
- 50 47. Hamilton, S.E. & Casey, D. 2016, "Creation of a high spatio-temporal resolution global database of continuous
51 mangrove forest cover for the 21st century (CGMFC-21)", *Global Ecology and Biogeography*, vol. 25, no. 6, pp. 729-
52 738.
- 53 48. Hamilton, S.E. & Friess, D.A. 2018, "Global carbon stocks and potential emissions due to mangrove deforestation from
54 2000 to 2012", *Nature Climate Change*, vol. 8, no. 3, pp. 240-244.
- 55 49. Lagomasino, D., Fatoyinbo, T., Lee, S., Feliciano, E., Trettin, C., Shapiro, A. & Mangora, M.M. 2019, "Measuring
56 mangrove carbon loss and gain in deltas", *Environmental Research Letters*, vol. 14, no. 2, pp. 025002.
- 57 50. Zhu, Y., Liu, K., Liu, L., Myint, S.W., Wang, S., Cao, J. & Wu, Z. 2020, "Estimating and Mapping Mangrove Biomass
58 Dynamic Change Using WorldView-2 Images and Digital Surface Models", *IEEE Journal of Selected Topics in*
59 *Applied Earth Observations and Remote Sensing*, vol. 13, pp. 2123-2134.
- 60 51. Zhu, Y., Liu, K., W Myint, S., Du, Z., Li, Y., Cao, J., Liu, L. and Wu, Z., 2020. Integration of GF2 Optical, GF3 SAR,
and UAV Data for Estimating Aboveground Biomass of China's Largest Artificially Planted Mangroves. *Remote*
Sensing, 12(12), p.2039.

52. Salum, R.B., Souza-Filho, P., Simard, M., Silva, C.A., Fernandes, M.E.B., Cougo, M.F., do Nascimento Junior, W. & Rogers, K. 2020, "Improving mangrove above-ground biomass estimates using LiDAR", *Estuarine Coastal and Shelf Science*, vol. 236.
53. Ghosh, S.M., Behera, M.D. & Paramanik, S. 2020, "Canopy height estimation using sentinel series images through machine learning models in a Mangrove Forest", *Remote Sensing*, vol. 12, no. 9, pp. 1519.
54. Anand, A., Pandey, P.C., Petropoulos, G.P., Pavlides, A., Srivastava, P.K., Sharma, J.K. & Malhi, R.K.M. 2020, "Use of Hyperion for Mangrove Forest Carbon Stock Assessment in Bhitarkanika Forest Reserve: A Contribution Towards Blue Carbon Initiative", *REMOTE SENSING*, vol. 12, no. 4.
55. Shrestha, S., Miranda, I., Kumar, A., Pardo, M.L.E., Dahal, S., Rashid, T., Remillard, C. & Mishra, D.R. 2019, "Identifying and forecasting potential biophysical risk areas within a tropical mangrove ecosystem using multi-sensor data", *International Journal of Applied Earth Observation and Geoinformation*, vol. 74, pp. 281-294.
56. Simard, M., Zhang, K., Rivera-Monroy, V.H., Ross, M.S., Ruiz, P.L., Castañeda-Moya, E., Twilley, R.R. & Rodriguez, E. 2006, "Mapping height and biomass of mangrove forests in Everglades National Park with SRTM elevation data", *Photogrammetric Engineering & Remote Sensing*, vol. 72, no. 3, pp. 299-311.
57. Elmahdy, S.I., Ali, T.A., Mohamed, M.M., Howari, F.M., Abouleish, M. & Simonet, D. 2020, "Spatiotemporal Mapping and Monitoring of Mangrove Forests Changes From 1990 to 2019 in the Northern Emirates, UAE Using Random Forest, Kernel Logistic Regression and Naive Bayes Tree Models", *Frontiers in Environmental Science*.
58. Nwobi, C., Williams, M. & Mitchard, E.T. 2020, "Rapid Mangrove Forest Loss and Nipa Palm (*Nypa fruticans*) Expansion in the Niger Delta, 2007–2017", *Remote Sensing*, vol. 12, no. 14, pp. 2344.
59. Suyadi, J.G., Lundquist, C.J. & Schwendenmann, L. 2020, "Aboveground Carbon Stocks in Rapidly Expanding Mangroves in New Zealand: Regional Assessment and Economic Valuation of Blue Carbon", *Estuaries and Coasts*, vol. 43, no. 6, pp. 1456-1469.
60. Lucas, R., De Kerchove, R.V., Otero, V., Lagomasino, D., Fatoyinbo, L., Omar, H., Satyanarayana, B. & Dandouh-Guebas, F. 2020, "Structural characterisation of mangrove forests achieved through combining multiple sources of remote sensing data", *REMOTE SENSING OF ENVIRONMENT*, vol. 237.
61. Jones, A.R., Raja Segaran, R., Clarke, K.D., Waycott, M., Goh, W.S. & Gillanders, B.M. 2020, "Estimating Mangrove Tree Biomass and Carbon Content: A Comparison of Forest Inventory Techniques and Drone Imagery", *Frontiers in Marine Science*, vol. 6, pp. 784.
62. Fatoyinbo, T.E. & Simard, M. 2013, "Height and biomass of mangroves in Africa from ICESat/GLAS and SRTM", *International Journal of Remote Sensing*, vol. 34, no. 2, pp. 668-681.
63. Hutchison, J., Manica, A., Swetnam, R., Balmford, A. & Spalding, M. 2014, "Predicting global patterns in mangrove forest biomass", *Conservation Letters*, vol. 7, no. 3, pp. 233-240.
64. Taureau, F., Robin, M., Proisy, C., Fromard, F.c., Imbert, D. & Debaine, F.c. 2019, "Mapping the mangrove forest canopy using spectral unmixing of very high spatial resolution satellite images", *Remote Sensing*, vol. 11, no. 3, pp. 367.
65. Tang, W., Zheng, M., Zhao, X., Shi, J., Yang, J. & Trettin, C.C. 2018, "Big Geospatial Data Analytics for Global Mangrove Biomass and Carbon Estimation", *Sustainability*, vol. 10, no. 2.
66. Rovai, A.S., Twilley, R.R., Castañeda-Moya, E., Riul, P., Cifuentes-Jara, M., Manrow-Villalobos, M., Horta, P.A., Simonassi, J.C., Fonseca, A.L. & Pagliosa, P.R. 2018, "Global controls on carbon storage in mangrove soils", *Nature Climate Change*, vol. 8, no. 6, pp. 534-538.
67. Kauffman, J.B., Adame, M.F., Arifanti, V.B., Schile-Beers, L.M., Bernardino, A.F., Bhomia, R.K., Donato, D.C., Feller, I.C., Ferreira, T.O., Jesus Garcia, M.D.C. and MacKenzie, R.A., 2020. Total ecosystem carbon stocks of mangroves across broad global environmental and physical gradients.
68. Jones, T.G., Ratsimba, H.R., Ravaoarinoroitsoharana, L., Cripps, G. & Bey, A. 2014, "Ecological variability and carbon stock estimates of mangrove ecosystems in northwestern Madagascar", *Forests*, vol. 5, no. 1, pp. 177-205.
69. Pandey, P.C., Anand, A. & Srivastava, P.K. 2019, "Spatial distribution of mangrove forest species and biomass assessment using field inventory and earth observation hyperspectral data", *Biodiversity and Conservation*, vol. 28, no. 8-9, pp. 2143-2162.
70. Li, Z., Zan, Q., Yang, Q., Zhu, D., Chen, Y. and Yu, S., 2019. Remote estimation of mangrove aboveground carbon stock at the species level using a low-cost unmanned aerial vehicle system. *Remote Sensing*, 11(9), p.1018.
71. Rahman, M.M., Lagomasino, D., Lee, S., Fatoyinbo, T., Ahmed, I. and Kanzaki, M., 2019. Improved assessment of mangrove forests in Sundarbans East Wildlife Sanctuary using WorldView 2 and Tan DEM-X high resolution imagery. *Remote Sensing in Ecology and Conservation*, 5(2), pp.136-149.
72. Wicaksono, Pramaditya and Danoedoro, Projo and Hartono & Nehren, U. 2016, "Mangrove biomass carbon stock mapping of the Karimunjawa Islands using multispectral remote sensing", *International Journal of Remote Sensing*, vol. 37, no. 1, pp. 26-52.
73. Pham, L.T.H. & Brabyn, L. 2017, "Monitoring mangrove biomass change in Vietnam using SPOT images and an object-based approach combined with machine learning algorithms", *ISPRS Journal of Photogrammetry and Remote Sensing*, vol. 128, pp. 86-97.
74. Pham, T.D., Yoshino, K., Nga, N.L. & Dieu, T.B. 2018, "Estimating aboveground biomass of a mangrove plantation on the Northern coast of Vietnam using machine learning techniques with an integration of ALOS-2 PALSAR-2 and Sentinel-2A data", *International Journal of Remote Sensing*, vol. 39, no. 22, pp. 7761-7788.

75. Shapiro, A.C, C.C. Trettin, H. Küchly, S. Alavinapanah, and S. Bandiera. The mangroves of the Zambezi Delta from 1995 to 2013 increase in extent observed via satellite. 2015. *Remote Sensing*, 7, 16504-16518. doi:10.3390/rs70x000x
76. Sannigrahi, S. 2017, "Modeling terrestrial ecosystem productivity of an estuarine ecosystem in the Sundarban Biosphere Region, India using seven ecosystem models", *Ecological Modelling*, vol. 356, pp. 73-90.
77. Lu, W., Xiao, J., Cui, X., Xu, F., Lin, G. & Lin, G. 2019, "Insect outbreaks have transient effects on carbon fluxes and vegetative growth but longer-term impacts on reproductive growth in a mangrove forest", *Agricultural and Forest Meteorology*, vol. 279.
78. Wicaksono, P., Danoedoro, P., Hartono, H., Nehren, U. & Ribbe, L. 2011, "Preliminary work of mangrove ecosystem carbon stock mapping in small island using remote sensing: above and below ground carbon stock mapping on medium resolution satellite image", *Remote Sensing for Agriculture, Ecosystems, and Hydrology XIII International Society for Optics and Photonics*.
79. Oostdijk, M., Santos, M.J., Whigham, D., Verhoeven, J. and Silvestri, S., 2018. Assessing rehabilitation of managed mangrove ecosystems using high resolution remote sensing. *Estuarine, Coastal and Shelf Science*, 211, pp.238-247.
80. Wang, M., Cao, W., Jiang, C., Yan, Y. & Guan, Q. 2018, "Potential ecosystem service values of mangrove forests in southeastern China using high-resolution satellite data", *Estuarine, Coastal and Shelf Science*, vol. 209, pp. 30-40.
81. Wang, M., Cao, W., Guan, Q., We, G., & Wang, F. 2018, "Assessing changes of mangrove forest in a coastal region of southeast China using multi-temporal satellite images", *Estuarine, Coastal and Shelf Science*, vol. 207, pp. 283-292.
82. Lee, S. & Fatoyinbo, T.E. 2015, "TanDEM-X Pol-InSAR inversion for mangrove canopy height estimation", *IEEE Journal of Selected Topics in Applied Earth Observations and Remote Sensing*, vol. 8, no. 7, pp. 3608-3618.
83. Lagomasino, D., Fatoyinbo, T., Lee, S. & Simard, M. 2015, "High-resolution forest canopy height estimation in an African blue carbon ecosystem", *Remote sensing in ecology and conservation*, vol. 1, no. 1, pp. 51-60.
84. Lagomasino, D., Fatoyinbo, T., Lee, S., Feliciano, E., Trettin, C. & Simard, M. 2016, "A Comparison of Mangrove Canopy Height Using Multiple Independent Measurements from Land, Air, and Space", *Remote Sensing*, vol. 8, no. 4.
85. Stringer, C.E., Trettin, C.C. & Zarnoch, S.J. 2016, "Soil properties of mangroves in contrasting geomorphic settings within the Zambezi River Delta, Mozambique", *Wetlands Ecology and Management*, vol. 24, no. 2, pp. 139-152.
86. Feliciano, E.A., Wdowinski, S., Potts, M.D., Lee, S. & Fatoyinbo, T.E. 2017, "Estimating Mangrove Canopy Height and Above-Ground Biomass in the Everglades National Park with Airborne LiDAR and TanDEM-X Data", *Remote Sensing*, vol. 9, no. 7.
87. Fatoyinbo, T., Feliciano, E.A., Lagomasino, D., Lee, S.K. & Trettin, C. 2018, "Estimating mangrove aboveground biomass from airborne LiDAR data: a case study from the Zambezi River delta", *Environmental Research Letters*, vol. 13, no. 2, pp. 025012.
88. Yin, D. & Wang, L. 2019, "Individual mangrove tree measurement using UAV-based LiDAR data: Possibilities and challenges", *Remote Sensing of Environment*, vol. 223, pp. 34-49.
89. Lee, S., Fatoyinbo, T.E., Lagomasino, D., Feliciano, E. & Trettin, C. 2018, "Multibaseline TanDEM-X Mangrove Height Estimation: The Selection of the Vertical Wavenumber", *IEEE JOURNAL OF SELECTED TOPICS IN APPLIED EARTH OBSERVATIONS AND REMOTE SENSING*, vol. 11, no. 10, pp. 3434-3442.
90. Thomas, Nathan, Richard Lucas, Peter Bunting, Andrew Hardy, Ake Rosenqvist, and Marc Simard. 2017b. "Distribution and Drivers of Global Mangrove Forest Change, 1996-2010." *PLoS ONE* 12 (6). <https://doi.org/10.1371/journal.pone.0179302>
91. Hansen, M.C., Potapov, P.V., Moore, R., Hancher, M., Turubanova, S.A., Tyukavina, A., Thau, D., Stehman, S.V., Goetz, S.J., Loveland, T.R. and Kommareddy, A., 2013. High-resolution global maps of 21st-century forest cover change. *science*, 342(6160), pp.850-853.
92. Hamdan, O., Aziz, H.K. and Hasmadi, I.M., 2014. L-band ALOS PALSAR for biomass estimation of Matang Mangroves, Malaysia. *Remote Sensing of Environment*, 155, pp.69-78.
93. Lucas, R., Otero, V., Van De Kerchove, R., Lagomasino, D., Satyanarayana, B., Fatoyinbo, T. and Dahdouh-Guebas, F., 2021. Monitoring Matang's Mangroves in Peninsular Malaysia through Earth observations: A globally relevant approach. *Land Degradation & Development*, 32(1), pp.354-373.
94. Wang, D., Wan, B., Liu, J., Su, Y., Guo, Q., Qiu, P. & Wu, X. 2020, "Estimating aboveground biomass of the mangrove forests on northeast Hainan Island in China using an upscaling method from field plots, UAV-LiDAR data and Sentinel-2 imagery", *International Journal of Applied Earth Observation and Geoinformation*, vol. 85, pp. 101986.
95. Navarro, J.A., Algeet, N., Fernández-Landa, A., Esteban, J., Rodríguez-Noriega, P. & Guillén-Climent, M.L. 2019, "Integration of UAV, Sentinel-1, and Sentinel-2 data for mangrove plantation aboveground biomass monitoring in Senegal", *Remote Sensing*, vol. 11, no. 1, pp. 77.
96. Hartoko, Agus and Chayaningrum, Siska and Febrianti, Dewati Ayu and Ariyanto, Dafit and Suryanti 2015, "Carbon Biomass Algorithms Development for Mangrove Vegetation in Kemujan, Parang Island Karimunjawa National Park and Demak Coastal Area - Indonesia", eds. H. Hady, H. Susanto & O. Radjasa, pp. 39.
97. Hickey, S.M., Callow, N.J., Phinn, S., Lovelock, C.E. & Duarte, C.M. 2018, "Spatial complexities in aboveground carbon stocks of a semi-arid mangrove community: A remote sensing height-biomass-carbon approach", *Estuarine Coastal and Shelf Science*, vol. 200, pp. 194-201.
98. Barr, J.G., Engel, V., Smith, T.J. & Fuentes, J.D. 2012, "Hurricane Disturbance and Recovery of Energy Balance, CO₂ Fluxes and Canopy Structure in a Mangrove Forest of the Florida Everglades", *Agricultural and Forest Meteorology*, vol. 153, no. 0, pp. 54-66.

99. Adame, M.F., Connolly, R.M., Turschwell, M.P., Lovelock, C.E., Fatoyinbo, T., Lagomasino, D., Goldberg, L.A., Holdorf, J., Friess, D.A., Sasmito, S.D., Sanderman, J., Sievers, M., Buelow, C., Kauffman, J.B., Bryan-Brown, D. & Brown, C.J. 2021, "Future carbon emissions from global mangrove forest loss", *Global Change Biology*.
100. Dai, Z., C.C. Trettin, R. Birdsie, S. Frolking. 2018. Mangrove carbon assessment tool: Model Development and sensitivity analyses. *Estuarine, Coastal and Shelf Science* 208:23-35. <https://doi.org/10.1016/j.ecss.2018.04.035>
101. Bournazel, J., Kumara, M.P., Jayatissa, L.P., Viergever, K., Morel, V. and Huxham, M., 2015. The impacts of shrimp farming on land-use and carbon storage around Puttalam lagoon, Sri Lanka. *Ocean & Coastal Management*, 113, pp.18-28.
102. Duncan, C., Primavera, J.H., Pettorelli, N., Thompson, J.R., Loma, R.J.A. & Koldewey, H.J. 2016, "Rehabilitating mangrove ecosystem services: A case study on the relative benefits of abandoned pond reversion from Panay Island, Philippines", *Marine Pollution Bulletin*, vol. 109, no. 2, pp. 772-782.
103. Yang, J., Gao, J., Cheung, A., Liu, B., Schwendenmann, L. & Costello, M.J. 2013, "Vegetation and sediment characteristics in an expanding mangrove forest in New Zealand", *Estuarine Coastal and Shelf Science*, vol. 134, pp. 11-18.
104. Ellegaard, M., Nguyen, N.T.G., Andersen, T.J., Michelsen, A., Nguyen, N.L., Doan, N.H., Kristensen, E., Weckström, K., Son, T.P.H. and Lund-Hansen, L.C., 2014. Temporal changes in physical, chemical and biological sediment parameters in a tropical estuary after mangrove deforestation. *Estuarine, Coastal and Shelf Science*, 142, pp.32-40.
105. Anne, N.J., Abd-Elrahman, A.H., Lewis, D.B. and Hewitt, N.A. 2014, "Modeling soil parameters using hyperspectral image reflectance in subtropical coastal wetlands", *International Journal of Applied Earth Observation and Geoinformation*, vol. 33, pp. 47-56.
106. Huang, T., Fu, Y., Pan, P. & Chen, C.A. 2012, "Fluvial carbon fluxes in tropical rivers", *Current Opinion in Environmental Sustainability*, vol. 4, no. 2, pp. 162-169.
107. Bauer, J.E.; Cai, W.-J.; Raymond, P.A.; Bianchi, T.S.; Hopkinson, C.S.; Regnier, P.A.G. The changing carbon cycle of the coastal ocean. *Nature* 2013, 504, 61–70
108. Alongi, D.M. 2020, "Carbon balance in salt marsh and mangrove ecosystems: A global synthesis", *Journal of Marine Science and Engineering*, vol. 8, no. 10, pp. 767.
109. Breithaupt, J.L., Smoak, J.M., Smith III, T.J., Sanders, C.J. & Hoare, A. 2012, "Organic carbon burial rates in mangrove sediments: Strengthening the global budget", *Global Biogeochemical Cycles*, vol. 26, no. 3.
110. Maher, D.T., Santos, I.R., Golsby-Smith, L., Gleeson, J. and Eyre, B.D., 2013. Groundwater-derived dissolved inorganic and organic carbon exports from a mangrove tidal creek: The missing mangrove carbon sink?. *Limnology and Oceanography*, 58(2), pp.475-488.
111. Sippo, J.Z., Maher, D.T., Tait, D.R., Holloway, C. and Santos, I.R., 2016. Are mangroves drivers or buffers of coastal acidification? Insights from alkalinity and dissolved inorganic carbon export estimates across a latitudinal transect. *Global Biogeochemical Cycles*, 30(5), pp.753-766.
112. Hansen, Angela M., Tamara EC Kraus, Brian A. Pellerin, Jacob A. Fleck, Bryan D. Downing, and Brian A. Bergamaschi. 2016. "Optical properties of dissolved organic matter (DOM): Effects of biological and photolytic degradation." *Limnology and oceanography* 61, no. 3 (2016): 1015-1032.
113. Lu, C.J., Benner, R., Fichot, C.G., Fukuda, H., Yamashita, Y. and Ogawa, H., 2016. Sources and transformations of dissolved lignin phenols and chromophoric dissolved organic matter in Otsuchi Bay, Japan. *Frontiers in Marine Science*, 3, p.85.
114. Sanyal, P., Ray, R., Paul, M., Gupta, V.K., Acharya, A., Bakshi, S., Jana, T.K. and Mukhopadhyay, S.K., 2020. Assessing the dynamics of dissolved organic matter (DOM) in the coastal environments dominated by mangroves, Indian Sundarbans. *Frontiers in Earth Science*, 8, p.218.
115. Friess, D.A., Rogers, K., Lovelock, C.E., Krauss, K.W., Hamilton, S.E., Lee, S.Y., Lucas, R., Primavera, J., Rajkaran, A. and Shi, S., 2019. The state of the world's mangrove forests: past, present, and future. *Annual Review of Environment and Resources*, 44, pp.89-115.
116. Krauss, K.W., From, A.S., Doyle, T.W., Doyle, T.J. & Barry, M.J. 2011, "Sea-level rise and landscape change influence mangrove encroachment onto marsh in the Ten Thousand Islands region of Florida, USA", *Journal of Coastal Conservation*, vol. 15, no. 4, pp. 629-638.
117. Ross, M.S., Meeder, J.F., Sah, J.P., Ruiz, P.L. & Telesnicki, G.J. 2000, "The southeast saline Everglades revisited: 50 years of coastal vegetation change", *Journal of Vegetation Science*, vol. 11, no. 1, pp. 101-112.
118. Osland, M.J., Day, R.H. & Michot, T.C. 2020, "Frequency of extreme freeze events controls the distribution and structure of black mangroves (*Avicennia germinans*) near their northern range limit in coastal Louisiana", *Diversity and Distributions*, vol. 26, no. 10, pp. 1366-1382.
119. Charles, S.P., Kominoski, J.S., Armitage, A.R., Guo, H., Weaver, C.A. and Pennings, S.C., 2020. Quantifying how changing mangrove cover affects ecosystem carbon storage in coastal wetlands. *Ecology*, 101(2), p.e02916.
120. Doughty, C.L., Langley, J.A., Walker, W.S., Feller, I.C., Schaub, R. and Chapman, S.K., 2016. Mangrove range expansion rapidly increases coastal wetland carbon storage. *Estuaries and Coasts*, 39(2), pp.385-396.
121. Yando, E.S., Osland, M.J., Willis, J.M., Day, R.H., Krauss, K.W. and Hester, M.W., 2016. Salt marsh-mangrove ecotones: using structural gradients to investigate the effects of woody plant encroachment on plant-soil interactions and ecosystem carbon pools. *Journal of Ecology*, 104(4), pp.1020-1031.

122. Worthington, T.A., Zu Ermgassen, P.S., Friess, D.A., Krauss, K.W., Lovelock, C.E., Thorley, J., Tingey, R., Woodroffe, C.D., Bunting, P., Cormier, N. and Lagomasino, D., 2020. A global biophysical typology of mangroves and its relevance for ecosystem structure and deforestation. *Scientific reports*, 10(1), pp.1-11.
123. Simard, M., Fatoyinbo, T., Smetanka, C., Rivera-Monroy, V.H., CASTANEDA, E., Thomas, N. and Van Der Stocken, T. 2019, "Global Mangrove Distribution, Aboveground Biomass, and Canopy Height", ORNL DAAC.
124. Rosentreter, J.A., Maher, D.T., Erler, D.V., Murray, R.H. & Eyre, B.D. 2018, "Methane emissions partially offset "blue carbon" burial in mangroves", *Science advances*, vol. 4, no. 6, pp. eaao4985.
125. Richards, D.R., Thompson, B.S. & Wijedasa, L. 2020, "Quantifying net loss of global mangrove carbon stocks from 20 years of land cover change", *Nature communications*, vol. 11, no. 1, pp. 1-7.
126. Twilley, R.R., Castañeda-Moya, E., Rivera-Monroy, V.H. & Rovai, A. 2017, "Productivity and carbon dynamics in mangrove wetlands" in *Mangrove ecosystems: A global biogeographic perspective* Springer, , pp. 113-162.
127. Duarte, C.M. & Cebrián, J. 1996, "The fate of marine autotrophic production", *Limnology and Oceanography*, vol. 41, no. 8, pp. 1758-1766.
128. Duarte, C.M., Losada, I.J., Hendriks, I.E., Mazarrasa, I. and Marbà, N. 2013, "The role of coastal plant communities for climate change mitigation and adaptation", *Nature Climate Change*, vol. 3, no. 11, pp. 961-968.
129. Barbier, E.B., Hacker, S.D., Kennedy, C., Koch, E.W., Stier, A.C. & Silliman, B.R. 2011, "The value of estuarine and coastal ecosystem services", *Ecological Monographs*, vol. 81, no. 2, pp. 169-193.
130. Mcowen, C.J., Weatherdon, L.V., Van Bochove, J., Sullivan, E., Blyth, S., Zockler, C., Stanwell-Smith, D., Kingston, N., Martin, C.S. and Spalding, M. 2017, "A global map of saltmarshes", *Biodiversity data journal*, no. 5.
131. Murray, N.J., Phinn, S.R., DeWitt, M., Ferrari, R., Johnston, R., Lyons, M.B., Clinton, N., Thau, D. and Fuller, R.A. 2019, "The global distribution and trajectory of tidal flats", *Nature*, vol. 565, no. 7738, pp. 222-225.
132. Sager, P.E., Richman, S., Harris, H.J. & Fewless, G. 1985, "Preliminary observations on the seiche-induced flux of carbon, nitrogen, and phosphorus in a Great Lakes coastal marsh", *Coastal Wetlands*, pp. 59-68.
133. Watson, E.B., Wigand, C., Davey, E.W., Andrews, H.M., Bishop, J. and Raposa, K.B. 2017, "Wetland Loss Patterns and Inundation-Productivity Relationships Prognosticate Widespread Salt Marsh Loss for Southern New England", *Estuaries and Coasts*, vol. 40, no. 3, pp. 662-681.
134. Deegan, L.A., Johnson, D.S., Warren, R.S., Peterson, B.J., Fleeger, J.W., Fagherazzi, S. and Wollheim, W.M. 2012, "Coastal eutrophication as a driver of salt marsh loss", *Nature*, vol. 490, no. 7420, pp. 388-392.
135. Wang, H., Ge, Z., Yuan, L. and Zhang, L. 2014, "Evaluation of the combined threat from sea-level rise and sedimentation reduction to the coastal wetlands in the Yangtze Estuary, China", *Ecological Engineering*, vol. 71, pp. 346-354.
136. Blum, M.D. and Roberts, H.H. 2009, "Drowning of the Mississippi Delta due to insufficient sediment supply and global sea-level rise", *Nature Geoscience*, vol. 2, no. 7, pp. 488-491.
137. Syvitski, J.P., Vörösmarty, C.J., Kettner, A.J. and Green, P. 2005, "Impact of humans on the flux of terrestrial sediment to the global coastal ocean", *Science*, vol. 308, no. 5720, pp. 376-380.
138. Poffenbarger, H.J., Needelman, B.A. & Magonigal, J.P. 2011, "Salinity influence on methane emissions from tidal marshes", *Wetlands*, vol. 31, no. 5, pp. 831-842.
139. Kroeger, K.D., Crooks, S., Moseman-Valtierra, S. & Tang, J. 2017, "Restoring tides to reduce methane emissions in impounded wetlands: A new and potent Blue Carbon climate change intervention", *Scientific reports*, vol. 7, no. 1, pp. 1-12.
140. Powell, E.B., Krause, J.R., Martin, R.M. and Watson, E.B. 2020, "Pond excavation reduces coastal wetland carbon dioxide assimilation", *Journal of Geophysical Research: Biogeosciences*, vol. 125, no. 2, pp. e2019JG005187.
141. Hopkinson, C.S., Morris, J.T., Fagherazzi, S., Wollheim, W.M. and Raymond, P.A. 2018, "Lateral marsh edge erosion as a source of sediments for vertical marsh accretion", *Journal of Geophysical Research: Biogeosciences*, vol. 123, no. 8, pp. 2444-2465.
142. Ghosh, S., Mishra, D.R. and Gitelson, A.A. 2016, "Long-term monitoring of biophysical characteristics of tidal wetlands in the northern Gulf of Mexico—A methodological approach using MODIS", *Remote Sensing of Environment*, vol. 173, pp. 39-58.
143. Kromkamp, J.C., Morris, E. and Forster, R.M. 2020, "Microscale variability in biomass and photosynthetic activity of microphytobenthos during a spring-neap tidal cycle", *Frontiers in Marine Science*.
144. Méléder, V., Savelli, R., Barnett, A., Polsenaere, P., Gernez, P., Cugier, P., Lerouxel, A., Le Bris, A., Dupuy, C. and Le Fouest, V. 2020, "Mapping the Intertidal Microphytobenthos Gross Primary Production Part I: Coupling Multispectral Remote Sensing and Physical Modeling", *Frontiers in Marine Science*.
145. Gao, Y., Ouyang, Z., Shao, C., Chu, H., Su, Y., Guo, H., Chen, J. and Zhao, B. 2018, "Field observation of lateral detritus carbon flux in a coastal wetland", *Wetlands*, vol. 38, no. 3, pp. 613-625.
146. Tao, J., Mishra, D.R., Cotten, D.L., O'Connell, J., Leclerc, M., Nahravi, H.B., Zhang, G. and Pahari, R. 2018, "A comparison between the MODIS product (MOD17A2) and a tide-robust empirical GPP model evaluated in a georgia wetland", *Remote Sensing*, vol. 10, no. 11, pp. 1831.
147. Yan, Y., Zhao, B., Chen, J., Guo, H., Gu, Y., Wu, Q. and Li, B. 2008, "Closing the carbon budget of estuarine wetlands with tower-based measurements and MODIS time series", *Global Change Biology*, vol. 14, no. 7, pp. 1690-1702.

148. Feagin, R.A., Forbrich, I., Huff, T.P., Barr, J.G., Ruiz-Plancarte, J., Fuentes, J.D., Najjar, R.G., Vargas, R., Vázquez-Lule, A. and Windham-Myers, L. 2020, "Tidal wetland gross primary production across the continental United States, 2000–2019", *Global Biogeochemical Cycles*, vol. 34, no. 2, pp. e2019GB006349.
149. Feagin, R.A., Forbrich, I., Huff, T.P., BARR, J.G., RUIZ-PLANCARTE, J., FUENTES, J.D., NAJJAR, R.G., VARGAS, R., VAZQUEZ-LULE, A. and WINDHAM-MYERS, L. 2020b, "Gross Primary Production Maps of Tidal Wetlands across Conterminous USA, 2000-2019", ORNL DAAC.
150. O'Connell, J.L., Mishra, D.R., Cotten, D.L., Wang, L. and Alber, M. 2017, "The Tidal Marsh Inundation Index (TMII): An inundation filter to flag flooded pixels and improve MODIS tidal marsh vegetation time-series analysis", *Remote Sensing of Environment*, vol. 201, pp. 34-46.
151. Gross, M.F., Klemas, V. and Levasseur, J.E. 1986, "Remote sensing of *Spartina anglica* biomass in five French salt marshes", *International Journal of Remote Sensing*, vol. 7, no. 5, pp. 657-664.
152. Gross, M.F., Hardisky, M.A., Klemas, V. and Wolf, P.L. 1987, "Quantification of biomass of the marsh grass *Spartina alterniflora* Loisel using Landsat Thematic Mapper imagery", *PHOTOGRAMMETRIC ENGINEERING and REMOTE SENSING*, vol. 53, no. 11.
153. Hardisky, M.A., Daiber, F.C., Roman, C.T. and Klemas, V. 1984, "Remote sensing of biomass and annual net aerial primary productivity of a salt marsh", *Remote Sensing of Environment*, vol. 16, no. 2, pp. 91-106.
154. Jensen, D., Cavanaugh, K.C., Simard, M., Christensen, A., Rovai, A. and Twilley, R. 2021 "Aboveground biomass distributions and vegetation composition changes in Louisiana's Wax Lake Delta", *Estuarine, Coastal and Shelf Science*, vol. 250, pp. 107139.
155. Doughty, C.L. and Cavanaugh, K.C. 2019, "Mapping coastal wetland biomass from high resolution unmanned aerial vehicle (UAV) imagery", *Remote Sensing*, vol. 11, no. 5, pp. 540.
156. Buffington, K.J., Dugger, B.D. and Thorne, K.M. 2018, "Climate-related variation in plant peak biomass and growth phenology across Pacific Northwest tidal marshes", *Estuarine, Coastal and Shelf Science*, vol. 202, pp. 212-221.
157. Rasel, S.M., Chang, H., Ralph, T.J., Saintilan, N. and Diti, I.J. 2019, "Application of feature selection methods and machine learning algorithms for saltmarsh biomass estimation using Worldview-2 imagery", *Geocarto International*, pp. 1-25.
158. Miller, G.J., Morris, J.T. and Wang, C. 2019, "Estimating aboveground biomass and its spatial distribution in coastal wetlands utilizing planet multispectral imagery", *Remote Sensing*, vol. 11, no. 17, pp. 2020.
159. Byrd, K.B., O'Connell, J.L., Di Tommaso, S. and Kelly, M. 2014, "Evaluation of sensor types and environmental controls on mapping biomass of coastal marsh emergent vegetation", *Remote Sensing of Environment*, vol. 149, pp. 166-180.
160. Zhang, C., Denka, S., Cooper, H. and Mishra, D.R. 2018, "Quantification of sawgrass marsh aboveground biomass in the coastal Everglades using object-based ensemble analysis and Landsat data", *Remote Sensing of Environment*, vol. 204, pp. 366-379.
161. Kulawardhana, R.W., Popescu, S.C. and Feagin, R.A. 2014, "Fusion of lidar and multispectral data to quantify salt marsh carbon stocks", *Remote Sensing of Environment*, vol. 154, pp. 345-357.
162. Byrd, K.B., Ballanti, L., Thomas, N., Nguyen, D., Holmquist, J.R., Simard, M. and Windham-Myers, L. 2018a, "Aboveground Biomass High-Resolution Maps for Selected US Tidal Marshes, 2015", *ORNL DAAC*.
163. Byrd, K.B., Ballanti, L., Thomas, N., Nguyen, D., Holmquist, J.R., Simard, M. and Windham-Myers, L. 2018b, "A remote sensing-based model of tidal marsh aboveground carbon stocks for the conterminous United States", *ISPRS Journal of Photogrammetry and Remote Sensing*, vol. 139, pp. 255-271.
164. Byrd, K.B., Ballanti, L., Thomas, N., Nguyen, D., Holmquist, J.R., Simard, M. and Windham-Myers, L. 2020, "Corrigendum to" A remote sensing-based model of tidal marsh aboveground carbon stocks for the conterminous United States"[*ISPRS J. Photogram. Rem. Sens.* 139 (2018) 255-271]", *ISPRS Journal of Photogrammetry and Remote Sensing*, vol. 166, pp. 63-67.
165. Xiangzhen, Q., Huiyu, L., Zhenshan, L., Xiang, L. and Haibo, G. 2019, "Impacts of age and expansion direction of invasive *Spartina alterniflora* on soil organic carbon dynamics in coastal salt marshes along eastern China", *Estuaries and Coasts*, vol. 42, no. 7, pp. 1858-1867.
166. Kulawardhana, R.W., Feagin, R.A., Popescu, S.C., Boutton, T.W., Yeager, K.M. and Bianchi, T.S. 2015, "The role of elevation, relative sea-level history and vegetation transition in determining carbon distribution in *Spartina alterniflora* dominated salt marshes", *Estuarine, Coastal and Shelf Science*, vol. 154, pp. 48-57.
167. Campbell, A.D. and Wang, Y. 2020, "Salt marsh monitoring along the mid-Atlantic coast by Google Earth Engine enabled time series", *PloS one*, vol. 15, no. 2, pp. e0229605.
168. Li, X., Ren, L., Liu, Y., Craft, C., Mander, Ü and Yang, S. 2014, "The impact of the change in vegetation structure on the ecological functions of salt marshes: the example of the Yangtze estuary", *Regional environmental change*, vol. 14, no. 2, pp. 623-632.
169. Thomas, N., Simard, M., Castañeda-Moya, E., Byrd, K.B., Windham-Myers, L., Bevington, A. and Twilley, R. 2019, "High-resolution mapping of biomass and distribution of marsh and forested wetlands in southeastern coastal Louisiana", *International Journal of Applied Earth Observation and Geoinformation*, vol. 80, pp. 257-267.
170. Zhao, G., Ye, S., Li, G., Yu, X. and McClellan, S.A. 2017, "Soil organic carbon storage changes in coastal wetlands of the Liaohe Delta, China, based on landscape patterns", *Estuaries and Coasts*, vol. 40, no. 4, pp. 967-976.

171. Jensen, L.A., Schmidt, L.B., Hollesen, J. and Elberling, B. 2006, "Accumulation of soil organic carbon linked to Holocene sea-level changes in west Greenland", *Arctic, Antarctic, and Alpine Research*, vol. 38, no. 3, pp. 378-383.
172. Braun, K.N., Theuerkauf, E.J., Masterson, A.L., Curry, B.B. and Horton, D.E. 2019, "Modeling organic carbon loss from a rapidly eroding freshwater coastal wetland", *Scientific reports*, vol. 9, no. 1, pp. 1-13.
173. Bianchi, T.S., Allison, M.A., Zhao, J., Li, X., Comeaux, R.S., Feagin, R.A. and Kulawardhana, R.W. 2013, "Historical reconstruction of mangrove expansion in the Gulf of Mexico: linking climate change with carbon sequestration in coastal wetlands", *Estuarine, Coastal and Shelf Science*, vol. 119, pp. 7-16.
174. Crooks, S., Sutton-Grier, A.E., Troxler, T.G., Herold, N., Bernal, B., Schile-Beers, L. and Wirth, T. 2018, "Coastal wetland management as a contribution to the US National Greenhouse Gas Inventory", *Nature climate change*, vol. 8, no. 12, pp. 1109-1112.
175. Holmquist, J. R., Windham-Myers, L., Bernal, B., Byrd, K. B., Crooks, S., Gonneea, M. E., ... & Weller, D. E. (2018). Uncertainty in United States coastal wetland greenhouse gas inventorying. *Environmental Research Letters*, 13(11), 115005.
176. Holmquist, J. R., Windham-Myers, L., Bliss, N., Crooks, S., Morris, J. T., Megonigal, J. P., ... & Woodrey, M. (2018). Accuracy and precision of tidal wetland soil carbon mapping in the conterminous United States. *Scientific reports*, 8(1), 1-16.
177. Holmquist, J.R., Windham-Myers, L., Bliss, N., Crooks, S., Morris, J.T., Megonigal, J.P., TROXLER, T., WELLER, D.E., CALLAWAY, J. and DREXLER, J. 2019, "Tidal wetland soil carbon stocks for the conterminous United States, 2006-2010", ORNL DAAC.
178. Callaway, J.C., Borgnis, E.L., Turner, R.E. & Milan, C.S. 2012, "Carbon sequestration and sediment accretion in San Francisco Bay tidal wetlands", *Estuaries and Coasts*, vol. 35, no. 5, pp. 1163-1181.
179. Peck, E.K., Wheatcroft, R.A. & Brophy, L.S. 2020, "Controls on sediment accretion and blue carbon burial in tidal saline wetlands: Insights from the Oregon coast, USA", *Journal of Geophysical Research: Biogeosciences*, vol. 125, no. 2.
180. Rogers, Kerrylee and Kelleway, Jeffrey J and Saintilan, Neil and Megonigal, J Patrick and Adams, Janine B and Holmquist, James R and Lu, Meng and Schile-Beers, Lisa and Zawadzki, Atun and Mazumder, Debashish and others 2019, "Wetland carbon storage controlled by millennial-scale variation in relative sea-level rise", *Nature*, vol. 567, no. 7746, pp. 91-95.
181. Duarte, C.M. 2017, "Reviews and syntheses: Hidden forests, the role of vegetated coastal habitats in the ocean carbon budget", *Biogeosciences*, vol. 14, no. 2, pp. 301-310.
182. Costanza, R., d'Arge, R., De Groot, R., Farber, S., Grasso, M., Hannon, B., Limburg, K., Naeem, S., O'Neill, R.V. & Paruelo, J. 1997, "The value of the world's ecosystem services and natural capital", *Nature*, vol. 387, no. 6630, pp. 253-260.
183. Duarte, C.M., Middelburg, J.J. and Caraco, N. 2005, "Major role of marine vegetation on the oceanic carbon cycle", *Biogeosciences*, vol. 2, no. 1, pp. 1-8.
184. Al-Haj, A.N. & Fulweiler, R.W. 2020, "A synthesis of methane emissions from shallow vegetated coastal ecosystems", *Global Change Biology*, vol. 26, no. 5, pp. 2988-3005.
185. Lin, W., Wu, J. & Lin, H. 2020, "Contribution of unvegetated tidal flats to coastal carbon flux", *Global Change Biology*, vol. 26, no. 6, pp. 3443-3454.
186. Teal, J.M. 1962, "Energy flow in the salt marsh ecosystem of Georgia", *Ecology*, vol. 43, no. 4, pp. 614-624.
187. Childers, D.L., Day, J.W. and Mckellar, H.N., 2002. Twenty more years of marsh and estuarine flux studies: revisiting Nixon (1980). *Concepts and controversies in tidal marsh ecology*, pp.391-423.
188. Tobias, C. & Neubauer, S.C. 2019, "Salt marsh biogeochemistry—an overview" In: Gerardo M. E. Perillo, Eric Wolanski, Donald R. Cahoon, Mark M. Brinson, editors, *Coastal Wetlands: An Integrated Ecosystem Approach.*, pp. 539-596.
189. Cao, F., Tzortziou, M., Hu, C., Mannino, A., Fichot, C.G., Del Vecchio, R., Najjar, R.G. and Novak, M. 2018, "Remote sensing retrievals of colored dissolved organic matter and dissolved organic carbon dynamics in North American estuaries and their margins", *Remote Sensing of Environment*, vol. 205, pp. 151-165.
190. Short, F., Carruthers, T., Dennison, W. and Waycott, M. 2007, "Global seagrass distribution and diversity: a bioregional model", *Journal of experimental marine biology and ecology*, vol. 350, no. 1-2, pp. 3-20.
191. Fourqurean, J.W., Duarte, C.M., Kennedy, H., Marbà, N., Holmer, M., Mateo, M.A., Apostolaki, E.T., Kendrick, G.A., Krause-Jensen, D. and McGlathery, K.J. 2012, "Seagrass ecosystems as a globally significant carbon stock", *Nature geoscience*, vol. 5, no. 7, pp. 505-509.
192. Salinas, C., Duarte, C.M., Lavery, P.S., Masque, P., Arias-Ortiz, A., Leon, J.X., Callaghan, D., Kendrick, G.A. and Serrano, O. 2020, "Seagrass losses since mid-20th century fuelled CO2 emissions from soil carbon stocks", *Global Change Biology*, vol. 26, no. 9, pp. 4772-4784.
193. Pollard, P.C. and Greenway, M. 2013, "Seagrasses in tropical Australia, productive and abundant for decades decimated overnight", *Journal of Biosciences*, vol. 38, no. 1, pp. 157-166.
194. Zhang, M., English, D., Hu, C., Carlson, P., Muller-Karger, F.E., Toro-Farmer, G. and Herwitz, S.R. 2016, "Short-term changes of remote sensing reflectance in a shallow-water environment: observations from repeated airborne hyperspectral measurements", *International Journal of Remote Sensing*, vol. 37, no. 7, pp. 1620-1638.

195. Lyons, M., Roelfsema, C., Kovacs, E., Samper-Villarreal, J., Saunders, M., Maxwell, P. and Phinn, S. 2015, "Rapid monitoring of seagrass biomass using a simple linear modelling approach, in the field and from space", *Marine Ecology Progress Series*, vol. 530, pp. 1-14.
196. Munir, M. and Wicaksono, P. 2019, "Support vector machine for seagrass percent cover mapping using PlanetScope image in Labuan Bajo, East Nusa Tenggara", Sixth International Symposium on LAPAN-IPB Satellite International Society for Optics and Photonics.
197. Misbari, S. and Hashim, M. 2016, "Change detection of submerged seagrass biomass in shallow coastal water", *Remote Sensing*, vol. 8, no. 3, pp. 200.
198. Tamondong, A., Cruz, C., Quides, R.R., Garcia, M., Cruz, J.A., Guihawan, J. and Blanco, A. 2018, "Remote sensing-based estimation of seagrass percent cover and LAI for above ground carbon sequestration mapping", *Remote Sensing of the Open and Coastal Ocean and Inland Waters* International Society for Optics and Photonics, , pp. 1077803.
199. Tamondong, A.M., Blanco, A.C., Fortes, M.D. and Nadaoka, K. 2013, "Mapping of seagrass and other benthic habitats in Bolinao, Pangasinan using Worldview-2 satellite image", *2013 IEEE International Geoscience and Remote Sensing Symposium-IGARSS/IEEE*, , pp. 1579.
200. Kakuta, S., Takeuchi, W. and Prathep, A. 2016, "Seaweed and seagrass mapping in thailand measured using Landsat 8 optical and textural image properties", *Journal of Marine Science and Technology*, vol. 24, no. 6, pp. 1155-1160.
201. Dierssen, H.M., Chlus, A. and Russell, B. 2015, "Hyperspectral discrimination of floating mats of seagrass wrack and the macroalgae *Sargassum* in coastal waters of Greater Florida Bay using airborne remote sensing", *Remote Sensing of Environment*, vol. 167, pp. 247-258.
202. Dierssen, H.M., Zimmerman, R.C., Drake, L.A. and Burdige, D. 2010, "Benthic ecology from space: optics and net primary production in seagrass and benthic algae across the Great Bahama Bank", *Marine Ecology Progress Series*, vol. 411, pp. 1-15.
203. Jayatilake, D.R. and Costello, M.J. 2018, "A modelled global distribution of the seagrass biome", *Biological Conservation*, vol. 226, pp. 120-126.
204. Duffy, J.E., Benedetti-Cecchi, L., Trinanes, J., Muller-Karger, F.E., Ambo-Rappe, R., Boström, C., Buschmann, A.H., Byrnes, J., Coles, R.G. and Creed, J. 2019, "Toward a coordinated global observing system for seagrasses and marine macroalgae", *Frontiers in Marine Science*, vol. 6, pp. 317.
205. McKenzie, L.J., Nordlund, L.M., Jones, B.L., Cullen-Unsworth, L.C., Roelfsema, C. and Unsworth, R.K. 2020, "The global distribution of seagrass meadows", *Environmental Research Letters*, vol. 15, no. 7, pp. 074041.
206. Pergent, G., Pergent-Martini, C., de Florinier, M. and Valette-Sansevin, A. 2015, "Assessment of carbon sequestration in *Posidonia* meadow", *MEDCOAST 2015*, pp. 231.
207. Lefcheck, J.S., Wilcox, D.J., Murphy, R.R., Marion, S.R. and Orth, R.J. 2017, "Multiple stressors threaten the imperiled coastal foundation species eelgrass (*Zostera marina*) in Chesapeake Bay, USA", *Global Change Biology*, vol. 23, no. 9, pp. 3474-3483.
208. Sousa, A.I., da Silva, J.F., Azevedo, A. and Lillebø, A.I. 2019, "Blue Carbon stock in *Zostera noltei* meadows at Ria de Aveiro coastal lagoon (Portugal) over a decade", *Scientific reports*, vol. 9, no. 1, pp. 1-13.
209. Zoffoli, M.L., Gernez, P., Rosa, P., Le Bris, A., Brando, V.E., Barillé, A., Harin, N., Peters, S., Poser, K. and Spaias, L. 2020, "Sentinel-2 remote sensing of *Zostera noltei*-dominated intertidal seagrass meadows", *Remote Sensing of Environment*, vol. 251, pp. 112020.
210. Hedley, J. and Enríquez, S. 2010, "Optical properties of canopies of the tropical seagrass *Thalassia testudinum* estimated by a three-dimensional radiative transfer model", *Limnology and Oceanography*, vol. 55, no. 4, pp. 1537-1550.
211. Hedley, J., Russell, B., Randolph, K. and Dierssen, H. 2016, "A physics-based method for the remote sensing of seagrasses", *Remote Sensing of Environment*, vol. 174, pp. 134-147.
212. Greene, A., Rahman, A.F., Kline, R. and Rahman, M.S. 2018, "Side scan sonar: A cost-efficient alternative method for measuring seagrass cover in shallow environments", *Estuarine, Coastal and Shelf Science*, vol. 207, pp. 250-258.
213. Rende, S.F., Bosman, A., Di Mento, R., Bruno, F., Lagudi, A., Irving, A.D., Dattola, L., Giambattista, L.D., Lanera, P. and Proietti, R. 2020, "Ultra-High-Resolution Mapping of *Posidonia oceanica* (L.) Delile Meadows through Acoustic, Optical Data and Object-based Image Classification", *Journal of Marine Science and Engineering*, vol. 8, no. 9, pp. 647.
214. Beca-Carretero, P., Varela, S. and Stengel, D.B. 2020, "A novel method combining species distribution models, remote sensing, and field surveys for detecting and mapping subtidal seagrass meadows", *Aquatic Conservation: Marine and Freshwater Ecosystems*, vol. 30, no. 6, pp. 1098-1110.
215. Poursanidis, D., Traganos, D., Teixeira, L., Shapiro, A. and Muaves, L. 2020, "Cloud-native Seascape Mapping of Mozambique's Quirimbas National Park with Sentinel-2", *Remote Sensing in Ecology and Conservation*.
216. UNEP-WCMC, Short FT (2021). Global distribution of seagrasses (version 7.1). Seventh update to the data layer used in Green and Short (2003). Cambridge (UK): UN Environment World Conservation Monitoring Centre. Data DOI: <https://doi.org/10.34892/x6r3-d211>
217. Waycott, M., Duarte, C.M., Carruthers, T.J., Orth, R.J., Dennison, W.C., Olyarnik, S., Calladine, A., Fourqurean, J.W., Heck, K.L. & Hughes, A.R. 2009, "Accelerating loss of seagrasses across the globe threatens coastal ecosystems", *Proceedings of the national academy of sciences*, vol. 106, no. 30, pp. 12377-12381.

- 1 218. Duffy, J.P., Pratt, L., Anderson, K., Land, P.E. and Shutler, J.D. 2018, "Spatial assessment of intertidal seagrass
2 meadows using optical imaging systems and a lightweight drone", *Estuarine, Coastal and Shelf Science*, vol. 200, pp.
3 169-180.
- 4 219. Ballard, M.S., Lee, K.M., Sagers, J.D., Venegas, G.R., McNeese, A.R., Wilson, P.S. and Rahman, A.F. 2020,
5 "Application of acoustical remote sensing techniques for ecosystem monitoring of a seagrass meadow", *The Journal of*
6 *the Acoustical Society of America*, vol. 147, no. 3, pp. 2002-2019.
- 7 220. Hays, G.C., Alcoverro, T., Christianen, M.J., Duarte, C.M., Hamann, M., Macreadie, P.I., Marsh, H.D., Rasheed, M.A.,
8 Thums, M. and Unsworth, R.K. 2018, "New tools to identify the location of seagrass meadows: marine grazers as
9 habitat indicators", *Frontiers in Marine Science*, vol. 5, pp. 9.
- 10 221. Traganos, D., Aggarwal, B., Poursanidis, D., Topouzelis, K., Chrysoulakis, N. and Reinartz, P. 2018, "Towards global-
11 scale seagrass mapping and monitoring using Sentinel-2 on Google Earth Engine: The case study of the aegean and
12 ionian seas", *Remote Sensing*, vol. 10, no. 8, pp. 1227.
- 13 222. Ha, N.T., Manley-Harris, M., Pham, T.D. and Hawes, I. 2020, "A comparative assessment of ensemble-based machine
14 learning and maximum likelihood methods for mapping seagrass using sentinel-2 imagery in tauranga harbor, New
15 Zealand", *Remote Sensing*, vol. 12, no. 3, pp. 355.
- 16 223. Brock, J.C., Yates, K.K., Halley, R.B., Kuffner, I.B., Wright, C.W. and Hatcher, B.G. 2006, "Northern Florida reef tract
17 benthic metabolism scaled by remote sensing", *Marine Ecology Progress Series*, vol. 312, pp. 123-139.
- 18 224. Moses, C.S., Andréfouët, S., Kranenburg, C.J. and Muller-Karger, F.E. 2009, "Regional estimates of reef carbonate
19 dynamics and productivity using Landsat 7 ETM , and potential impacts from ocean acidification", *Marine Ecology*
20 *Progress Series*, vol. 380, pp. 103-115.
- 21 225. Clavier, J., Chauvaud, L., Carlier, A., Amice, E., Van der Geest, M., Labrosse, P., Diagne, A. and Hily, C. 2011,
22 "Aerial and underwater carbon metabolism of a *Zostera noltii* seagrass bed in the Banc d'Arguin, Mauritania", *Aquatic*
23 *Botany*, vol. 95, no. 1, pp. 24-30.
- 24 226. Van Dam, B., Zeller, M., Lopes, C., Smyth, A., Böttcher, M., Osburn, C., Zimmerman, T., Pröfrock, D., Fourqurean, J.
25 and Thomas, H. 2021, "Calcification-driven CO₂ emissions exceed "Blue Carbon" sequestration in a carbonate seagrass
26 meadow".
- 27 227. Polsenaere, P., Lamaud, E., Lafon, V., Bonnefond, J., Bretel, P., Delille, B., Deborde, J., Loustau, D. and Abril, G.
28 2012, "Spatial and temporal CO₂ exchanges measured by Eddy Covariance over a temperate intertidal flat and their
29 relationships to net ecosystem production", *Biogeosciences*, vol. 9, no. 1, pp. 249-268.
- 30 228. Samper-Villarreal, J., Lovelock, C.E., Saunders, M.I., Roelfsema, C. and Mumby, P.J. 2016, "Organic carbon in
31 seagrass sediments is influenced by seagrass canopy complexity, turbidity, wave height, and water depth", *Limnology*
32 *and Oceanography*, vol. 61, no. 3, pp. 938-952.
- 33 229. Serrano, O., Lavery, P.S., Rozaimi, M. and Mateo, M.A. 2014, "Influence of water depth on the carbon sequestration
34 capacity of seagrasses", *Global Biogeochemical Cycles*, vol. 28, no. 9, pp. 950-961.
- 35 230. Traganos, D. and Reinartz, P. 2018, "Machine learning-based retrieval of benthic reflectance and *Posidonia oceanica*
36 seagrass extent using a semi-analytical inversion of Sentinel-2 satellite data", *International Journal of Remote*
37 *Sensing*, vol. 39, no. 24, pp. 9428-9452.
- 38 231. Thomas, N., Pertiwi, A.P., Traganos, D., Lagomasino, D., Poursanidis, D., Moreno, S. and Fatoyinbo, L. 2021,
39 "SPACE-BORNE CLOUD-NATIVE SATELLITE-DERIVED BATHYMETRY (SDB) MODELS USING ICESat-2
40 and SENTINEL-2", *Geophysical Research Letters*, , pp. e2020GL092170.
- 41 232. Saunders, M.I., Bayraktarov, E., Roelfsema, C.M., Leon, J.X., Samper-Villarreal, J., Phinn, S.R., Lovelock, C.E. and
42 Mumby, P.J. 2015, "Spatial and temporal variability of seagrass at Lizard Island, Great Barrier Reef", *Botanica*
43 *Marina*, vol. 58, no. 1, pp. 35-49.
- 44 233. Ouisse, V., Marchand-Jouravleff, I., Fiandrino, A., Feunteun, E. and Ysnel, F. 2020, "Swinging boat moorings: Spatial
45 heterogeneous damage to eelgrass beds in a tidal ecosystem", *Estuarine, Coastal and Shelf Science*, vol. 235, pp.
46 106581.
- 47 234. Glasby, T.M. and West, G. 2018, "Dragging the chain: Quantifying continued losses of seagrasses from boat
48 moorings", *Aquatic Conservation: Marine and Freshwater Ecosystems*, vol. 28, no. 2, pp. 383-394.
- 49 235. Kelly, J.J., Orr, D. and Takekawa, J.Y. 2019, "Quantification of damage to eelgrass (*Zostera marina*) beds and
50 evidence-based management strategies for boats anchoring in San Francisco Bay", *Environmental management*, vol. 64,
51 no. 1, pp. 20-26.
- 52 236. Thorhaug, A., Berlyn, G.P., Poulos, H.M. and Goodale, U.M. 2015, "Pollutant tracking for 3 Western North Atlantic
53 sea grasses by remote sensing: Preliminary diminishing white light responses of *Thalassia testudinum*, *Halodule*
54 *wrightii*, and *Zostera marina*", *Marine pollution bulletin*, vol. 97, no. 1-2, pp. 460-469.
- 55 237. Carnell, P.E., Ierodiaconou, D., Atwood, T.B. and Macreadie, P.I. 2020, "Overgrazing of seagrass by sea urchins
56 diminishes blue carbon stocks", *Ecosystems*, vol. 23, no. 7, pp. 1437-1448.
- 57 238. Arias-Ortiz, A., Serrano, O., Masqué, P., Lavery, P.S., Mueller, U., Kendrick, G.A., Rozaimi, M., Esteban, A.,
58 Fourqurean, J.W. and Marbà, N. 2018, "A marine heatwave drives massive losses from the world's largest seagrass
59 carbon stocks", *Nature Climate Change*, vol. 8, no. 4, pp. 338-344.
- 60 239. Davenport, A.E., Davis, J.D., Woo, I., Grossman, E.E., Barham, J., Ellings, C.S. and Takekawa, J.Y. 2017, "Comparing
automated classification and digitization approaches to detect change in eelgrass bed extent during restoration of a large
river delta", *Northwest Science*, vol. 91, no. 3, pp. 272-282.

- 1 240. McGlathery, K.J., Reynolds, L.K., Cole, L.W., Orth, R.J., Marion, S.R. and Schwarzschild, A. 2012, "Recovery
2 trajectories during state change from bare sediment to eelgrass dominance", *Marine Ecology Progress Series*, vol. 448,
3 pp. 209-221.
- 4 241. Valdez, S.R., Zhang, Y.S., van der Heide, T., Vanderklift, M.A., Tarquinio, F., Orth, R.J. and Silliman, B.R. 2020,
5 "Positive ecological interactions and the success of seagrass restoration", *Frontiers in Marine Science*, vol. 7, pp. 91.
- 6 242. Kolka R, Trettin C, Tang W, Krauss K, Bansal S, Drexler J, Wickland K, Chimner R, Hogan D, Pindilli E, Benscoter B,
7 Tangen B, Kane E, Bridgham S, Richardson C, 2018. "Terrestrial wetlands". In: Cavallaro, N.; Shrestha, G.; Birdsey,
8 R.; Mayes, A.M.; Najjar, R.G.; Reed, S.C.; Romero-Lankao, P.; Zhu, Z, eds. Second state of the carbon cycle report
9 (SOCCR2): A sustained assessment report. Washington, DC: U.S. Global Change Research Program: 507-567.
10 [Chapter 13]. <https://doi.org/10.7930/SOCCR2.2018.Ch13>.
- 11 243. Cowardin, L.M., Carter, V., Golet, F.C. and LaRoe, E.T. 1979, Classification of wetlands and deepwater habitats of the
12 United States, US Department of the Interior, US Fish and Wildlife Service, Washington, D.C.
- 13 244. Dahl, T.E. 1990, Wetlands losses in the United States, 1780's to 1980's. Report to the Congress, National Wetlands
14 Inventory, St. Petersburg, FL (USA).
- 15 245. Lal, R. 2008, "Carbon sequestration", *Philosophical Transactions of the Royal Society B: Biological Sciences*, vol. 363,
16 no. 1492, pp. 815-830.
- 17 246. Nahlik, A.M. and Fennessy, M.S. 2016, "Carbon storage in US wetlands", *Nature Communications*, vol. 7, no. 1, pp. 1-
18 9.
- 19 247. Davidson, N.C., Fluet-Chouinard, E. & Finlayson, C.M. 2018, "Global extent and distribution of wetlands: trends and
20 issues", *Marine and Freshwater Research*, vol. 69, no. 4, pp. 620-627.
- 21 248. Dahl, T.E., Johnson, C.E. and Frayer, W.E., 1991. *Wetlands, status and trends in the conterminous United States mid-
22 1970's to mid-1980's*. US Fish and Wildlife Service.
- 23 249. Halabisky, M., Moskal, L.M., Gillespie, A. & Hannam, M. 2016, "Reconstructing semi-arid wetland surface water
24 dynamics through spectral mixture analysis of a time series of Landsat satellite images (1984–2011)", *Remote Sensing
25 of Environment*, vol. 177, pp. 171-183.
- 26 250. Kissel, A.M., Halabisky, M., Scherer, R.D., Ryan, M.E. & Hansen, E.C. 2020, "Expanding wetland hydroperiod data
27 via satellite imagery for ecological applications", *Frontiers in Ecology and the Environment*, vol. 18, no. 8, pp. 432-438.
- 28 251. Lang, M., McCarty, G., Oesterling, R. & Yeo, J. 2013, "Topographic metrics for improved mapping of forested
29 wetlands", *Wetlands*, vol. 33, no. 1, pp. 141-155.
- 30 252. O'Neil, G.L., Saby, L., Band, L.E. & Goodall, J.L. 2019, "Effects of LiDAR DEM smoothing and conditioning
31 techniques on a topography-based wetland identification model", *Water Resources Research*, vol. 55, no. 5, pp. 4343-
32 4363.
- 33 253. Adeli, S., Salehi, B., Mahdianpari, M., Quaekenbush, L.J., Brisco, B., Tamiminia, H. & Shaw, S. 2020, "Wetland
34 monitoring using SAR data: A meta-analysis and comprehensive review", *Remote Sensing*, vol. 12, no. 14, pp. 2190.
- 35 254. Descloux, S., Chanudet, V., Poilvé, H. & Grégoire, A. 2011, "Co-assessment of biomass and soil organic carbon stocks
36 in a future reservoir area located in Southeast Asia", *Environmental monitoring and assessment*, vol. 173, no. 1, pp.
37 723-741.
- 38 255. Suchenwirth, L., Stümer, W., Schmidt, T., Förster, M. and Kleinschmit, B. 2014, "Large-scale mapping of carbon
39 stocks in riparian forests with self-organizing maps and the k-nearest-neighbor algorithm", *Forests*, vol. 5, no. 7, pp.
40 1635-1652.
- 41 256. Sanders, L.M., Taffs, K., Stokes, D., Sanders, C.J., Enrich-Prast, A., Amora-Nogueira, L. & Marotta, H. 2018, "Historic
42 carbon burial spike in an Amazon floodplain lake linked to riparian deforestation near Santarém, Brazil",
43 *Biogeosciences*, vol. 15, no. 2, pp. 447-455.
- 44 257. Graves, B.P., Ralph, T.J., Hesse, P.P., Westaway, K.E., Kobayashi, T., Gadd, P.S. & Mazumder, D. 2019, "Macro-
45 charcoal accumulation in floodplain wetlands: Problems and prospects for reconstruction of fire regimes and
46 environmental conditions", *PloS one*, vol. 14, no. 10, pp. e0224011.
- 47 258. Fernandes, M.R., Aguiar, F.C., Martins, M.J., Rico, N., Ferreira, M.T. and Correia, A.C. 2020, "Carbon Stock
48 Estimations in a Mediterranean Riparian Forest: A Case Study Combining Field Data and UAV Imagery", *Forests*, vol.
49 11, no. 4, pp. 376.
- 50 259. McClellan, M., Comas, X., Benscoter, B., Hinkle, R. & Sumner, D. 2017, "Estimating belowground carbon stocks in
51 isolated wetlands of the Northern Everglades Watershed, central Florida, using ground penetrating radar and aerial
52 imagery", *Journal of Geophysical Research: Biogeosciences*, vol. 122, no. 11, pp. 2804-2816.
- 53 260. Buma, B., Krapek, J. and Edwards, R.T. 2016, "Watershed-scale forest biomass distribution in a perhumid temperate
54 rainforest as driven by topographic, soil, and disturbance variables", *Canadian Journal of Forest Research*, vol. 46, no.
55 6, pp. 844-854.
- 56 261. Buras, A., Thevs, N., Zerbe, S. and Wilmking, M. 2013, "Productivity and carbon sequestration of *Populus euphratica*
57 at the Amu River, Turkmenistan", *Forestry*, vol. 86, no. 4, pp. 429-439.
- 58 262. Filippi, A.M., Güneralp, İ and Randall, J. 2014, "Hyperspectral remote sensing of aboveground biomass on a river
59 meander bend using multivariate adaptive regression splines and stochastic gradient boosting", *Remote Sensing
60 Letters*, vol. 5, no. 5, pp. 432-441.

- 1 263. Chabi, A., Lautenbach, S., Orekan, V.O.A. and Kyei-Baffour, N. 2016, "Allometric models and aboveground biomass
2 stocks of a West African Sudan Savannah watershed in Benin", *Carbon balance and management*, vol. 11, no. 1, pp. 1-
3 18.
- 4 264. Riegel, J.B., Bernhardt, E. and Swenson, J. 2013, "Estimating above-ground carbon biomass in a newly restored coastal
5 plain wetland using remote sensing", *Plos one*, vol. 8, no. 6, pp. e68251.
- 6 265. Taddeo, S., Dronova, I. and Depsky, N. 2019, "Spectral vegetation indices of wetland greenness: Responses to
7 vegetation structure, composition, and spatial distribution", *Remote Sensing of Environment*, vol. 234, pp. 111467.
- 8 266. Lumbierres, M., Méndez, P.F., Bustamante, J., Soriguer, R. & Santamaría, L. 2017, "Modeling biomass production in
9 seasonal wetlands using MODIS NDVI land surface phenology", *Remote Sensing*, vol. 9, no. 4, pp. 392.
- 10 267. O'Connell, J.L., Byrd, K.B. and Kelly, M. 2014, "Remotely-sensed indicators of N-related biomass allocation in
11 *Schoenoplectus acutus*", *PLoS One*, vol. 9, no. 3, pp. e90870.
- 12 268. Ling, C., Sun, H., Zhang, H., Lin, H., Ju, H. & Liu, H. 2014, "Study on above-ground biomass estimation of East Dong
13 Ting lake wetland based on Worldview-2 data", *2014 Third International Workshop on Earth Observation and Remote
14 Sensing Applications (EORSIA)IEEE*, pp. 428.
- 15 269. Budzynska, M., Dabrowska-Zielinska, K., Kowalik, W., Malek, I. and Turlej, K. 2010, "Study in Biebrza Wetlands
16 using optical and microwave satellite data", *2010 IEEE International Geoscience and Remote Sensing
17 SymposiumIEEE*, , pp. 393.
- 18 270. Knox, S.H., Dronova, I., Sturtevant, C., Oikawa, P.Y., Matthes, J.H., Verfaillie, J. and Baldocchi, D. 2017, "Using
19 digital camera and Landsat imagery with eddy covariance data to model gross primary production in restored
20 wetlands", *Agricultural and Forest Meteorology*, vol. 237, pp. 233-245.
- 21 271. Poulter, B., Bousquet, P., Canadell, J.G., Ciais, P., Peregon, A., Saunio, M., Arora, V.K., Beerling, D.J., Brovkin, V.
22 and Jones, C.D. 2017, "Global wetland contribution to 2000–2012 atmospheric methane growth rate
23 dynamics", *Environmental Research Letters*, vol. 12, no. 9, pp. 094013.
- 24 272. Potter, C., Klooster, S., Hiatt, S., Fladeland, M., Genovese, V. and Gross, P. 2006, "Methane emissions from natural
25 wetlands in the United States: satellite-derived estimation based on ecosystem carbon cycling", *Earth Interactions*, vol.
26 10, no. 22, pp. 1-12.
- 27 273. Melton, J.R., Wania, R., Hodson, E.L., Poulter, B., Ringeval, B., Spahni, R., Bohn, T., Avis, C.A., Beerling, D.J. &
28 Chen, G. 2013, "Present state of global wetland extent and wetland methane modelling: conclusions from a model inter-
29 comparison project (WETCHIMP)", *Biogeosciences*, vol. 10, no. 2, pp. 753-788.
- 30 274. Wania, R., Melton, J.R., Hodson, E.L., Poulter, B., Ringeval, B., Spahni, R., Bohn, T., Avis, C.A., Chen, G. and
31 Eliseev, A.V. 2013, "Present state of global wetland extent and wetland methane modelling: methodology of a model
32 inter-comparison project (WETCHIMP)", *Geoscientific Model Development*, vol. 6, no. 3, pp. 617-641.
- 33 275. Hondula, K.L., DeVries, B., Jones, C.N. & Palmer, M.A. "Effects of Using High Resolution Satellite-based Inundation
34 Time Series to Estimate Methane Fluxes from Forested Wetlands", 2021, *Geophysical Research Letters*, , pp.
35 e2021GL092556.
- 36 276. Lu, W., Xiao, J., Liu, F., Zhang, Y., Liu, C. & Lin, G. 2017, "Contrasting ecosystem CO₂ fluxes of inland and coastal
37 wetlands: a meta-analysis of eddy covariance data", *Global Change Biology*, vol. 23, no. 3, pp. 1180-1198.
- 38 277. Fluet-Chouinard, E., Lehner, B., Rebelo, L., Papa, F. & Hamilton, S.K. 2015, "Development of a global inundation map
39 at high spatial resolution from topographic downscaling of coarse-scale remote sensing data", *Remote Sensing of
40 Environment*, vol. 158, pp. 348-361.
- 41 278. Mendez-Estrella, R., Romo-Leon, J.R. and Castellanos, A.E. 2017, "Mapping changes in carbon storage and
42 productivity services provided by riparian ecosystems of semi-arid environments in Northwestern Mexico", *ISPRS
43 International Journal of Geo-Information*, vol. 6, no. 10, pp. 298.
- 44 279. Prigent, C., Papa, F., Aires, F., Rossow, W.B. & Matthews, E. 2007, "Global inundation dynamics inferred from
45 multiple satellite observations, 1993–2000", *Journal of Geophysical Research: Atmospheres*, vol. 112, no. D12.
- 46 280. Lehner, B. & Döll, P. 2004, "Development and validation of a global database of lakes, reservoirs and wetlands",
47 *Journal of hydrology*, vol. 296, no. 1-4, pp. 1-22.
- 48 281. Aselmann, I. & Crutzen, P.J. 1989, "Global distribution of natural freshwater wetlands and rice paddies, their net
49 primary productivity, seasonality and possible methane emissions", *Journal of Atmospheric Chemistry*, vol. 8, no. 4, pp.
50 307-358.
- 51 282. Matthews, E. & Fung, I. 1987, "Methane emission from natural wetlands: Global distribution, area, and environmental
52 characteristics of sources", *Global Biogeochemical Cycles*, vol. 1, no. 1, pp. 61-86.
- 53 283. Roehm C L 2005 Respiration in wetland ecosystems Respiration in Aquatic Ecosystems (Oxford University Press) pp
54 83–102 Online:
55 [https://oxford.universitypressscholarship.com/view/10.1093/acprof:oso/9780198527084.001.0001/acprof-
56 9780198527084-chapter-6](https://oxford.universitypressscholarship.com/view/10.1093/acprof:oso/9780198527084.001.0001/acprof-9780198527084-chapter-6)
- 57 284. Campbell, C., Vitt, D.H., Halsey, L.A., Campbell, I.D., Thormann, M.N. & Bayley, S.E. 2000, "Net primary production
58 and standing biomass in northern continental wetlands.", *Information Report-Northern Forestry Centre, Canadian Forest
59 Service*, , no. NOR-X-369.
- 60 285. Mitsch, W.J. & Gosselink, J.G. 2000, "The value of wetlands: importance of scale and landscape setting", *Ecological
Economics*, vol. 35, no. 1, pp. 25-33.

286. Xu, J., Morris, P.J., Liu, J. and Holden, J. 2018, "PEATMAP: Refining estimates of global peatland distribution based on a meta-analysis", *Catena*, vol. 160, pp. 134-140.
287. Hodgkins, S.B., Richardson, C.J., Dommain, R., Wang, H., Glaser, P.H., Verbeke, B., Winkler, B.R., Cobb, A.R., Rich, V.I. and Missilmani, M. 2018, "Tropical peatland carbon storage linked to global latitudinal trends in peat recalcitrance", *Nature communications*, vol. 9, no. 1, pp. 1-13.
288. Yu, Z., Loisel, J., Brosseau, D.P., Beilman, D.W. and Hunt, S.J., 2010. Global peatland dynamics since the Last Glacial Maximum. *Geophysical research letters*, 37(13).
289. Leifeld, J. & Menichetti, L. 2018, "The underappreciated potential of peatlands in global climate change mitigation strategies", *Nature communications*, vol. 9, no. 1, pp. 1-7.
290. Loisel, J., Gallego-Sala, A.V., Amesbury, M.J., Magnan, G., Anshari, G., Beilman, D.W., Benavides, J.C., Blewett, J., Camill, P. and Charman, D.J. 2021, "Expert assessment of future vulnerability of the global peatland carbon sink", *Nature climate change*, vol. 11, no. 1, pp. 70-77.
291. Bourgeau-Chavez, L.L., Endres, S.L., Graham, J.A., Hribljan, J.A., Chimner, R.A., Lilleskov, E.A. and Battaglia, M.J. 2018, "Mapping peatlands in boreal and tropical ecoregions", In: Liang, S., ed. *Comprehensive Remote Sensing*, vol. 6. Oxford, UK: Elsevier: 24-44., , pp. 24-44.
292. Limpens, J., Berendse, F., Blodau, C., Canadell, J.G., Freeman, C., Holden, J., Roulet, N., Rydin, H. and Schaepman-Strub, G., 2008. Peatlands and the carbon cycle: from local processes to global implications—a synthesis. *Biogeosciences*, 5(5), pp.1475-1491.
293. Turunen, J., Tomppo, E., Tolonen, K. & Reinikainen, A. 2002, "Estimating carbon accumulation rates of undrained mires in Finland—application to boreal and subarctic regions", *The Holocene*, vol. 12, no. 1, pp. 69-80.
294. Bourgeau-Chavez, L.L., Grelik, S.L., Billimire, M.G., Jenkins, L., Kasischke, E.S. and Turetsky, M.R. 2020, "Assessing boreal peat fire severity and vulnerability of peatlands to early season wildland fire", *Frontiers in Forests and Global Change*, vol. 3, pp. 20.
295. Craft, C., Washburn, C. and Parker, A. 2008, "Latitudinal trends in organic carbon accumulation in temperate freshwater peatlands" in *Wastewater treatment, plant dynamics and management in constructed and natural wetlands* Springer, , pp. 23-31.
296. Charman, D.J., Beilman, D.W., Blaauw, M., Booth, R.K., Brewer, S., Chambers, F.M., Christen, J.A., Gallego-Sala, A., Harrison, S.P. and Hughes, P.D. 2013, "Climate-related changes in peatland carbon accumulation during the last millennium", *Biogeosciences*, vol. 10, no. 2, pp. 929-944.
297. Bourgeau-Chavez, L.L., Grelik, S.L., Battaglia, M.J., Leisman, D. J., Chimner, R. A., Hribljan, J. A., Lilleskov, E. A., Draper, F. C., Zutta, B. R., Hergoualc'h, K., Bhomia, R. K., and Lähteenoja, O. 2021. Advances in Amazonian Peatland Discrimination with Multi-Temporal PALSAR Refines Estimates of Peatland Distribution, C Stocks and Deforestation. *Front. Earth Sci.* 9:676748. doi: 10.3389/feart.2021.676748
298. Bourgeau-Chavez, L.L., Grelik, S.L., Battaglia, M.J., Leisman, D.J., Chimner, R.A., Hribljan, J.A., Lilleskov, E.A., Draper, F.C., Zutta, B.R., Kristell Hergoualc'h, Rupesh Bhomia, Outi, Lähteenoja. 2021. Essential New Mapping of Peruvian Tropical Lowland Peatland Distribution, C Stocks and Deforestation. *Frontiers in Earth Science*, in review
299. Draper, F.C., Roucoux, K.H., Lawson, I.T., Mitchard, E.T., Coronado, E.N.H., Lähteenoja, O., Montenegro, L.T., Sandoval, E.V., Zarate, R. and Baker, T.R. 2014, "The distribution and amount of carbon in the largest peatland complex in Amazonia", *Environmental Research Letters*, vol. 9, no. 12, pp. 124017.
300. Silva, M.L.d., Silva, A.C., Silva, B.P.C., Barral, U.M., Soares, P.G. and Vidal-Torrado, P. 2013, "Surface mapping, organic matter and water stocks in peatlands of the Serra do Espinhaço Meridional-Brazil", *Revista Brasileira de Ciência do Solo*, vol. 37, no. 5, pp. 1149-1157.
301. Lähteenoja, O., Reátegui, Y.R., Räsänen, M., Torres, D.D.C., Oinonen, M. and Page, S. 2012, "The large Amazonian peatland carbon sink in the subsiding Pastaza-Marañón foreland basin, Peru", *Global Change Biology*, vol. 18, no. 1, pp. 164-178.
302. Hergoualc'h, K., Gutiérrez-Vélez, V.H., Menton, M. and Verchot, L.V. 2017, "Characterizing degradation of palm swamp peatlands from space and on the ground: An exploratory study in the Peruvian Amazon", *Forest Ecology and Management*, vol. 393, pp. 63-73.
303. Chimner, R.A., Bourgeau-Chavez, L., Grelik, S., Hribljan, J.A., Clarke, A.M.P., Polk, M.H., Lilleskov, E.A. and Fuentealba, B. 2019, "Mapping mountain peatlands and wet meadows using multi-date, multi-sensor remote sensing in the Cordillera Blanca, Peru", *Wetlands*, vol. 39, no. 5, pp. 1057-1067.
304. Hribljan, J.A., Suarez, E., Bourgeau-Chavez, L., Endres, S., Lilleskov, E.A., Chimbolema, S., Wayson, C., Serocki, E. and Chimner, R.A. 2017, "Multidate, multisensor remote sensing reveals high density of carbon-rich mountain peatlands in the páramo of Ecuador", *Global Change Biology*, vol. 23, no. 12, pp. 5412-5425.
305. Davenport, I.J., McNicol, I., Mitchard, E.T., Dargie, G., Suspense, I., Milongo, B., Bocko, Y.E., Hawthorne, D., Lawson, I. and Baird, A.J. 2020, "First Evidence of Peat Domes in the Congo Basin using LiDAR from a Fixed-Wing Drone", *Remote Sensing*, vol. 12, no. 14, pp. 2196.
306. Dargie, G.C., Lewis, S.L., Lawson, I.T., Mitchard, E.T., Page, S.E., Bocko, Y.E. and Ifo, S.A. 2017, "Age, extent and carbon storage of the central Congo Basin peatland complex", *Nature*, vol. 542, no. 7639, pp. 86-90.
307. Wedeux, B., Dalponte, M., Schlund, M., Hagen, S., Cochrane, M., Graham, L., Usup, A., Thomas, A. and Coomes, D. 2020, "Dynamics of a human-modified tropical peat swamp forest revealed by repeat lidar surveys", *Global Change Biology*, vol. 26, no. 7, pp. 3947-3964.

308. Vernimmen, R., Hooijer, A., Akmalia, R., Fitranatanegara, N., Mulyadi, D., Yuherdha, A., Andreas, H. and Page, S. 2020, "Mapping deep peat carbon stock from a LiDAR based DTM and field measurements, with application to eastern Sumatra", *Carbon balance and management*, vol. 15, pp. 1-18.
309. Thapa, R.B., Watanabe, M., Motohka, T., Shiraiishi, T. and Shimada, M. 2014, "Calibration of aboveground forest carbon stock models for major tropical forests in central Sumatra using airborne LiDAR and field measurement data", *IEEE Journal of Selected Topics in Applied Earth Observations and Remote Sensing*, vol. 8, no. 2, pp. 661-673.
310. Minasny, B., Sulaeman, Y. and Setiawan, B.I., 2019, November. Open digital mapping for accurate assessment of tropical peatlands. In *Tropical Wetlands-Innovation in Mapping and Management: Proceedings of the International Workshop on Tropical Wetlands: Innovation in Mapping and Management, October 19-20, 2018, Banjarmasin, Indonesia* (p. 3). CRC Press.
311. Hoyt, A.M., Chaussard, E., Seppalainen, S.S. and Harvey, C.F. 2020, "Widespread subsidence and carbon emissions across Southeast Asian peatlands", *Nature Geoscience*, vol. 13, no. 6, pp. 435-440.
312. Enghart, S., Keuck, V. and Siegert, F. 2011, "Modeling aboveground biomass in tropical forests using multi-frequency SAR data—A comparison of methods", *IEEE Journal of Selected Topics in Applied Earth Observations and Remote Sensing*, vol. 5, no. 1, pp. 298-306.
313. Noojipady, P., Morton, D.C., Schroeder, W., Carlson, K.M., Huang, C., Gibbs, H.K., Burns, D., Walker, N.F. and Prince, S.D. 2017, "Managing fire risk during drought: The influence of certification and El Niño on fire-driven forest conversion for oil palm in Southeast Asia", *Earth System Dynamics*, vol. 8, no. 3, pp. 749-771.
314. Adesiji, A.R., Mohammed, T.A., Daud, N.N., Saari, M., Gbadebo, A.O. and Jacdonmi, I. 2015, "Impacts of land use change on peatland degradation: a review", *Ethiopian Journal of Environmental Studies and Management*, vol. 8, no. 2, pp. 225-234.
315. Tsvetkov, P.S. 2017, "The history, present status and future prospects of the Russian fuel peat industry", *Mires and Peat*, vol. 19, no. 14, pp. 1-12
316. Lees, K.J., Artz, R.R., Khomik, M., Clark, J.M., Ritson, J., Hancock, M.H., Cowie, N.R. and Quaipe, T. 2020, "Using spectral indices to estimate water content and GPP in Sphagnum moss and other peatland vegetation", *IEEE Transactions on Geoscience and Remote Sensing*, vol. 58, no. 7, pp. 4547-4557.
317. Tampuu, T., Praks, J., Uiboupin, R. and Kull, A. 2020, "Long term interferometric temporal coherence and DInSAR phase in Northern Peatlands", *Remote Sensing*, vol. 12, no. 10, pp. 1566.
318. Medcalf, K.A., Jarman, M.W. and Keyworth, S.J. 2010, "Assessing the extent and severity of erosion on the upland organic soils of Scotland using earth observation and object orientated classification methods " eds. E.A. Addink and F. VanCoillie, Int Soc Photogrammetry and Remote Sensing; COPERNICUS GESELLSCHAFT MBH, BAHNHOFALLE 1E, GOTTINGEN, 37081, GERMANY.
319. Connolly, J., Holden, N.M., Connolly, J., Seaquist, J.W. and Ward, S.M. 2011, "Detecting recent disturbance on Montane blanket bogs in the Wicklow Mountains, Ireland using the MODIS enhanced vegetation index", *International Journal of Remote Sensing*, vol. 32, no. 9, pp. 2377-2393.
320. Aitkenhead, M. and Coull, M. 2020, "Mapping soil profile depth, bulk density and carbon stock in Scotland using remote sensing and spatial covariates", *European Journal of Soil Science*, vol. 71, no. 4, pp. 553-567.
321. Lees, K.J., Quaipe, T., Artz, R., Khomik, M., Sottocornola, M., Kiely, G., Hambley, G., Hill, T., Saunders, M. and Cowie, N.R. 2019, "A model of gross primary productivity based on satellite data suggests formerly afforested peatlands undergoing restoration regain full photosynthesis capacity after five to ten years", *Journal of environmental management*, vol. 246, pp. 594-604.
322. Williamson, J., Rowe, E., Reed, D., Ruffino, L., Jones, P., Dolan, R., Buckingham, H., Norris, D., Astbury, S. and Evans, C.D. 2017, "Historical peat loss explains limited short-term response of drained blanket bogs to rewetting", *Journal of environmental management*, vol. 188, pp. 278-286.
323. Patberg, W., Baaijens, G.J., Smolders, A.J., Grootjans, A.P. and Elzenga, J.T.M. 2013, "The importance of groundwater-derived carbon dioxide in the restoration of small Sphagnum bogs", *Preslia*, vol. 85, no. 3, pp. 389-403.
324. Henman, J. and Poulter, B. 2008, "Inundation of freshwater peatlands by sea-level rise: uncertainty and potential carbon cycle feedbacks", *Journal of Geophysical Research: Biogeosciences*, vol. 113, no. G1.
325. Connolly, J. and Holden, N.M. 2011, "Mapping peatland disturbance in Ireland: an object oriented approach", *Remote Sensing for Agriculture, Ecosystems, and Hydrology XIII* International Society for Optics and Photonics.
326. Gunnarsson, U., Borešjö Bronge, L., Rydin, H. and Ohlson, M. 2008, "Near-zero recent carbon accumulation in a bog with high nitrogen deposition in SW Sweden", *Global Change Biology*, vol. 14, no. 9, pp. 2152-2165.
327. Scholefield, P., Morton, D., McShane, G., Carrasco, L., Whitfield, M.G., Rowland, C., Rose, R., Wood, C., Tebbs, E. and Dodd, B. 2019, "Estimating habitat extent and carbon loss from an eroded northern blanket bog using UAV derived imagery and topography", *Progress in Physical Geography: Earth and Environment*, vol. 43, no. 2, pp. 282-298.
328. Borge, A.F., Westermann, S., Solheim, I. and Etzelmüller, B. 2017, "Strong degradation of palsas and peat plateaus in northern Norway during the last 60 years", *The Cryosphere*, vol. 11, no. 1, pp. 1-16.
329. Chasmer, L., Lima, E.M., Mahoney, C., Hopkinson, C., Montgomery, J. & Cobbaert, D. 2021, "Shrub changes with proximity to anthropogenic disturbance in boreal wetlands determined using bi-temporal airborne lidar in the Oil Sands Region, Alberta Canada", *Science of the Total Environment*, vol. 780

- 1 330. Chaudhary, N., Westermann, S., Lamba, S., Shurpali, N., Sannel, A.B.K., Schurgers, G., Miller, P.A. and Smith, B.
2 2020, "Modelling past and future peatland carbon dynamics across the pan-Arctic", *Global Change Biology*, vol. 26, no.
3 7, pp. 4119-4133.
- 4 331. Beamish, A., Reynolds, M.K., Epstein, H., Frost, G.V., Macander, M.J., Bergstedt, H., Bartsch, A., Kruse, S., Miles, V.
5 and Tanis, C.M. 2020, "Recent trends and remaining challenges for optical remote sensing of Arctic tundra vegetation:
6 A review and outlook", *Remote Sensing of Environment*, vol. 246, pp. 111872.
- 7 332. Kirkwood, A., Roy-Léveillé, P., Packalen, M., McLaughlin, J. and Basiliko, N. 2019, "Evolution of Palsas and Peat
8 Plateaus in the Hudson Bay Lowlands: Permafrost Degradation and the Production of Greenhouse Gases" in *Cold
9 Regions Engineering 2019 American Society of Civil Engineers Reston, VA*, pp. 597-606.
- 10 333. Korpela, I., Haapanen, R., Korrensalo, A., Tuittila, E.S. and Vesala, T. 2020, "Fine-resolution mapping of microforms
11 of a boreal bog using aerial images and waveform-recording LiDAR", *Mires and Peat*.
- 12 334. Jones, M.C., Grosse, G., Jones, B.M. and Walter Anthony, K. 2012, "Peat accumulation in drained thermokarst lake
13 basins in continuous, ice-rich permafrost, northern Seward Peninsula, Alaska", *Journal of Geophysical Research:
14 Biogeosciences*, vol. 117, no. G2.
- 15 335. Sannel, A. and Kuhry, P. 2011, "Warming-induced destabilization of peat plateau/thermokarst lake complexes", *Journal
16 of Geophysical Research: Biogeosciences*, vol. 116, no. G3.
- 17 336. Podest, E., McDonald, K.C. and Kimball, J.S. 2014, "Multisensor microwave sensitivity to freeze/thaw dynamics across
18 a complex boreal landscape", *IEEE Transactions on Geoscience and Remote Sensing*, vol. 52, no. 11, pp. 6818-6828.
- 19 337. Minsley, B.J., Abraham, J.D., Smith, B.D., Cannia, J.C., Voss, C.I., Jorgenson, M.T., Walvoord, M.A., Wylie, B.K.,
20 Anderson, L. & Ball, L.B. 2012, "Airborne electromagnetic imaging of discontinuous permafrost", *Geophysical
21 Research Letters*, vol. 39, no. 2.
- 22 338. Cooley, S.W., Smith, L.C., Ryan, J.C., Pitcher, L.H. and Pavelsky, T.M. 2019, "Arctic-Boreal lake dynamics revealed
23 using CubeSat imagery", *Geophysical Research Letters*, vol. 46, no. 4, pp. 2111-2120.
- 24 339. Bourgeau-Chavez, L.L., Endres, S., Powell, R., Battaglia, M.J., Benschoter, B., Turetsky, M., Kasischke, E.S. and
25 Banda, E. 2017, "Mapping boreal peatland ecosystem types from multitemporal radar and optical satellite imagery",
26 *Canadian Journal of Forest Research*, vol. 47, no. 4, pp. 545-559.
- 27 340. Tan, Z., Zhuang, Q., Henze, D.K., Frankenberg, C., Dlugokencky, E., Sweeney, C., Turner, A.J., Sasakawa, M. and
28 Machida, T. 2016, "Inverse modeling of pan-Arctic methane emissions at high spatial resolution: what can we learn
29 from assimilating satellite retrievals and using different process-based wetland and lake biogeochemical
30 models?", *Atmospheric Chemistry and Physics*, vol. 16, no. 19, pp. 12649-12666.
- 31 341. Watts, J.D., Kimball, J.S., Bartsch, A. and McDonald, K.C. 2014, "Surface water inundation in the boreal-Arctic:
32 potential impacts on regional methane emissions", *Environmental Research Letters*, vol. 9, no. 7, pp. 075001.
- 33 342. Hugelius, G., Kuhry, P., Tarnocai, C. and Virtanen, T. 2010, "Soil organic carbon pools in a periglacial landscape: a
34 case study from the central Canadian Arctic", *Permafrost and Periglacial Processes*, vol. 21, no. 1, pp. 16-29.
- 35 343. Sheng, Y., Smith, L.C., MacDonald, G.M., Kremenetski, K.V., Frey, K.E., Velichko, A.A., Lee, M., Beilman, D.W.
36 and Dubinin, P. 2004, "A high-resolution GIS-based inventory of the west Siberian peat carbon pool", *Global
37 Biogeochemical Cycles*, vol. 18, no. 3.
- 38 344. Takeuchi, W., Nakano, T., Ochi, S. and Yasuoka, Y. 2002, "Estimation of methane emission from West Siberian
39 Lowland with sub-pixel land cover characterization", *IEEE International Geoscience and Remote Sensing
40 Symposium IEEE*, pp. 2351.
- 41 345. DeLancey, E.R., Kariyeva, J., Bried, J.T. and Hird, J.N. 2019, "Large-scale probabilistic identification of boreal
42 peatlands using Google Earth Engine, open-access satellite data, and machine learning", *PLoS one*, vol. 14, no. 6, pp.
43 e0218165.
- 44 346. McPartland, M.Y., Falkowski, M.J., Reinhardt, J.R., Kane, E.S., Kolka, R., Turetsky, M.R., Douglas, T.A., Anderson,
45 J., Edwards, J.D. and Palik, B. 2019 a, "Characterizing boreal peatland plant composition and species diversity with
46 hyperspectral remote sensing", *Remote Sensing*, vol. 11, no. 14, pp. 1685.
- 47 347. McPartland, M.Y., Kane, E.S., Falkowski, M.J., Kolka, R., Turetsky, M.R., Palik, B. and Montgomery, R.A. 2019 b,
48 "The response of boreal peatland community composition and NDVI to hydrologic change, warming, and elevated
49 carbon dioxide", *Global Change Biology*, vol. 25, no. 1, pp. 93-107.
- 50 348. Warren, R.K., Pappas, C., Helbig, M., Chasmer, L.E., Berg, A.A., Baltzer, J.L., Quinton, W.L. and Sonnentag, O. 2018,
51 "Minor contribution of overstorey transpiration to landscape evapotranspiration in boreal permafrost
52 peatlands", *Ecohydrology*, vol. 11, no. 5, pp. e1975.
- 53 349. Potter, C. 2018, "Recovery rates of wetland vegetation greenness in severely burned ecosystems of Alaska derived from
54 satellite image analysis", *Remote Sensing*, vol. 10, no. 9, pp. 1456.
- 55 350. Evangelidou, N., Kylling, A., Eckhardt, S., Myroniuk, V., Stebel, K., Paugam, R., Zibitsev, S. and Stohl, A. 2019, "Open
56 fires in Greenland in summer 2017: transport, deposition and radiative effects of BC, OC and BrC
57 emissions", *Atmospheric Chemistry and Physics*, vol. 19, no. 2, pp. 1393-1411.
- 58 351. Kasischke, E.S., Goetz, S.J., Kimball, J.S. and Mack, M.M. 2010, "The Arctic-Boreal Vulnerability Experiment
59 (ABoVE): A concise plan for a NASA-sponsored field campaign", Final report on the VuRSAL/ABoVE scoping Study.
- 60 352. Ballhorn, U., Siegert, F., Mason, M. and Limin, S. 2009, "Derivation of burn scar depths and estimation of carbon
emissions with LIDAR in Indonesian peatlands", *Proceedings of the National Academy of Sciences*, vol. 106, no. 50,
pp. 21213-21218.

- 1 353. Van der Werf, Guido R, Randerson, J.T., Giglio, L., Collatz, G.J., Mu, M., Kasibhatla, P.S., Morton, D.C., DeFries,
2 R.S., Jin, Y.v. and van Leeuwen, T.T. 2010, "Global fire emissions and the contribution of deforestation, savanna,
3 forest, agricultural, and peat fires (1997–2009)", *Atmospheric chemistry and physics*, vol. 10, no. 23, pp. 11707-11735.
- 4 354. Fokeeva, E.V., Safronov, A.N., Rakitin, V.S., Yurganov, L.N., Grechko, E.I. and Shumskii, R.A. 2011, "Investigation
5 of the 2010 July–August fires impact on carbon monoxide atmospheric pollution in Moscow and its outskirts,
6 estimating of emissions", *Izvestiya, Atmospheric and Oceanic Physics*, vol. 47, no. 6, pp. 682-698.
- 7 355. Shi, Y., Sasai, T. and Yamaguchi, Y. 2014, "Spatio-temporal evaluation of carbon emissions from biomass burning in
8 Southeast Asia during the period 2001–2010", *Ecological Modelling*, vol. 272, pp. 98-115.
- 9 356. Dadap, N.C., Cobb, A.R., Hoyt, A.M., Harvey, C.F. and Konings, A.G. 2019, "Satellite soil moisture observations
10 predict burned area in Southeast Asian peatlands", *Environmental Research Letters*, vol. 14, no. 9, pp. 094014.
- 11 357. Kiely, L., Spracklen, D.V., Wiedinmyer, C., Conibear, L., Reddington, C.L., Archer-Nicholls, S., Lowe, D., Arnold,
12 S.R., Knote, C. and Khan, M.F. 2019, "New estimate of particulate emissions from Indonesian peat fires in
13 2015", *Atmospheric Chemistry and Physics*, vol. 19, no. 17, pp. 11105-11121.
- 14 358. Poulter, B., Christensen Jr, N.L. and Halpin, P.N. 2006, "Carbon emissions from a temperate peat fire and its relevance
15 to interannual variability of trace atmospheric greenhouse gases", *Journal of Geophysical Research: Atmospheres*, vol.
16 111, no. D6.
- 17 359. VETRITA, Y. and COCHRANE, M.A. 2019, "Annual Burned Area from Landsat, Mawas, Central Kalimantan,
18 Indonesia, 1997-2015", *ORNL DAAC*.
- 19 360. Andela, N., Morton, D.C., Giglio, L. and Randerson, J.T. 2019, "Global Fire Atlas with Characteristics of Individual
20 Fires, 2003-2016", *ORNL DAAC*.
- 21 361. Nitze, I., Grosse, G., Jones, B.M., Romanovsky, V.E. & Boike, J. 2018, "Remote sensing quantifies widespread
22 abundance of permafrost region disturbances across the Arctic and Subarctic", *Nature communications*, vol. 9, no. 1,
23 pp. 1-11.
- 24 362. Jones, B.M., Grosse, G., Arp, C.D., Miller, E., Liu, L., Hayes, D.J. & Larsen, C.F. 2015, "Recent Arctic tundra fire
25 initiates widespread thermokarst development", *Scientific reports*, vol. 5, no. 1, pp. 1-13.
- 26 363. Abe, T., Iwahana, G., Efremov, P.V., Desyatkin, A.R., Kawamura, T., Fedorov, A., Zhegusov, Y., Yanagiya, K. &
27 Tadono, T. 2020, "Surface displacement revealed by L-band InSAR analysis in the Mayya area, Central Yakutia,
28 underlain by continuous permafrost", *Earth, Planets and Space*, vol. 72, no. 1, pp. 1-16.
- 29 364. Iwahana, G., Uchida, M., Liu, L., Gong, W., Meyer, F.J., Guritz, R., Yamanokuchi, T. & Hinzman, L. 2016, "InSAR
30 detection and field evidence for thermokarst after a tundra wildfire, using ALOS-PALSAR", *Remote Sensing*, vol. 8,
31 no. 3, pp. 218.
- 32 365. Schaefer, K., Elshorbany, Y., Jafarov, E., Schuster, P.F., Striegl, R.G., Wickland, K.P. & Sunderland, E.M. 2020,
33 "Potential impacts of mercury released from thawing permafrost", *Nature communications*, vol. 11, no. 1, pp. 1-6.
- 34 366. French, N.H., Graham, J., Whitman, E. and Bourgeau-Chavez, L.L., 2020. Quantifying surface severity of the 2014 and
35 2015 fires in the Great Slave Lake area of Canada. *International journal of wildland fire*, 29(10), pp.892-906.
- 36 367. Turetsky, M.R., Abbott, B.W., Jones, M.C., Anthony, K.W., Olefeldt, D., Schuur, E.A., Koven, C., McGuire, A.D.,
37 Grosse, G. & Kuhry, P. 2019, "Permafrost collapse is accelerating carbon release".
- 38 368. Wieder, R.K., Vitt, D.H. & Benscoter, B.W. 2006, "Peatlands and the boreal forest" in *Boreal peatland
39 ecosystems* Springer, , pp. 1-8.
- 40 369. Page, S.E., Rieley, J.O. and Banks, C.J. 2011, "Global and regional importance of the tropical peatland carbon pool",
41 *Global Change Biology*, vol. 17, no. 2, pp. 798-818.
- 42 370. Poulter, B., Fluet-Chouinard, E., Hugelius, G., Koven, C., Fatoyinbo, L., Page, S.E., Rosentreter, J.A., Smart, L.S.,
43 Taillie, P.J. & Thomas, N. 2021, "A review of global wetland carbon stocks and management challenges", *Wetland
44 Carbon and Environmental Management*, pp. 1-20.
- 45 371. Rieley, J. and Page, S. 2016, "Tropical peatland of the world" in *Tropical peatland ecosystems* Springer, pp. 3-32.
- 46 372. Lähteenoja, O., Ruokolainen, K., Schulman, L. & Oinonen, M. 2009, "Amazonian peatlands: an ignored C sink and
47 potential source", *Global Change Biology*, vol. 15, no. 9, pp. 2311-2320.
- 48 373. Chimner, R.A. 2004, "Soil respiration rates of tropical peatlands in Micronesia and Hawaii", *Wetlands*, vol. 24, no. 1,
49 pp. 51-56.
- 50 374. Chimner, R.A. & Karberg, J.M. 2008, "Long-term carbon accumulation in two tropical mountain peatlands, Andes
51 Mountains, Ecuador.", *Mires & Peat*, vol. 3.
- 52 375. Schuur, E.A., Bockheim, J., Canadell, J.G., Euskirchen, E., Field, C.B., Goryachkin, S.V., Hagemann, S., Kuhry, P.,
53 Lafleur, P.M. and Lee, H. 2008, "Vulnerability of permafrost carbon to climate change: Implications for the global
54 carbon cycle", *Bioscience*, vol. 58, no. 8, pp. 701-714.
- 55 376. Schuur, E.A., McGuire, A.D., Schädel, C., Grosse, G., Harden, J.W., Hayes, D.J., Hugelius, G., Koven, C.D., Kuhry, P.
56 and Lawrence, D.M. 2015, "Climate change and the permafrost carbon feedback", *Nature*, vol. 520, no. 7546, pp. 171-
57 179.
- 58 377. Gibson, C.M., Chasmer, L.E., Thompson, D.K., Quinton, W.L., Flannigan, M.D. and Olefeldt, D. 2018, "Wildfire as a
59 major driver of recent permafrost thaw in boreal peatlands", *Nature communications*, vol. 9, no. 1, pp. 1-9.
- 60 378. Hugelius, G., Strauss, J., Zubrzycki, S., Harden, J.W., Schuur, E., Ping, C., Schirrmeister, L., Grosse, G., Michaelson,
G.J. and Koven, C.D. 2014, "Estimated stocks of circumpolar permafrost carbon with quantified uncertainty ranges and
identified data gaps", *Biogeosciences*, vol. 11, no. 23, pp. 6573-6593.

379. Gumbrecht, T., Roman-Cuesta, R.M., Verchot, L., Herold, M., Wittmann, F., Householder, E., Herold, N. and Murdiyarto, D. 2017, "An expert system model for mapping tropical wetlands and peatlands reveals South America as the largest contributor", *Global Change Biology*, vol. 23, no. 9, pp. 3581-3599.
380. Gruber, S. 2012, "Derivation and analysis of a high-resolution estimate of global permafrost zonation", *The Cryosphere*, vol. 6, no. 1, pp. 221-233.
381. Joosten, H. 2009, "The Global Peatland CO₂ Picture: peatland status and drainage related emissions in all countries of the world.", *The Global Peatland CO₂ Picture: peatland status and drainage related emissions in all countries of the world*
382. Gallego-Sala, A.V., Charman, D.J., Brewer, S., Page, S.E., Prentice, I.C., Friedlingstein, P., Moreton, S., Amesbury, M.J., Beilman, D.W. & Björck, S. 2018, "Latitudinal limits to the predicted increase of the peatland carbon sink with warming", *Nature Climate Change*, vol. 8, no. 10, pp. 907-913
383. Schaphoff, S., Heyder, U., Ostberg, S., Gerten, D., Heinke, J. & Lucht, W. 2013, "Contribution of permafrost soils to the global carbon budget", *Environmental Research Letters*, vol. 8, no. 1, pp. 014026.
384. Leifeld, J., Wüst-Galley, C. & Page, S. 2019, "Intact and managed peatland soils as a source and sink of GHGs from 1850 to 2100", *Nature Climate Change*, vol. 9, no. 12, pp. 945-947.
385. Cole, J.J., Prairie, Y.T., Caraco, N.F., McDowell, W.H., Tranvik, L.J., Striegl, R.G., Duarte, C.M., Kortelainen, P., Downing, J.A. and Middelburg, J.J. 2007, "Plumbing the global carbon cycle: integrating inland waters into the terrestrial carbon budget", *Ecosystems*, vol. 10, no. 1, pp. 172-185.
386. Tranvik, L.J., Downing, J.A., Cotner, J.B., Loiselle, S.A., Striegl, R.G., Ballatore, T.J., Dillon, P., Finlay, K., Fortino, K. and Knoll, L.B. 2009, "Lakes and reservoirs as regulators of carbon cycling and climate", *Limnology and Oceanography*, vol. 54, no. 6part2, pp. 2298-2314.
387. Williamson, C.E., Saros, J.E., Vincent, W.F. and Smol, J.P. 2009, "Lakes and reservoirs as sentinels, integrators, and regulators of climate change", *Limnology and Oceanography*, vol. 54, no. 6part2, pp. 2273-2282.
388. Buffam, I., Turner, M.G., Desai, A.R., Hanson, P.C., Rusak, J.A., Lottig, N.R., Stanley, E.H. and Carpenter, S.R. 2011, "Integrating aquatic and terrestrial components to construct a complete carbon budget for a north temperate lake district", *Global Change Biology*, vol. 17, no. 2, pp. 1193-1211.
389. Bennington, V., McKinley, G.A., Urban, N.R. and McDonald, C.P. 2012, "Can spatial heterogeneity explain the perceived imbalance in Lake Superior's carbon budget? A model study", *Journal of Geophysical Research: Biogeosciences*, vol. 117, no. G3.
- Lohila, A., Tuovinen, J., Hatakka, J., Aurela, M., Vuorenmaa, J., Haakana, M. and Laurila, T. 2015, "Carbon dioxide and energy fluxes over a northern boreal lake"
390. Williamson, C.E., Saros, J.E., Vincent, W.F. & Smol, J.P. 2009, "Lakes and reservoirs as sentinels, integrators, and regulators of climate change", *Limnology and Oceanography*, vol. 54, no. 6part2, pp. 2273-2282
391. Larsen, S., Andersen, T. and Hessen, D.O. 2011, "Climate change predicted to cause severe increase of organic carbon in lakes", *Global Change Biology*, vol. 17, no. 2, pp. 1186-1192.
392. Moss, B., Kosten, S., Meerhoff, M., Battarbee, R.W., Jeppesen, E., Mazzeo, N., Havens, K., Lacerot, G., Liu, Z. and De Meester, L. 2011, "Allied attack: climate change and eutrophication", *Inland waters*, vol. 1, no. 2, pp. 101-105.
393. Bergmann, T., Fahnenstiel, G., Lohrenz, S., Millie, D. and Schofield, O. 2004, "Impacts of a recurrent resuspension event and variable phytoplankton community composition on remote sensing reflectance", *Journal of Geophysical Research: Oceans*, vol. 109, no. C10.
394. Gons, H.J., Auer, M.T. and Effler, S.W. 2008, "MERIS satellite chlorophyll mapping of oligotrophic and eutrophic waters in the Laurentian Great Lakes", *Remote Sensing of Environment*, vol. 112, no. 11, pp. 4098-4106.
395. Lohrenz, S.E., Fahnenstiel, G.L., Schofield, O. and Millie, D.F. 2008, "Coastal Sediment Dynamics and River Discharge as Key Factors Influencing: Coastal Ecosystem Productivity in Southeastern Lake Michigan", *Oceanography*, vol. 21, no. 4, pp. 60-69.
396. Hunter, P.D., Tyler, A.N., Carvalho, L., Codd, G.A. and Maberly, S.C. 2010, "Hyperspectral remote sensing of cyanobacterial pigments as indicators for cell populations and toxins in eutrophic lakes", *Remote Sensing of Environment*, vol. 114, no. 11, pp. 2705-2718.
397. Shuchman, R.A., Sayers, M., Fahnenstiel, G.L. and Leshkevich, G. 2013, "A model for determining satellite-derived primary productivity estimates for Lake Michigan", *Journal of Great Lakes Research*, vol. 39, pp. 46-54.
398. Fahnenstiel, G.L., Sayers, M.J., Shuchman, R.A., Yousef, F. and Pothoven, S.A. 2016, "Lake-wide phytoplankton production and abundance in the Upper Great Lakes: 2010–2013", *Journal of Great Lakes Research*, vol. 42, no. 3, pp. 619-629.
399. Sayers, M.J., Grimm, A.G., Shuchman, R.A., Deines, A.M., Bunnell, D.B., Raymer, Z.B., Rogers, M.W., Woelmer, W., Bennion, D.H. and Brooks, C.N. 2015, "A new method to generate a high-resolution global distribution map of lake chlorophyll", *International Journal of Remote Sensing*, vol. 36, no. 7, pp. 1942-1964.
400. Ho, J.C., Michalak, A.M. and Pahlevan, N. 2019, "Widespread global increase in intense lake phytoplankton blooms since the 1980s", *Nature*, vol. 574, no. 7780, pp. 667-670.
401. Mouw, C.B., Greb, S., Aurin, D., DiGiacomo, P.M., Lee, Z., Twardowski, M., Binding, C., Hu, C., Ma, R. and Moore, T. 2015, "Aquatic color radiometry remote sensing of coastal and inland waters: Challenges and recommendations for future satellite missions", *Remote Sensing of Environment*, vol. 160, pp. 15-30.

402. Werdell, P. J. *et al.* The Plankton, Aerosol, Cloud, ocean Ecosystem mission: status, science, advances. *Bull. Am. Meteorol. Soc.* **100**, 1775-1794 (2019).
403. Sayers, M., Bosse, K., Fahnenstiel, G. and Shuchman, R. 2020, "Carbon Fixation Trends in Eleven of the World's Largest Lakes: 2003–2018", *Water*, vol. 12, no. 12, pp. 3500.
404. Sayers, M.J., Fahnenstiel, G.L., Shuchman, R.A. and Bosse, K.R. 2021, "A new method to estimate global freshwater phytoplankton carbon fixation using satellite remote sensing: initial results", *International Journal of Remote Sensing*, vol. 42, no. 10, pp. 3708-3730.
405. Verpoorter, C., Kutser, T., Seekell, D.A. & Tranvik, L.J. 2014, "A global inventory of lakes based on high-resolution satellite imagery", *Geophysical Research Letters*, vol. 41, no. 18, pp. 6396-6402.
406. Mendonça, R., Müller, R.A., Clow, D., Verpoorter, C., Raymond, P., Tranvik, L.J. and Sobek, S. 2017, "Organic carbon burial in global lakes and reservoirs", *Nature communications*, vol. 8, no. 1, pp. 1-7.
407. Lewis Jr, W.M. 2011, "Global primary production of lakes: 19th Baldi Memorial Lecture", *Inland Waters*, vol. 1, no. 1, pp. 1-28.
408. Einsele G, Yan J, Hinderer M. 2001. Atmospheric carbon burial in modern lake basins and its significance for the global carbon budget. *Global Planet Change* 30:167–95
409. Bastviken, D., Tranvik, L.J., Downing, J.A., Crill, P.M. and Enrich-Prast, A. 2011, "Freshwater methane emissions offset the continental carbon sink", *Science*, vol. 331, no. 6013, pp. 50.
410. Warner, D.M. and Lesht, B.M. 2015, "Relative importance of phosphorus, invasive mussels and climate for patterns in chlorophyll a and primary production in Lakes Michigan and Huron", *Freshwater Biology*, vol. 60, no. 5, pp. 1029-1043.
411. Kauer, T., Kutser, T., Arst, H., Danckaert, T. and Nöges, T. 2015, "Modelling primary production in shallow well mixed lakes based on MERIS satellite data", *Remote Sensing of Environment*, vol. 163, pp. 253-261.
412. Soomets, T., Kutser, T., Wüest, A. and Bouffard, D. 2019, "Spatial and temporal changes of primary production in a deep peri-alpine lake", *Inland Waters*, vol. 9, no. 1, pp. 49-60.
413. McDonald, C.P., Rover, J.A., Stets, E.G. and Striegl, R.G. 2012, "The regional abundance and size distribution of lakes and reservoirs in the United States and implications for estimates of global lake extent", *Limnology and Oceanography*, vol. 57, no. 2, pp. 597-606.
414. Kuhn, C., Bogard, M., Johnston, S.E., John, A., Vermote, E., Spencer, R., Dornblaser, M., Wickland, K., Striegl, R. & Butman, D. 2020, "Satellite and airborne remote sensing of gross primary productivity in boreal Alaskan lakes", *Environmental Research Letters*, vol. 15, no. 10, pp. 105001.
415. Bogard, M.J., Kuhn, C.D., Johnston, S.E., Striegl, R.G., Holtgrieve, G.W., Dornblaser, M.M., Spencer, R.G., Wickland, K.P. & Butman, D.E. 2019, "Negligible cycling of terrestrial carbon in many lakes of the arid circumpolar landscape", *Nature Geoscience*, vol. 12, no. 3, pp. 180-185.
416. Kuhn, C. & Butman, D. 2021, "Declining greenness in Arctic-boreal lakes", *Proceedings of the National Academy of Sciences*, vol. 118, no. 15.
417. Rey, D.M., Walvoord, M., Minsley, B., Rover, J. & Singha, K. 2019, "Investigating lake-area dynamics across a permafrost-thaw spectrum using airborne electromagnetic surveys and remote sensing time-series data in Yukon Flats, Alaska", *Environmental Research Letters*, vol. 14, no. 2, pp. 025001.
418. Palmer, S.C., Kutser, T. and Hunter, P.D. 2015, "Remote sensing of inland waters: Challenges, progress and future directions", *Remote Sensing of Environment*.
419. Mishra, D.R., Ogashawara, I. and Gitelson, A.A. 2017, *Bio-optical modeling and remote sensing of inland waters*, Elsevier.
420. Tyler, A.N., Hunter, P.D., Spyarakos, E., Neil, C., Simis, S., Groom, S., Merchant, C.J., Miller, C.A., O'Donnell, R. and Scott, E.M. 2017, "A Global Observatory of Lake Water Quality", *EGU General Assembly Conference Abstracts*, pp. 10609.
421. Zhu, W., Yu, Q., Tian, Y.Q., Becker, B.L., Zheng, T. & Carrick, H.J. 2014, "An assessment of remote sensing algorithms for colored dissolved organic matter in complex freshwater environments", *Remote Sensing of Environment*, vol. 140, pp. 766-778.
422. Li, J., Yu, Q., Tian, Y.Q., Becker, B.L., Siqueira, P. & Torbick, N. 2018, "Spatio-temporal variations of CDOM in shallow inland waters from a semi-analytical inversion of Landsat-8", *Remote Sensing of Environment*, vol. 218, pp. 189-200.
423. Brezonik, P.L., Olmanson, L.G., Finlay, J.C. and Bauer, M.E. 2015, "Factors affecting the measurement of CDOM by remote sensing of optically complex inland waters", *Remote Sensing of Environment*, vol. 157, pp. 199-215.
424. Kutser, T., Casal Pascual, G., Barbosa, C., Paavel, B., Ferreira, R., Carvalho, L. and Toming, K. 2016, "Mapping inland water carbon content with Landsat 8 data", *International Journal of Remote Sensing*, vol. 37, no. 13, pp. 2950-2961.
425. Lohrenz, S.E., Cai, W., Chakraborty, S., Huang, W., Guo, X., He, R., Xue, Z., Fennel, K., Howden, S. and Tian, H. 2018, "Satellite estimation of coastal $p\text{CO}_2$ and air-sea flux of carbon dioxide in the northern Gulf of Mexico", *Remote Sensing of Environment*, vol. 207, pp. 71-83.
426. Ouyang, Z., Shao, C., Chu, H., Becker, R., Bridgeman, T., Stepien, C.A., John, R. and Chen, J. 2017, "The effect of algal blooms on carbon emissions in western Lake Erie: An integration of remote sensing and eddy covariance measurements", *Remote Sensing*, vol. 9, no. 1, pp. 44.

- 1
2
3
4
5
6
7
8
9
10
11
12
13
14
15
16
17
18
19
20
21
22
23
24
25
26
27
28
29
30
31
32
33
34
35
36
37
38
39
40
41
42
43
44
45
46
47
48
49
50
51
52
53
54
55
56
57
58
59
60
427. Kutser, T., Verpoorter, C., Paavel, B. and Tranvik, L.J. 2015, "Estimating lake carbon fractions from remote sensing data", *Remote Sensing of Environment*, vol. 157, pp. 138-146.
428. Battin, T.J., Luysaert, S., Kaplan, L.A., Aufdenkampe, A.K., Richter, A. and Tranvik, L.J. 2009, "The boundless carbon cycle", *Nature Geoscience*, vol. 2, no. 9, pp. 598-600.
429. Aufdenkampe, A.K., Mayorga, E., Raymond, P.A., Melack, J.M., Doney, S.C., Alin, S.R., Aalto, R.E. and Yoo, K. 2011, "Riverine coupling of biogeochemical cycles between land, oceans, and atmosphere", *Frontiers in Ecology and the Environment*, vol. 9, no. 1, pp. 53-60.
430. Wehrli, B. 2013, "Conduits of the carbon cycle", *Nature*, vol. 503, no. 7476, pp. 346-347.
431. Raymond, P.A., Hartmann, J., Lauerwald, R., Sobek, S., McDonald, C., Hoover, M., Butman, D., Striegl, R., Mayorga, E. and Humborg, C. 2013, "Global carbon dioxide emissions from inland waters", *Nature*, vol. 503, no. 7476, pp. 355-359.
432. Sawakuchi, H.O., Neu, V., Ward, N.D., Barros, Maria de Lourdes C, Valerio, A.M., Gagne-Maynard, W., Cunha, A.C., Less, D.F., Diniz, J.E. and Brito, D.C. 2017, "Carbon dioxide emissions along the lower Amazon River", *Frontiers in Marine Science*, vol. 4, pp. 76.
433. Tranvik, L.J., Cole, J.J. and Prairie, Y.T. 2018, "The study of carbon in inland waters—from isolated ecosystems to players in the global carbon cycle", *Limnology and Oceanography Letters*, vol. 3, no. 3, pp. 41-48.
434. Drake, T.W., Raymond, P.A. and Spencer, R.G. 2018, "Terrestrial carbon inputs to inland waters: A current synthesis of estimates and uncertainty", *Limnology and Oceanography Letters*, vol. 3, no. 3, pp. 132-142.
435. Vachon, D., Sponseller, R.A. and Karlsson, J. 2021, "Integrating carbon emission, accumulation and transport in inland waters to understand their role in the global carbon cycle", *Global Change Biology*, vol. 27, no. 4, pp. 719-727.
436. USGCRP 2018. Second State of the Carbon Cycle Report (SOCCR2): A Sustained Assessment Report [Cavallaro, N., G. Shrestha, R. Birdsey, M. A. Mayes, R. G. Najjar, S. C. Reed, P. Romero-Lankao, and Z. Zhu (eds)]. U.S. Global Change Research Program, Washington, DC, USA. <https://carbon2018.globalchange.gov/>.
437. Stets, E.G. and Striegl, R.G. 2012, "Carbon export by rivers draining the conterminous United States", *Inland Waters*, vol. 2, no. 4, pp. 177-184.
438. Meybeck, M. 1982, "Carbon, nitrogen, and phosphorus transport by world rivers", *Am.J.Sci.*, vol. 282, no. 4, pp. 401-450.
439. Meybeck, M. and Ragu, A. 2012, "GEMS-GLORI world river discharge database", *Laboratoire de Géologie Appliquée, Université Pierre et Marie Curie, Paris, France*.
440. Li, M., Peng, C., Wang, M., Xue, W., Zhang, K., Wang, K., Shi, G. and Zhu, Q. 2017, "The carbon flux of global rivers: a re-evaluation of amount and spatial patterns", *Ecological Indicators*, vol. 80, pp. 40-51.
441. Karaska, M.A., Huguenin, R.L., Beacham, J.L., Wang, M., Jensen, J.R. and Kaufmann, R.S. 2004, "AVIRIS measurements of chlorophyll, suspended minerals, dissolved organic carbon, and turbidity in the Neuse River, North Carolina", *Photogrammetric Engineering and Remote Sensing*, vol. 70, no. 1, pp. 125-133.
442. Herrault, P., Gandois, L., Gascoïn, S., Tananaev, N., Le Dantec, T. and Teisserenc, R. 2016, "Using high spatio-temporal optical remote sensing to monitor dissolved organic carbon in the Arctic river Yenisei", *Remote Sensing*, vol. 8, no. 10, pp. 803.
443. Chen, J., Zhu, W., Tian, Y.Q. and Yu, Q. 2020, "Monitoring dissolved organic carbon by combining Landsat-8 and Sentinel-2 satellites: Case study in Saginaw River estuary, Lake Huron", *Science of The Total Environment*, vol. 718, pp. 137374.
444. Liu, B., D'Sa, E.J. and Joshi, I. 2019a, "Multi-decadal trends and influences on dissolved organic carbon distribution in the Barataria Basin, Louisiana from in-situ and Landsat/MODIS observations", *Remote Sensing of Environment*, vol. 228, pp. 183-202.
445. Liu, D., Pan, D., Bai, Y., He, X., Wang, D., Wei, J. and Zhang, L. 2015, "Remote sensing observation of particulate organic carbon in the Pearl River Estuary", *Remote Sensing*, vol. 7, no. 7, pp. 8683-8704.
446. Del Castillo, C.E. and Miller, R.L. 2008, "On the use of ocean color remote sensing to measure the transport of dissolved organic carbon by the Mississippi River Plume", *Remote Sensing of Environment*, vol. 112, no. 3, pp. 836-844.
447. Olmanson, L.G., Brezonik, P.L., Finlay, J.C. and Bauer, M.E. 2016, "Comparison of Landsat 8 and Landsat 7 for regional measurements of CDOM and water clarity in lakes", *Remote Sensing of Environment*, vol. 185, pp. 119-128.
448. Massicotte, P., Asmala, E., Stedmon, C. and Markager, S. 2017, "Global distribution of dissolved organic matter along the aquatic continuum: Across rivers, lakes and oceans", *Science of the Total Environment*, vol. 609, pp. 180-191.
449. ChunHock, S., Cherukuru, N., Mujahid, A., Martin, P., Sanwlani, N., Warneke, T., Rixen, T., Notholt, J. and Müller, M. 2020, "A New Remote Sensing Method to Estimate River to Ocean DOC Flux in Peatland Dominated Sarawak Coastal Regions, Borneo", *Remote Sensing*, vol. 12, no. 20, pp. 3380.
450. Liu, D., Bai, Y., He, X., Pan, D., Chen, C.A., Li, T., Xu, Y., Gong, C. and Zhang, L. 2019, "Satellite-derived particulate organic carbon flux in the Changjiang River through different stages of the Three Gorges Dam", *Remote Sensing of Environment*, vol. 223, pp. 154-165.
451. Griffin, C.G., Frey, K.E., Rogan, J. and Holmes, R.M. 2011, "Spatial and interannual variability of dissolved organic matter in the Kolyma River, East Siberia, observed using satellite imagery", *Journal of geophysical research: Biogeosciences*, vol. 116, no. G3.

- 1 452. Larson, M.D., Simic Milas, A., Vincent, R.K. and Evans, J.E. 2018, "Multi-depth suspended sediment estimation using
2 high-resolution remote-sensing UAV in Maumee River, Ohio", *International Journal of Remote Sensing*, vol. 39, no.
3 15-16, pp. 5472-5489.
- 4 453. Su, J., Dai, M., He, B., Wang, L., Gan, J., Guo, X., Zhao, H. & Yu, F. 2017, "Tracing the origin of the oxygen-
5 consuming organic matter in the hypoxic zone in a large eutrophic estuary: the lower reach of the Pearl River Estuary,
6 China", *Biogeosciences*, vol. 14, no. 18, pp. 4085-4099
- 7 454. Richey, J.E., Melack, J.M., Aufdenkampe, A.K., Ballester, V.M. and Hess, L.L. 2002, "Outgassing from Amazonian
8 rivers and wetlands as a large tropical source of atmospheric CO₂", *Nature*, vol. 416, no. 6881, pp. 617-620.
- 9 455. Johnson, M.S., Lehmann, J., Riha, S.J., Krusche, A.V., Richey, J.E., Ometto, J.P.H. and Couto, E.G. 2008, "CO₂ efflux
10 from Amazonian headwater streams represents a significant fate for deep soil respiration", *Geophysical Research
11 Letters*, vol. 35, no. 17.
- 12 456. de Fátima, M., FL Rasera, Maria, Ballester, M.V.R., Krusche, A.V., Salimon, C., Montebelo, L.A., Alin, S.R., Victoria,
13 R.L. and Richey, J.E. 2008, "Estimating the surface area of small rivers in the southwestern Amazon and their role in
14 CO₂ outgassing", *Earth Interactions*, vol. 12, no. 6, pp. 1-16.
- 15 457. de Fátima, M., FL, Krusche, A.V., Richey, J.E., Ballester, M.V. and Victória, R.L. 2013, "Spatial and temporal
16 variability of pCO₂ and CO₂ efflux in seven Amazonian Rivers", *Biogeochemistry*, vol. 116, no. 1, pp. 241-259.
- 17 458. Butman, D. and Raymond, P.A. 2011, "Significant efflux of carbon dioxide from streams and rivers in the United
18 States", *Nature Geoscience*, vol. 4, no. 12, pp. 839-842.
- 19 459. Buto, S.G. and Anderson, R.D., 2020. NHDPlus High Resolution (NHDPlus HR)---A hydrography framework for the
20 Nation (No. 2020-3033). US Geological Survey.
- 21 460. Cole, J.J. and Caraco, N.F. 2001, "Carbon in catchments: connecting terrestrial carbon losses with aquatic
22 metabolism", *Marine and Freshwater Research*, vol. 52, no. 1, pp. 101-110.
- 23 461. Battin, T.J., Kaplan, L.A., Findlay, S., Hopkinson, C.S., Marti, E., Packman, A.I., Newbold, J.D. and Sabater, F. 2008,
24 "Biophysical controls on organic carbon fluxes in fluvial networks", *Nature geoscience*, vol. 1, no. 2, pp. 95-100.
- 25 462. Schiller, D.v., Marcé, R., Obrador, B., Gómez-Gener, L., Casas-Ruiz, J.P., Acuña, V. and Koschorreck, M. 2014,
26 "Carbon dioxide emissions from dry watercourses", *Inland waters*, vol. 4, no. 4, pp. 377-382.
- 27 463. Marcé, R., Obrador, B., Gómez-Gener, L., Catalán, N., Koschorreck, M., Arce, M.I., Singer, G. and von Schiller, D.
28 2019, "Emissions from dry inland waters are a blind spot in the global carbon cycle", *Earth-Science Reviews*, vol. 188,
29 pp. 240-248.
- 30 464. Keller, P.S., Catalán, N., von Schiller, D., Grossart, H., Koschorreck, M., Obrador, B., Frassl, M.A., Karakaya, N.,
31 Barros, N. and Howitt, J.A. 2020, "Global CO₂ emissions from dry inland waters share common drivers across
32 ecosystems", *Nature communications*, vol. 11, no. 1, pp. 1-8.
- 33 465. Downing, J. and Duarte, C.M. 2009, "Lakes (formation, diversity, distribution): abundance and size distribution of
34 lakes, ponds and impoundments", *Encyclopedia of inland waters* (editor-in-chief: GE Likens), , pp. 469-478.
- 35 466. USGS. 2021. U.S. Geological Survey National Elevation Dataset (NED) website.
36 <https://www.sciencebase.gov/catalog/item/4f4e48b1e4b07f02db530759>. Accessed on March 22, 2021.
- 37 467. Lang, M., McDonough, O., McCarty, G., Oesterling, R. and Wilen, B. 2012, "Enhanced detection of wetland-stream
38 connectivity using LiDAR", *Wetlands*, vol. 32, no. 3, pp. 461-473.
- 39 468. Priestnall, G. and Aplin, P. 2006, "Cover: Spatial and temporal remote sensing requirements for river
40 monitoring", *International Journal of Remote Sensing*, vol. 27, no. 11, pp. 2111-2120.
- 41 469. Langat, P.K., Kumar, L. and Koech, R. 2019, "Monitoring river channel dynamics using remote sensing and GIS
42 techniques", *Geomorphology*, vol. 325, pp. 92-102.
- 43 470. Legleiter, C.J. and Harrison, L.R. 2019, "Remote sensing of river bathymetry: Evaluating a range of sensors, platforms,
44 and algorithms on the upper Sacramento River, California, USA", *Water Resources Research*, vol. 55, no. 3, pp. 2142-
45 2169.
- 46 471. Bizzi, S., Demarchi, L., Grabowski, R.C., Weissteiner, C.J. and Van de Bund, W. 2016, "The use of remote sensing to
47 characterise hydromorphological properties of European rivers", *Aquatic Sciences*, vol. 78, no. 1, pp. 57-70.
- 48 472. Tomsett, C. and Leyland, J. 2019, "Remote sensing of river corridors: A review of current trends and future
49 directions", *River Research and Applications*, vol. 35, no. 7, pp. 779-803.
- 50 473. Gleason, C., Garambois, P. and Durand, M. 2017, "Tracking river flows from space", *EOS Earth and Space Science
51 News*, , no. 98.
- 52 474. Frasson, R., Durand, M., Callahan, P., Turk, J., Pottier, C., Biancamaria, S., Williams, B., AND Wei, R. 2018. River
53 Vector Product Status. Montreal, Canada: SWOT 3rd Science Team Meeting.
- 54 475. Stuurman, C. and Pottier, C. 2020. Level 2 KaRIn high rate river single pass vector product Surface Water and Ocean
55 Topography (SWOT) Project, SWOT Product Description. California Institute of Technology. Available online:
56 [https://podaac-tools.jpl.nasa.gov/drive/files/misc/web/misc/swot_mission_docs/pdd/D-
57 56413_SWOT_Product_Description_L2_HR_RiverSP_20200825a.pdf](https://podaac-tools.jpl.nasa.gov/drive/files/misc/web/misc/swot_mission_docs/pdd/D-56413_SWOT_Product_Description_L2_HR_RiverSP_20200825a.pdf)
- 58 476. Stallard, R.F. 1998, "Terrestrial sedimentation and the carbon cycle: Coupling weathering and erosion to carbon
59 burial", *Global Biogeochemical Cycles*, vol. 12, no. 2, pp. 231-257.
- 60 477. Qi, J., Du, X., Zhang, X., Lee, S., Wu, Y., Deng, J., Moglen, G.E., Sadeghi, A.M. and McCarty, G.W. 2020a,
"Modeling riverine dissolved and particulate organic carbon fluxes from two small watersheds in the northeastern
United States", *Environmental Modelling and Software*, vol. 124, pp. 104601.

- 1 478. Qi, J., Zhang, X., Lee, S., Wu, Y., Moglen, G.E. and McCarty, G.W. 2020b, "Modeling sediment diagenesis processes
2 on riverbed to better quantify aquatic carbon fluxes and stocks in a small watershed of the Mid-Atlantic region", *Carbon*
3 *Balance and Management*, vol. 15, no. 1, pp. 1-14.
- 4 479. Allen, G.H. & Pavelsky, T.M. 2018, "Global extent of rivers and streams", *Science*, vol. 361, no. 6402, pp. 585-588.
- 5 480. Rödenbeck, C., Bakker, D.C., Gruber, N., Iida, Y., Jacobson, A.R., Jones, S., Landschützer, P., Metzl, N., Nakaoka, S.
6 and Olsen, A. 2015, "Data-based estimates of the ocean carbon sink variability—first results of the Surface Ocean pCO₂
7 Mapping intercomparison (SOCOM)", *Biogeosciences*, vol. 12, no. 23, pp. 7251-7278.
- 8 481. Buitenhuis, E.T., Hashioka, T. and Quéré, C.L. 2013, "Combined constraints on global ocean primary production using
9 observations and models", *Global Biogeochemical Cycles*, vol. 27, no. 3, pp. 847-858.
- 10 482. Ott, L.E., Pawson, S., Collatz, G.J., Gregg, W.W., Menemenlis, D., Brix, H., Rousseaux, C.S., Bowman, K.W., Liu, J.
11 and Elderling, A. 2015, "Assessing the magnitude of CO₂ flux uncertainty in atmospheric CO₂ records using products
12 from NASA's Carbon Monitoring Flux Pilot Project", *Journal of Geophysical Research: Atmospheres*, vol. 120, no. 2,
13 pp. 734-765.
- 14 483. Berthet, S., Séférian, R., Bricaud, C., Chevallier, M., Voltaire, A. and Ethé, C. 2019, "Evaluation of an online grid-
15 coarsening algorithm in a global eddy-admitting ocean biogeochemical model", *Journal of Advances in Modeling Earth*
16 *Systems*, vol. 11, no. 6, pp. 1759-1783.
- 17 484. Fay, A.R. and McKinley, G.A. 2014, "Global open-ocean biomes: mean and temporal variability", *Earth System*
18 *Science Data*, vol. 6, no. 2, pp. 273-284.
- 19 485. DeVries, T., Le Quéré, C., Andrews, O., Berthet, S., Hauck, J., Ilyina, T., Landschützer, P., Lenton, A., Lima, I.D. and
20 Nowicki, M. 2019, "Decadal trends in the ocean carbon sink", *Proceedings of the National Academy of Sciences*, vol.
21 116, no. 24, pp. 11646-11651.
- 22 486. McKinley, G.A., Pilcher, D.J., Fay, A.R., Lindsay, K., Long, M.C. and Lovenduski, N.S. 2016, "Timescales for
23 detection of trends in the ocean carbon sink", *Nature*, vol. 530, no. 7591, pp. 469-472.
- 24 487. Liao, E., Resplandy, L., Liu, J. and Bowman, K.W. 2020, "Amplification of the Ocean Carbon Sink During El Ninos:
25 Role of Poleward Ekman Transport and Influence on Atmospheric CO₂", *Global Biogeochemical Cycles*, vol. 34, no. 9.
- 26 488. Rödenbeck, C., Keeling, R.F., Bakker, D.C., Metzl, N., Olsen, A., Sabine, C. and Heimann, M. 2013, "Global surface-
27 ocean p CO₂ and sea-air CO₂ flux variability from an observation-driven ocean mixed-layer scheme", *Ocean Science*,
28 vol. 9, no. 2, pp. 193-216.
- 29 489. Landschützer, P., Gruber, N., Bakker, D.C.E. and Schuster, U. 2014, "Recent variability of the global ocean carbon
30 sink", *Global Biogeochemical Cycles*, vol. 28, no. 9, pp. 927-949.
- 31 490. Landschützer, P., Gruber, N. and Bakker, D.C.E. 2016, "Decadal variations and trends of the global ocean carbon
32 sink", *Global Biogeochemical Cycles*, vol. 30, no. 10, pp. 1396-1417.
- 33 491. Watson, A.J., Schuster, U., Shutler, J.D., Holding, T., Ashton, I.G., Landschützer, P., Woolf, D.K. and Goddijn-
34 Murphy, L. 2020, "Revised estimates of ocean-atmosphere CO₂ flux are consistent with ocean carbon
35 inventory", *Nature communications*, vol. 11, no. 1, pp. 1-6.
- 36 492. Gruber, N., Clement, D., Carter, B.R., Feely, R.A., van Heuven, S., Hoppema, M., Ishii, M., Key, R.M., Kozyr, A.,
37 Lauvset, S.K., Lo Monaco, C., Mathis, J.T., Murata, A., Olsen, A., Perez, F.F., Sabine, C.L., Tanhua, T. and
38 Wanninkhof, R. 2019, "The oceanic sink for anthropogenic CO₂ from 1994 to 2007", *SCIENCE*, vol. 363, no. 6432, SI,
39 pp. 1193.
- 40 493. Wang, J.S., Kawa, S.R., Collatz, G.J., Sasakawa, M., Gatti, L.V., Machida, T., Liu, Y. and Manyin, M.E. 2018, "A
41 global synthesis inversion analysis of recent variability in CO₂ fluxes using GOSAT and *in situ*
42 observations", *Atmospheric Chemistry and Physics*, vol. 18, no. 15, pp. 11097-11124.
- 43 494. Waga, H., Hirawake, T., Fujiwara, A., Grebmeier, J.M. and Saitoh, S. 2019, "Impact of spatiotemporal variability in
44 phytoplankton size structure on benthic macrofaunal distribution in the Pacific Arctic", *Deep Sea Research Part II:
45 Topical Studies in Oceanography*, vol. 162, pp. 114-126.
- 46 495. Corliss, B.H., Brown, C.W., Sun, X. and Showers, W.J. 2009, "Deep-sea benthic diversity linked to seasonality of
47 pelagic productivity", *Deep Sea Research Part I: Oceanographic Research Papers*, vol. 56, no. 5, pp. 835-841.
- 48 496. Biggs, D.C., Hu, C. and Müller-Karger, F.E. 2008, "Remotely sensed sea-surface chlorophyll and POC flux at Deep
49 Gulf of Mexico Benthos sampling stations", *Deep Sea Research Part II: Topical Studies in Oceanography*, vol. 55, no.
50 24-26, pp. 2555-2562.
- 51 497. Dierssen, H.M., Zimmerman, R.C., Drake, L.A. and Burdige, D.J. 2009, "Potential export of unattached benthic
52 macroalgae to the deep sea through wind-driven Langmuir circulation", *Geophysical Research Letters*, vol. 36, no. 4.
- 53 498. Field, C.B., Behrenfeld, M.J., Randerson, J.T. and Falkowski, P. 1998, "Primary production of the biosphere:
54 integrating terrestrial and oceanic components", *Science*, vol. 281, no. 5374, pp. 237-240.
- 55 499. Boyd, P.W., Claustre, H., Levy, M., Siegel, D.A. and Weber, T. 2019, "Multi-faceted particle pumps drive carbon
56 sequestration in the ocean", *Nature*, vol. 568, no. 7752, pp. 327-335.
- 57 500. Bopp, L., Monfray, P., Aumont, O., Dufresne, J., Le Treut, H., Madec, G., Terray, L. and Orr, J.C. 2001, "Potential
58 impact of climate change on marine export production", *Global Biogeochemical Cycles*, vol. 15, no. 1, pp. 81-99.
- 59 501. Eppley, R.W. and Peterson, B.J. 1979, "Particulate organic matter flux and planktonic new production in the deep
ocean", *Nature*, vol. 282, no. 5740, pp. 677-680.
502. Eppley, R.W. and Renger, E.H. 1988, "Nanomolar increase in surface layer nitrate concentration following a small
wind event", *Deep Sea Research Part A. Oceanographic Research Papers*, vol. 35, no. 7, pp. 1119-1125.

- 1 503. Carr, M., Friedrichs, M.A., Schmeltz, M., Aita, M.N., Antoine, D., Arrigo, K.R., Asanuma, I., Aumont, O., Barber, R.
2 and Behrenfeld, M. 2006, "A comparison of global estimates of marine primary production from ocean color", *Deep*
3 *Sea Research Part II: Topical Studies in Oceanography*, vol. 53, no. 5-7, pp. 741-770.
- 4 504. Regaudie-de-Gioux, A., Huete-Ortega, M., Sobrino, C., López-Sandoval, D.C., González, N., Fernández-Carrera, A.,
5 Vidal, M., Marañón, E., Cermeño, P. and Latasa, M. 2019, "Multi-model remote sensing assessment of primary
6 production in the subtropical gyres", *Journal of Marine Systems*, vol. 196, pp. 97-106.
- 7 505. Saba, V.S., Friedrichs, M.A., Antoine, D., Armstrong, R.A., Asanuma, I., Behrenfeld, M.J., Ciotti, A.M., Dowell, M.,
8 Hoepffner, N. and Hyde, K. 2011, "An evaluation of ocean color model estimates of marine primary productivity in
9 coastal and pelagic regions across the globe", *Biogeosciences*, vol. 8, no. 2, pp. 489-503.
- 10 506. Silsbe, G.M., Behrenfeld, M.J., Halsey, K.H., Milligan, A.J. and Westberry, T.K. 2016, "The CAFE model: A net
11 production model for global ocean phytoplankton", *Global Biogeochemical Cycles*, vol. 30, no. 12, pp. 1756-1777.
- 12 507. Boyd, P.W. and Trull, T.W. 2007, "Understanding the export of biogenic particles in oceanic waters: Is there
13 consensus?", *Progress in Oceanography*, vol. 72, no. 4, pp. 276-312.
- 14 508. Henson, S.A., Sanders, R., Madsen, E., Morris, P.J., Le Moigne, F. and Quartly, G.D. 2011, "A reduced estimate of the
15 strength of the ocean's biological carbon pump", *Geophysical Research Letters*, vol. 38.
- 16 509. Siegel, D.A., Buesseler, K.O., Doney, S.C., Sailley, S.F., Behrenfeld, M.J. and Boyd, P.W. 2014, "Global assessment of
17 ocean carbon export by combining satellite observations and food-web models", *Global Biogeochemical Cycles*, vol.
18 28, no. 3, pp. 181-196.
- 19 510. Eppley, R.W., Stewart, E., Abbott, M.R. and Heyman, U. 1985, "Estimating ocean primary production from satellite
20 chlorophyll. Introduction to regional differences and statistics for the Southern California Bight", *Journal of Plankton*
21 *Research*, vol. 7, no. 1, pp. 57-70.
- 22 511. Behrenfeld, M.J. and Falkowski, P.G. 1997, "A consumer's guide to phytoplankton primary productivity
23 models", *Limnology and Oceanography*, vol. 42, no. 7, pp. 1479-1491.
- 24 512. Platt, T., Sathyendranath, S. and Ravindran, P. 1990, "Primary production by phytoplankton: analytic solutions for daily
25 rates per unit area of water surface", *Proceedings of the Royal Society of London. Series B: Biological Sciences*, vol.
26 241, no. 1301, pp. 101-111.
- 27 513. Lee, Y.J., Matrai, P.A., Friedrichs, M.A.M., Saba, V.S., Antoine, D., Ardyna, M., Asanuma, I., Babin, M., Belanger, S.,
28 Benoit-Gagne, M., Devred, E., Fernandez-Mendez, M., Gentili, B., Hirawake, T., Kang, S., Kameda, T., Katlein, C.,
29 Lee, S.H., Lee, Z., Melin, F., Scardi, M., Smyth, T.J., Tang, S., Turpie, K.R., Waters, K.J. and Westberry, T.K. 2015,
30 "An assessment of phytoplankton primary productivity in the Arctic Ocean from satellite ocean color/*in situ*
31 chlorophyll-a based models", *Journal of Geophysical Research-Oceans*, vol. 120, no. 9, pp. 6508-6541.
- 32 514. Arrigo, K.R., Robinson, D.H., Worthen, D.L., Schieber, B. and Lizotte, M.P. 1998, "Bio-optical properties of the
33 southwestern Ross Sea", *Journal of Geophysical Research: Oceans*, vol. 103, no. C10, pp. 21683-21695.
- 34 515. Arrigo, K.R., van Dijken, G.L. and Bushinsky, S. 2008, "Primary production in the Southern Ocean, 1997-
35 2006", *Journal of Geophysical Research: Oceans*, vol. 113, no. C8.
- 36 516. Behrenfeld, M.J. and Falkowski, P.G. 1997, "Photosynthetic rates derived from satellite-based chlorophyll
37 concentration", *Limnology and Oceanography*, vol. 42, no. 1, pp. 1-20.
- 38 517. Campbell, J., Antoine, D., Armstrong, R., Arrigo, K., Balch, W., Barber, R., Behrenfeld, M., Bidigare, R., Bishop, J.
39 and Carr, M. 2002, "Comparison of algorithms for estimating ocean primary production from surface chlorophyll,
40 temperature, and irradiance", *Global Biogeochemical Cycles*, vol. 16, no. 3, pp. 9-15.
- 41 518. Longhurst, A., Sathyendranath, S., Platt, T. and Caverhill, C. 1995, "An Estimate of Global Primary Production in the
42 Ocean from Satellite Radiometer Data", *Journal of Plankton Research*, vol. 17, no. 6, pp. 1245-1271.
- 43 519. Platt, T. and Sathyendranath, S. 1988, "Oceanic primary production: estimation by remote sensing at local and regional
44 scales", *Science*, vol. 241, no. 4873, pp. 1613-1620.
- 45 520. Ryther, J.H. and Yentsch, C.S. 1957, "The Estimation of Phytoplankton Production in the Ocean from Chlorophyll and
46 Light Data I", *Limnology and Oceanography*, vol. 2, no. 3, pp. 281-286.
- 47 521. Behrenfeld, M.J., Boss, E., Siegel, D.A. and Shea, D.M. 2005, "Carbon-based ocean productivity and phytoplankton
48 physiology from space", *Global Biogeochemical Cycles*, vol. 19, no. 1.
- 49 522. Stramski, D., Boss, E., Bogucki, D. and Voss, K.J. 2004, "The role of seawater constituents in light backscattering in
50 the ocean", *Progress in Oceanography*, vol. 61, no. 1, pp. 27-56.
- 51 523. Stramski, D., Reynolds, R.A., Babin, M., Kaczmarek, S., Lewis, M.R., Röttgers, R., Sciandra, A., Stramska, M.,
52 Twardowski, M.S. and Franz, B.A. 2008, "Relationships between the surface concentration of particulate organic
53 carbon and optical properties in the eastern South Pacific and eastern Atlantic Oceans", *Biogeosciences*, vol. 5, no. 1,
54 pp. 171-201.
- 55 524. Zhang, X., Lewis, M. and Johnson, B. 1998, "Influence of bubbles on scattering of light in the ocean", *Applied*
56 *Optics*, vol. 37, no. 27, pp. 6525-6536.
- 57 525. Morel, A. and Bricaud, A. 1981, "Theoretical results concerning light absorption in a discrete medium, and application
58 to specific absorption of phytoplankton", *Deep Sea Research Part A. Oceanographic Research Papers*, vol. 28, no. 11,
59 pp. 1375-1393.
- 60 526. Antoine, D. and Morel, A. 1996, "Oceanic primary production: 1. Adaptation of a spectral light-photosynthesis model
in view of application to satellite chlorophyll observations", *Global Biogeochemical Cycles*, vol. 10, no. 1, pp. 43-55.

- 1 527. Hirawake, T., Takao, S., Horimoto, N., Ishimaru, T., Yamaguchi, Y. and Fukuchi, M. 2011, "A phytoplankton
2 absorption-based primary productivity model for remote sensing in the Southern Ocean", *POLAR BIOLOGY*, vol. 34,
3 no. 2, pp. 291-302.
- 4 528. Kiefer, D.A. and Mitchell, B.G. 1983, "A Simple, Steady-State Description of Phytoplankton Growth Based on
5 Absorption Cross-Section and Quantum Efficiency", *LIMNOLOGY AND OCEANOGRAPHY*, vol. 28, no. 4, pp. 770-
6 776.
- 7 529. Lee, Z.P., Carder, K.L., Peacock, T.G., Davis, C.O. and Mueller, J.L. 1996, "Method to derive ocean absorption
8 coefficients from remote-sensing reflectance", *Applied Optics*, vol. 35, no. 3, pp. 453-462.
- 9 530. Ma, S., Tao, Z., Yang, X., Yu, Y., Zhou, X., Ma, W. and Li, Z. 2014, "Estimation of marine primary productivity from
10 satellite-derived phytoplankton absorption data", *IEEE Journal of Selected Topics in Applied Earth Observations and
11 Remote Sensing*, vol. 7, no. 7, pp. 3084-3092.
- 12 531. Marra, J. 1993, "Proportionality between *in situ* carbon assimilation and bio-optical measures of primary production in
13 the Gulf of Maine in summer". *Limnology and Oceanography*, vol. 38, pp. 232-238.
- 14 532. Marra, J., Ho, C. and Trees, C. 2003, "An alternative algorithm for the calculation of primary productivity from remote
15 sensing data", *Lamont Doherty Earth Observatory Technical Report (LDEO-2003-1)*.
- 16 533. Smyth, T.J., Tilstone, G.H. and Groom, S.B. 2005, "Integration of radiative transfer into satellite models of ocean
17 primary production", *Journal of Geophysical Research: Oceans*, vol. 110, no. C10.
- 18 534. Zoffoli, M.L., Lee, Z. and Marra, J.F. 2018, "Regionalization and Dynamic Parameterization of Quantum Yield of
19 Photosynthesis to Improve the Ocean Primary Production Estimates From Remote Sensing", *Frontiers in Marine
20 Science*, vol. 5, pp. 446.
- 21 535. Marra, J., Trees, C.C., Bidigare, R.R. and Barber, R.T. 2000, "Pigment absorption and quantum yields in the Arabian
22 Sea", *Deep Sea Research Part II: Topical Studies in Oceanography*, vol. 47, no. 7-8, pp. 1279-1299.
- 23 536. Ostrowska, M., Woźniak, B. and Dera, J. 2012, "Modelled quantum yields and energy efficiency of fluorescence,
24 photosynthesis and heat production by phytoplankton in the World Ocean", *Oceanologia*, vol. 54, no. 4, pp. 565-610.
- 25 537. Sorensen, J.C. and Siegel, D.A. 2001, "Variability of the effective quantum yield for carbon assimilation in the
26 Sargasso Sea", *Deep Sea Research Part II: Topical Studies in Oceanography*, vol. 48, no. 8-9, pp. 2005-2035.
- 27 538. Iluz, D. and Dubinsky, Z., 2013. Quantum yields in aquatic photosynthesis. In *Photosynthesis* (pp. 135-158). Intech.
- 28 539. DeVries, T. and Weber, T. 2017, "The export and fate of organic matter in the ocean: New constraints from combining
29 satellite and oceanographic tracer observations", *Global Biogeochemical Cycles*, vol. 31, no. 3, pp. 535-555.
- 30 540. Arteaga, L., Haëntjens, N., Boss, E., Johnson, K.S. and Sarmiento, J.L. 2018, "Assessment of export efficiency
31 equations in the southern ocean applied to satellite-based net primary production", *Journal of Geophysical Research:
32 Oceans*, vol. 123, no. 4, pp. 2945-2964.
- 33 541. Goes, J.I., do R Gomes, H., Limsakul, A., Balch, W.M. and Saino, T. 2001, "El Niño related interannual variations in
34 biological production in the North Pacific as evidenced by satellite and ship data", *Progress in Oceanography*, vol. 49,
35 no. 1-4, pp. 211-225.
- 36 542. Goes, J.I., Saino, T., Oaku, H., Ishizaka, J., Wong, C.S. and Nojiri, Y. 2000, "Basin scale estimates of sea surface
37 nitrate and new production from remotely sensed sea surface temperature and chlorophyll", *Geophysical Research
38 Letters*, vol. 27, no. 9, pp. 1263-1266.
- 39 543. Siegel, D.A., Buesseler, K.O., Behrenfeld, M.J., Benitez-Nelson, C.R., Boss, E., Brzezinski, M.A., Burd, A., Carlson,
40 C.A., D'Asaro, E.A. and Doney, S.C. 2016, "Prediction of the export and fate of global ocean net primary production:
41 The EXPORTS science plan", *Frontiers in Marine Science*, vol. 3, pp. 22.
- 42 544. Matsuoka, A., Hooker, S.B., Bricaud, A., Gentili, B. and Babin, M. 2013, "Estimating absorption coefficients of
43 colored dissolved organic matter (CDOM) using a semi-analytical algorithm for southern Beaufort Sea waters:
44 application to deriving concentrations of dissolved organic carbon from space", *Biogeosciences*, vol. 10, no. 2, pp. 917-
45 927.
- 46 545. Le, C., Zhou, X., Hu, C., Lee, Z., Li, L. and Stramski, D. 2018, "A Color-Index-Based Empirical Algorithm for
47 Determining Particulate Organic Carbon Concentration in the Ocean From Satellite Observations", *Journal of
48 Geophysical Research-Oceans*, vol. 123, no. 10, pp. 7407-7419.
- 49 546. Gordon, H.R., Boynton, G.C., Balch, W.M., Groom, S.B., Harbour, D.S. and Smyth, T.J. 2001, "Retrieval of
50 coccolithophore calcite concentration from SeaWiFS imagery", *Geophysical Research Letters*, vol. 28, no. 8, pp. 1587-
51 1590.
- 52 547. Balch, W.M., Gordon, H.R., Bowler, B.C., Drapeau, D.T. and Booth, E.S. 2005, "Calcium carbonate measurements in
53 the surface global ocean based on Moderate-Resolution Imaging Spectroradiometer data", *Journal of Geophysical
54 Research: Oceans*, vol. 110, no. C7.
- 55 548. Mitchell, C., Hu, C., Bowler, B., Drapeau, D. and Balch, W.M. 2017, "Estimating particulate inorganic carbon
56 concentrations of the global ocean from ocean color measurements using a reflectance difference approach", *Journal of
57 Geophysical Research: Oceans*, vol. 122, no. 11, pp. 8707-8720.
- 58 549. Evers-King, H., Martinez-Vicente, V., Brewin, R.J., Dall'Olmo, G., Hickman, A.E., Jackson, T., Kostadinov, T.S.,
59 Krasemann, H., Loisel, H. and Röttgers, R. 2017, "Validation and intercomparison of ocean color algorithms for
60 estimating particulate organic carbon in the oceans", *Frontiers in Marine Science*, vol. 4, pp. 251.
550. Behrenfeld, M.J., Hu, Y., Hostetler, C.A., Dall'Olmo, G., Rodier, S.D., Hair, J.W. and Trepte, C.R. 2013, "Space-based
lidar measurements of global ocean carbon stocks", *Geophysical Research Letters*, vol. 40, no. 16, pp. 4355-4360.

- 1 551. Balch, W.M., Bowler, B.C., Drapeau, D.T., Lubelczyk, L.C. and Lyczkowski, E. 2018, "Vertical distributions of
2 coccolithophores, PIC, POC, biogenic Silica, and chlorophyll a throughout the global ocean", *Global Biogeochemical
3 Cycles*, vol. 32, no. 1, pp. 2-17.
- 4 552. Hedges, J.I. and Keil, R.G. 1995, "Sedimentary organic matter preservation: an assessment and speculative synthesis",
5 *Marine Chemistry*, vol. 49, no. 2-3, pp. 81-115.
- 6 553. Dunne, J., Sarmiento, J. and Gnanadesikan, A. 2007 "A synthesis of global particle export from the surface ocean and
7 cycling", *Global Biogeochem. Cy.*, vol. 21.
- 8 554. DeVries, B., Huang, C., Lang, M.W., Jones, J.W., Huang, W., Creed, I.F. and Carroll, M.L. 2017, "Automated
9 quantification of surface water inundation in wetlands using optical satellite imagery", *Remote Sensing*, vol. 9, no. 8,
10 pp. 807.
- 11 555. Moore, J. K., Doney, S. C., Glover, D. M., & Fung, I. Y. (2002). Iron cycling and nutrient-limitation patterns in surface
12 waters of the World Ocean. *Deep-Sea Research Part II: Topical Studies in Oceanography*, 49, 463–507
- 13 556. Muller-Karger, F.E., Varela, R., Thunell, R., Luerssen, R., Hu, C. and Walsh, J.J. 2005, "The importance of continental
14 margins in the global carbon cycle", *Geophysical Research Letters*, vol. 32, no. 1.
- 15 557. Jahnke, R. A. 2010, *Global Synthesis, in Carbon and Nutrient Fluxes in Continental Margins*, edited by K. K. Liu, L.
16 Atkinson, R. Quinones and L. Talaue-McManus, pp. 597-615, Springer-Verlag, Berlin Heidelberg, doi:10.1007/978-3-
17 540-92735-2.
- 18 558. Cai, W. 2011, "Estuarine and coastal ocean carbon paradox: CO2 sinks or sites of terrestrial carbon
19 incineration?", *Annual review of marine science*, vol. 3, pp. 123-145. DOI 10.1146/annurev-marine-120709-142723.
- 20 559. Bourgeois, T., J. C. Orr, L. Resplandy, J. Terhaar, C. Ethé, M. Gehlen, and L. Bopp (2016), Coastal-ocean uptake of
21 anthropogenic carbon, *Biogeosciences*, 13(14), 4167-4185, doi:10.5194/bg-13-4167-2016.
- 22 560. Gattuso, J., Frankignoulle, M. and Wollast, R. 1998, "Carbon and carbonate metabolism in coastal aquatic
23 ecosystems", *Annual Review of Ecology and Systematics*, vol. 29, no. 1, pp. 405-434.
- 24 561. Hopkins, J. & Balch, W.M. 2018, "A new approach to estimating coccolithophore calcification rates from
25 space", *Journal of Geophysical Research: Biogeosciences*, vol. 123, no. 5, pp. 1447-1459
- 26 562. Benway, H. M., S. R. Alin, E. Boyer, W.-J. Cai, P. G. Coble, J. N. Cross, M. A. Friedrichs, M. Goni, P. Griffith, M.
27 Herrmann, S. Lohrenz, J. T. Mathis, G. A. McKinley, R. G. Najjar, C. H. Pilskaln, S. A. Siedlecki, and R. Smith 2016,
28 A science plan for carbon cycle research in North American coastal waters. Report of the Coastal CARBON Synthesis
29 (CCARS) community workshop, August 19-21, 2014, edited, Ocean Carbon and Biogeochemistry Program and North
30 American Carbon Program, 84 pp., Woods Hole, MA, doi:10.1575/1912/7777.
- 31 563. Fennel, K., Alin, S., Barbero, L., Evans, W., Bourgeois, T., Cooley, S., Dunne, J., Feely, R.A., Hernandez-Ayon, J.M.
32 and Hu, X. 2019, "Carbon cycling in the North American coastal ocean: a synthesis", *Biogeosciences*, vol. 16, no. 6, pp.
33 1281-1304.
- 34 564. Signorini, S.R., Mannino, A., Najjar, J., Raymond G., Friedrichs, M.A.M., Cai, W., Salisbury, J., Wang, Z.A., Thomas,
35 H. & Shadwick, E. 2013, "Surface ocean pCO₂ seasonality and sea-air CO₂ flux estimates for the North American
36 east coast", *JOURNAL OF GEOPHYSICAL RESEARCH-OCEANS*, vol. 118, no. 10, pp. 5439-5460.
- 37 565. Najjar, Raymond G., Maria Herrmann, R. Alexander, Elizabeth W. Boyer, D. J. Burdige, D. Butman, W-J. Cai et al.
38 2018 "Carbon budget of tidal wetlands, estuaries, and shelf waters of eastern North America." *Global Biogeochemical
39 Cycles* 32, no. 3 (2018): 389-416.
- 40 566. Bélanger, S., Babin, M. and Tremblay, J. 2013, "Increasing cloudiness in Arctic damps the increase in phytoplankton
41 primary production due to sea ice receding", *Biogeosciences*, vol. 10, no. 6, pp. 4087-4101.
- 42 567. Huot, Y., Babin, M. and Bruyant, F. 2013, "Photosynthetic parameters in the Beaufort Sea in relation to the
43 phytoplankton community structure", *Biogeosciences*, vol. 10, no. 5, pp. 3445-3454.
- 44 568. Liu, M., Tian, H., Yang, Q., Yang, J., Song, X., Lohrenz, S.E. and Cai, W. 2013, "Long-term trends in
45 evapotranspiration and runoff over the drainage basins of the Gulf of Mexico during 1901–2008", *Water Resources
46 Research*, vol. 49, no. 4, pp. 1988-2012.
- 47 569. Lohrenz, S.E., Cai, W., Chakraborty, S., Gundersen, K. and Murrell, M.C. 2014, "Nutrient and carbon dynamics in a
48 large river-dominated coastal ecosystem: The Mississippi-Atchafalaya River system", *Biogeochemical Dynamics at
49 Major River-Coastal Interfaces: Linkages with Global Change*, , pp. 448-472.
- 50 570. Ren, W., Tian, H., Tao, B., Yang, J., Pan, S., Cai, W., Lohrenz, S.E., He, R. and Hopkinson, C.S. 2015, "Large increase
51 in dissolved inorganic carbon flux from the Mississippi River to Gulf of Mexico due to climatic and anthropogenic
52 changes over the 21st century", *Journal of Geophysical Research: Biogeosciences*, vol. 120, no. 4, pp. 724-736.
- 53 571. Ren, W., Tian, H., Cai, W., Lohrenz, S.E., Hopkinson, C.S., Huang, W., Yang, J., Tao, B., Pan, S. and He, R. 2016,
54 "Century-long increasing trend and variability of dissolved organic carbon export from the Mississippi River basin
55 driven by natural and anthropogenic forcing", *Global Biogeochemical Cycles*, vol. 30, no. 9, pp. 1288-1299.
- 56 572. Tao, B., Tian, H., Ren, W., Yang, J., Yang, Q., He, R., Cai, W. and Lohrenz, S. 2014, "Increasing Mississippi river
57 discharge throughout the 21st century influenced by changes in climate, land use, and atmospheric CO₂", *Geophysical
58 Research Letters*, vol. 41, no. 14, pp. 4978-4986.
- 59 573. Tian, H., Ren, W., Yang, J., Tao, B., Cai, W., Lohrenz, S.E., Hopkinson, C.S., Liu, M., Yang, Q. and Lu, C. 2015,
60 "Climate extremes dominating seasonal and interannual variations in carbon export from the Mississippi River
Basin", *Global Biogeochemical Cycles*, vol. 29, no. 9, pp. 1333-1347.

574. Tian, H., Yang, Q., Najjar, R.G., Ren, W., Friedrichs, M.A., Hopkinson, C.S. and Pan, S. 2015, "Anthropogenic and climatic influences on carbon fluxes from eastern North America to the Atlantic Ocean: A process-based modeling study", *Journal of Geophysical Research: Biogeosciences*, vol. 120, no. 4, pp. 757-772.
575. Xue, Z., He, R., Fennel, K., Cai, W., Lohrenz, S. and Hopkinson, C. 2013, "Modeling ocean circulation and biogeochemical variability in the Gulf of Mexico", *Biogeosciences*, vol. 10, no. 11, pp. 7219-7234.
576. Signorini, S.R., Mannino, A., Friedrichs, M.A.M., St-Laurent, P., Wilkin, J., Tabatabai, A., Najjar, R.G., Hofmann, E.E., Da, F., Tian, H. & Yao, Y. 2019, "Estuarine Dissolved Organic Carbon Flux From Space: With Application to Chesapeake and Delaware Bays", *JOURNAL OF GEOPHYSICAL RESEARCH-OCEANS*, vol. 124, no. 6, pp. 3755-3778.
577. Shanmugam, P., Varunan, T., Jaiganesh, S.N.N., Sahay, A. & Chauhan, P. 2016, "Optical assessment of colored dissolved organic matter and its related parameters in dynamic coastal water systems", *ESTUARINE COASTAL AND SHELF SCIENCE*, vol. 175, pp. 126-145.
578. Mannino, A., Russ, M.E. and Hooker, S.B. 2008, "Algorithm development and validation for satellite-derived distributions of DOC and CDOM in the US Middle Atlantic Bight", *Journal of Geophysical Research: Oceans*, vol. 113, no. C7.
579. Balch, W., Huntington, T., Aiken, G., Drapeau, D., Bowler, B., Lubelczyk, L. and Butler, K. 2016, "Toward a quantitative and empirical dissolved organic carbon budget for the Gulf of Maine, a semienclosed shelf sea", *Global Biogeochemical Cycles*, vol. 30, no. 2, pp. 268-292.
580. Vantrepotte, V., Danhiez, F., Loisel, H., Ouilon, S., Mériaux, X., Cauvin, A. and Dessailly, D. 2015, "CDOM-DOC relationship in contrasted coastal waters: implication for DOC retrieval from ocean color remote sensing observation.", *Optics express*, vol. 23, no. 1, pp. 33-54.
581. Cai, W.J., Chen, C.A. and Borges, A. 2013, "Carbon dioxide dynamics and fluxes in coastal waters influenced by river plumes", *Biogeochemical Dynamics at Major River-Coastal Interfaces*, edited by: Bianchi, TS, Allison MA, and Cai, W.-J., Cambridge University Press, Cambridge, , pp. 155-173.
582. Guo, X., Cai, W., Huang, W., Wang, Y., Chen, F., Murrell, M.C., Lohrenz, S.E., Jiang, L., Dai, M. and Hartmann, J. 2012, "Carbon dynamics and community production in the Mississippi River plume", *Limnology and Oceanography*, vol. 57, no. 1, pp. 1-17.
583. Huang, W., Cai, W., Wang, Y., Lohrenz, S.E. and Murrell, M.C. 2015a, "The carbon dioxide system on the Mississippi River-dominated continental shelf in the northern Gulf of Mexico: 1. Distribution and air-sea CO₂ flux", *Journal of Geophysical Research: Oceans*, vol. 120, no. 3, pp. 1429-1445.
584. Huang, W., Cai, W., Wang, Y., Hu, X., Chen, B., Lohrenz, S.E., Chakraborty, S., He, R., Brandes, J. and Hopkinson, C.S. 2015b, "The response of inorganic carbon distributions and dynamics to upwelling-favorable winds on the northern Gulf of Mexico during summer", *Continental Shelf Research*, vol. 111, pp. 211-222.
585. Huang, W., Cai, W., Castelao, R.M., Wang, Y. and Lohrenz, S.E. 2013, "Effects of a wind-driven cross-shelf large river plume on biological production and CO₂ uptake on the Gulf of Mexico during spring", *Limnology and Oceanography*, vol. 58, no. 5, pp. 1727-1735.
586. Xue, Z., He, R., Fennel, K., Cai, W., Lohrenz, S., Huang, W. and Tian, H. 2014, "Modeling pCO₂ variability in the Gulf of Mexico", *Biogeosciences Discussions*, vol. 11, no. 8, pp. 12673-12695.
587. Chakraborty, S. and Lohrenz, S.E. 2015, "Phytoplankton community structure in the river-influenced continental margin of the northern Gulf of Mexico", *Marine Ecology Progress Series*, vol. 521, pp. 31-47.
588. Chakraborty, S., Lohrenz, S.E. and Gundersen, K. 2017, "Photophysiological and light absorption properties of phytoplankton communities in the river-dominated margin of the northern Gulf of Mexico", *Journal of Geophysical Research: Oceans*, vol. 122, no. 6, pp. 4922-4938.
589. Wang, Z.A., Wanninkhof, R., Cai, W., Byrne, R.H., Hu, X., Peng, T. & Huang, W. 2013, "The marine inorganic carbon system along the Gulf of Mexico and Atlantic coasts of the United States: Insights from a transregional coastal carbon study", *Limnology and Oceanography*, vol. 58, no. 1, pp. 325-342.
590. O'Mara, N.A. and Dunne, J.P. 2019, "Hot spots of carbon and alkalinity cycling in the coastal oceans", *Scientific reports*, vol. 9, no. 1, pp. 1-8.
591. Dale, A.W., Graco, M. and Wallmann, K. 2017, "Strong and dynamic benthic-pelagic coupling and feedbacks in a coastal upwelling system (Peruvian shelf)", *Frontiers in Marine Science*, vol. 4, pp. 29.
592. Theodor, M., Schmiedl, G., Jorissen, F. and Mackensen, A. 2016, "Stable carbon isotope gradients in benthic foraminifera as proxy for organic carbon fluxes in the Mediterranean Sea", *Biogeosciences*, vol. 13, no. 23, pp. 6385-6404.
593. Sanchez-Vidal, A., Pasqual, C., Kerhervé, P., Calafat, A., Heussner, S., Palanques, A., Durrieu de Madron, X., Canals, M. & Puig, P. 2008, "Impact of dense shelf water cascading on the transfer of organic matter to the deep western Mediterranean basin", *Geophysical Research Letters*, vol. 35, no. 5.
594. Kwon, E. Y., T. DeVries, E. Galbraith, J. Hwang, G. Kim, and A. Timmermann Stable Carbon Isotopes. 2020, Suggest Large Terrestrial Carbon Inputs to the Global Ocean, *Global Biogeochemical Cycles*, e2020GB006684, doi:<https://doi.org/10.1029/2020GB006684>.
595. UNFCCC. 1997, "United Nations framework convention on climate change", Kyoto Protocol, Kyoto, vol. 19, pp. 497.
596. Hiraishi, T., Krug, T., Tanabe, K., Srivastava, N., Baasansuren, J., Fukuda, M. and Troxler, T.G. 2014, "2013 supplement to the 2006 IPCC guidelines for national greenhouse gas inventories: Wetlands", IPCC, Switzerland.

- 1 597. Rehdanz, K., Tol, R.S. and Wetzel, P. 2006, "Ocean carbon sinks and international climate policy", *Energy Policy*, vol.
2 34, no. 18, pp. 3516-3526.
- 3 598. IPCC, 2019: IPCC Special Report on the Ocean and Cryosphere in a Changing Climate [H.-O. Pörtner, D.C. Roberts,
4 V. Masson-Delmotte, P. Zhai, M. Tignor, E. Poloczanska, K. Mintenbeck, A. Alegría, M. Nicolai, A. Okem, J. Petzold,
5 B. Rama, N.M. Weyer (eds.)].
- 6 599. UNFCCC. 2015, "1/CP. 21, Adoption of the Paris Agreement", Report of the Conference of the Parties on Its Twenty-
7 First Session, Held in Paris.
- 8 600. Zeng, Y., Friess, D.A., Sarira, T.V., Siman, K. and Koh, L.P., 2021. Global potential and limits of mangrove blue
9 carbon for climate change mitigation. *Current Biology*.
- 10 601. Pindilli, E., Sleeter, R. & Hogan, D. 2018, "Estimating the societal benefits of carbon dioxide sequestration through
11 peatland restoration", *Ecological Economics*, vol. 154, pp. 145-155.
- 12 602. Chimner, R.A., Cooper, D.J., Wurster, F.C. and Rochefort, L., 2017. An overview of peatland restoration in North
13 America: where are we after 25 years?. *Restoration Ecology*, 25(2):283-292.
- 14 603. Halabisky, M., Moskal, L.M. and Hall, S.A. 2011, "Object-based classification of semi-arid wetlands", *Journal of*
15 *Applied Remote Sensing*, vol. 5, no. 1, pp. 053511.
- 16 604. Kennedy, R.E., Yang, Z., Gorelick, N., Braaten, J., Cavalcante, L., Cohen, W.B. and Healey, S. 2018, "Implementation
17 of the LandTrendr algorithm on google earth engine", *Remote Sensing*, vol. 10, no. 5, pp. 691.
- 18 605. Sharma, S., MacKenzie, R.A., Tieng, T., Soben, K., Tulyasuwan, N., Resanond, A., Blate, G. and Litton, C.M. 2020,
19 "The impacts of degradation, deforestation and restoration on mangrove ecosystem carbon stocks across Cambodia",
20 *Science of the Total Environment*, vol. 706, pp. 135416.
- 21 606. Chmura, G.L. 2013, "What do we need to assess the sustainability of the tidal salt marsh carbon sink?", *Ocean and*
22 *Coastal Management*, vol. 83, pp. 25-31.
- 23 607. Krishna, K.V., Shanmugam, P. and Nagamani, P.V. 2020, "A Multiparametric Nonlinear Regression Approach for the
24 Estimation of Global Surface Ocean $p\text{CO}_2$ Using Satellite Oceanographic Data", *IEEE Journal of Selected Topics in*
25 *Applied Earth Observations and Remote Sensing*, vol. 13, pp. 6220-6235.
- 26 608. Sasmito, S.D., Taillardat, P., Clendenning, J.N., Cameron, C., Friess, D.A., Murdiyarso, D. & Hutley, L.B. 2019,
27 "Effect of land-use and land-cover change on mangrove blue carbon: A systematic review", *Global Change Biology*,
28 vol. 25, no. 12, pp. 4291-4302.
- 29 609. Lagomasino, D., Fatoyinbo, L., Castaneda, E., Cook, B., Montesano, P., Neigh, C., Ott, L., Chavez, S. and Morton, D.,
30 2020. Storm surge, not wind, caused mangrove dieback in southwest Florida following Hurricane Irma.
- 31 610. Krauss, K.W. & Osland, M.J. 2020, "Tropical cyclones and the organization of mangrove forests: a review", *Annals of*
32 *botany*, vol. 125, no. 2, pp. 213-234.
- 33 611. Osland, M.J., Feher, L.C., Spivak, A.C., Nestlerode, J.A., Almario, A.E., Cormier, N., From, A.S., Krauss, K.W.,
34 Russell, M.J., Alvarez, F. and Dantin, D.D., 2020b. Rapid peat development beneath created, maturing mangrove
35 forests: ecosystem changes across a 25-yr chronosequence. *Ecological Applications*, 30(4), p.e02085.
- 36 612. Shutler, J.D., Wanninkhof, R., Nightingale, P.D., Woolf, D.K., Bakker, D.C., Watson, A., Ashton, I., Holding, T.,
37 Chapron, B. and Quilfen, Y. 2020, "Satellites will address critical science priorities for quantifying ocean
38 carbon", *Frontiers in Ecology and the Environment*, vol. 18, no. 1, pp. 27-35.
- 39
40
41
42
43
44
45
46
47
48
49
50
51
52
53
54
55
56
57
58
59
60